Ministry of Higher Education
And Scientific Research
University of Kerbala
College of Engineering
Mechanical Engineering Department

EXPERIMENTAL AND NUMERICAL STUDY OF TWO- PHASE FLOW IN THE RIBBED DIVERGENT RECTANGULAR DUCTS

A Thesis
Submitted to the
Mechanical Engineering Department
of the University of Kerbala in a Partial Fulfillment of
the Requirements for the Degree of Master of Science in
Mechanical Engineering

By

Ali Abdalaimma Hassan AL-Genaby

(B.Sc. University of Babylon 2004)

Supervisors

Assist. Prof. Dr. Abbas Sahi Shareef

Assist. Prof. Dr. Riyadh S. Saleh Al-Turaihi

2018 A.D. **1440** A.H.

Abstract

Two-phase flow in the ribbed divergent\convergent rectangular duct for two cases: upward vertical and inclined were studied in this thesis. The materials used for two-phase, water and air were used. Experimental and numerical studies have been performed to test the influence of increased air and water discharges on the pressure profile and difference pressure through the divergent\convergent section, As the effect of increasing the divergent/ convergent angle on the pressure difference across the divergent/convergent section was studied.

The characterizations of flow patterns are achieved via visual observation. A pressure sensor with interphase and video camera recording were used to study flow regimes through the test channel. Water inlet discharges used were between (5-20 L/min), and air discharges were between (5.833-16.666 L/min). Two test channels with divergent\convergent angles (10 and 15 degrees) were used.

An experimental rig was constructed with dimensions were (2 * 6) cm of the cross-section area before the divergent\convergent section with length were 50 cm long, while the section area was (2 * 8) cm after the divergent\convergent section with length were 50 cm too.

Computational fluid dynamics for a three-dimensional model was simulated with ANSYS fluent 18 depending on the boundary condition obtained experimentally and governed by equations of Eulerian multiphase flow model.

A agree was observed between the experimental and numerical values of pressure with maximum deviation was 9 %, as a similarity was observed in the flow behavior between experimental and numerical work.

The results indicated that the pressure along the test channel raises as water and air discharge rise. for vertical test channel with divergent section (10 degree) , as the water discharge increased from (5 L/min to 20 L/min) at the same location of the pressure transducer and constant air discharge (35 cm and 5.833 L/min), respectively, the value of pressure increase from (14.6 kpa to 16.7 kpa).

For the divergent section, It was observed that as the divergence opening angle increases, the pressure recovery decreases. While in the case of the convergence section, the pressure drop increases with the increase of the convergence angle.

It was observed that the dominant flow pattern within the range of discharges used was a slug flow pattern. The values of air and water discharges were represented on the Hewitt and Roberts flow maps (1969) for vertical flow, as the Barnea flow map (1980) was used for inclined flow. A good agreement was observed between the type of flow that appeared in the experiments and the flow maps.

A numerical study only was conducted to study the effect of the ribs on flow behavior and pressure recovery, It was noted that the value of the recovery of the pressure across the divergence section of the absence of ribs is higher than the case of presence ribs by 8.333%.

Introduction

1.1. Overview

Two-phase flow is defined as two-phase flow simultaneously in the same pipe like gas and liquid, gas and solid, two dissimilar liquids or liquid and solid .the most complexes of these types is the flow of gas -liquids due to the compressibility and deformation of both phases. Two-phase flow can be often met in chemical or mechanical engineering applications, oil wells, power generation, reactors, boilers, condensers, evaporators and combustion systems [1]. The existence of singularities in channels may great impact the behavior of two-phase flow and thus the resulting pressure drop.

Therefore, it is a significant issue of study in specific when the application relates safety valves. The investigates of two-phase flow in constant area channels are numerous in the survey review. In contrast to the studies of two-phase flow in diffuser, nozzle, bows and other types of singularities are somewhat few. The purpose of research these singularities is to know how these shapes influnce the two-phase flow patterns and pressure profile. Especially, the comprehension of the flow in these singularities can lead to an improved performance of safety systems. Two-phase flow can be classified as the classification given by Naji[2] as:

- According to the matter of phase:
    1. Two-phase, one-component. (e.g. water-steam flow)
    2. Two-phase, two-components. (e.g. water-gas flow)
- According to the external wall state:
    1. Adiabatic flow (e.g. generally gas- liquids flow)
    2. Heating flow (e.g. pipes in boiler)
    3. Cooling flow (e.g. pipes in condenser)

- According to the inclination of the pipe which carries the flow:
    1. Horizontal flow.
    2. Vertical flow. (Upwardly or downwardly).
    3. Inclined flow. (Upwardly or downwardly).

Two-phase, two components (air-water), adiabatic and upward flow is the case under consideration in the present study.

Manufacture ducts or pipes with ribs is widely. The rib in channels contribute to an increase mass and heat transfer and produce flow circulation leading to increased turbulence. In channels, ribs drive steam toward the core of the channel while liquid toward the channel wall [3]. In the present work, the ribs are used to create strong turbulence intensity inside the divergence section by breaking the laminar-sub layer leading to rapid mixing between the phases.

The employ of numerical simulation has increased in the recently years. Numerical guess of the behavior of two-phase flows be more necessary. The evolution of computational codes for the numerical simulation of two-phase flows depend on the physical comprehension of the two-phase flow phenomena, like bubble interactions, distribution of phases , two-phase flow turbulence, condensation, and boiling, etc. For successful modeling, information accurate and clear about flow should be provided [4].

1.2. Flow Pattern

A locative configuration of liquid and gas happens when liquid and gas are flow together within the same tube, due to different fluid properties. This configuration is called the flow pattern [5]. Flow patterns are considered important problems because design variables depend on them such as mass transfer, momentum and energy and pressure drop. Therefore, It is necessary to know the correct prediction of the flow pattern

in order to obtain a successful design for two-phase flow systems [6]. In present work, upward vertical and inclined flow was treated. Therefor the flow patterns of these types of flow will be mentioned.

1.2.1. Flow Patterns in Vertical Systems

At low gas discharges, the gas phase begins to uplift through the continuous liquid Such as small and separate bubbles, this flow is known as bubble flow. Whenever the gas discharge increases, the smaller bubbles tend to join and form bigger bubbles. At suitably high gas discharges, the agglomerated bubbles become big sufficient to occupy nearly the complete pipe area. These type of bubbles are called Taylor bubbles, liquid slug separates between these bubbles, which usually contain smaller gas bubbles, and this type of flow pattern is called slug flow. With continuing to increase gas discharge, the shear stress between the liquid film and Taylor bubble increases, finally producing a collapse of the liquid film and the bubbles. That leading to happening churning motion of the fluids. Hence, this flow is named churn flow. At very high gas discharge, which causes the complete gas phase to flow through the core of the channel. Some liquid phase is entrained in the gas central as droplets, while the remainder of the liquid flows between the tube wall and the gas core. This type of flow is called annular flow.

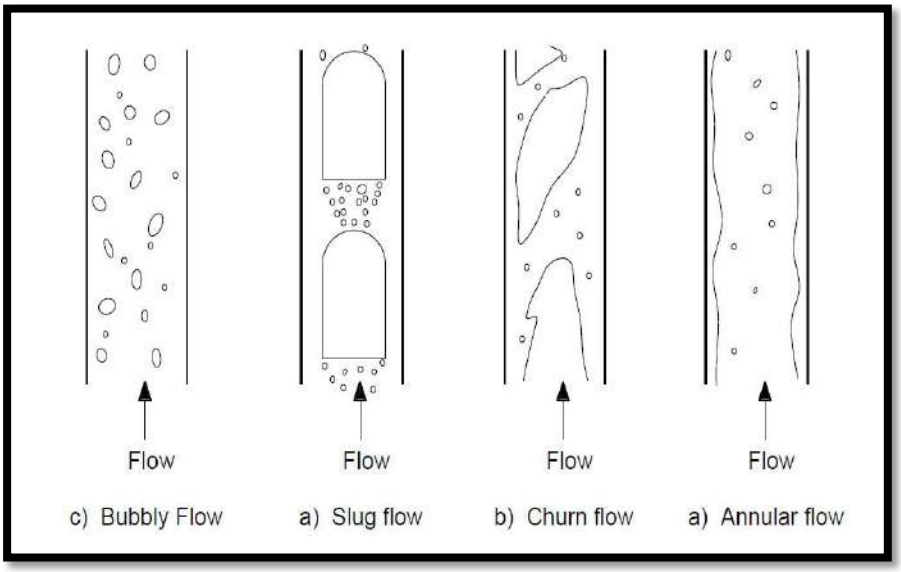

Figure 1.1: Flow patterns in the vertical upward flow.

1.2.2. Flow Patterns in Inclined Systems

Flow patterns noted in upward inclined systems are extremely like to those noted in vertical upward flow, particularly for near-vertical systems. It involves bubbly, slug, churn and annular. , Figure 1.3.

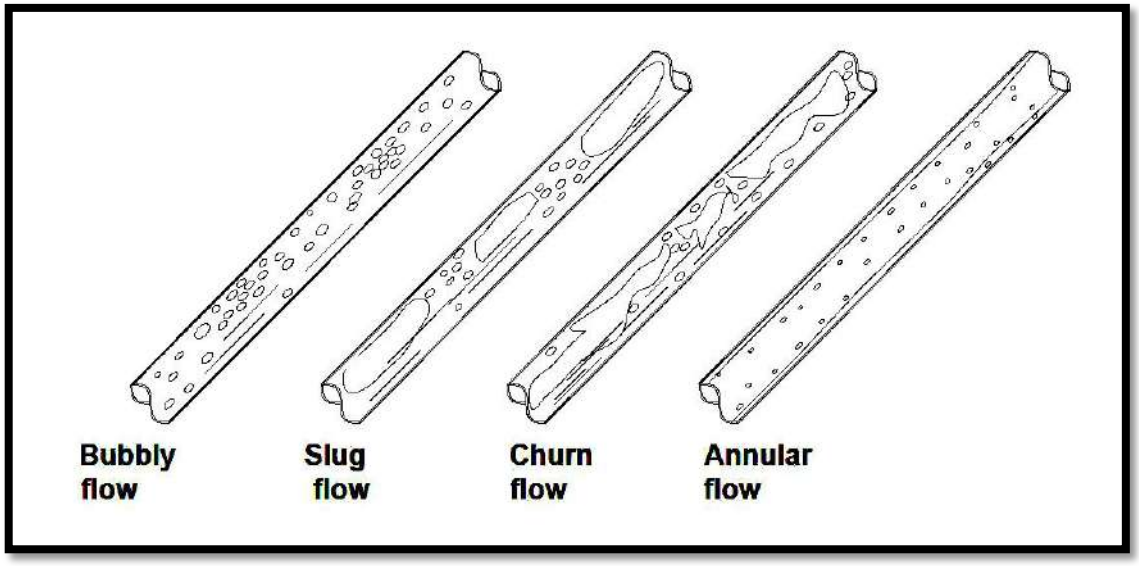

Figure 1.2: Flow patterns in inclined pipes.

1.3. Flow Pattern Map

To predict which of the flow pattern exist in available flow conditions in the flow pattern series, many investigations draw maps to locate that depending on flow conditions. These maps of flow patterns are described by chart has many lines to separate the consequent flow pattern. Otherwise, maps are described by a set of equations called "Flow pattern Transitions". The difference between various maps is due to their specification, some for single inclination angle, while the other is for the whole range of inclination angles. Hewitt and Roberts flow maps (1969) [7]. Is used for vertical upward two-phase flow.as shown in figure 1.3.

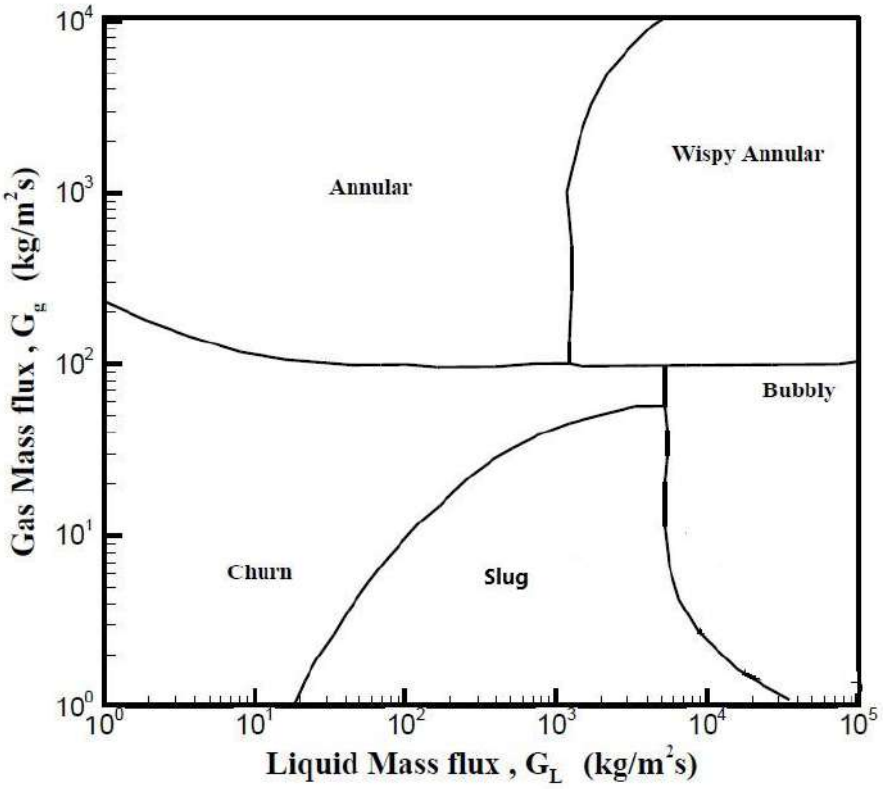

Figure 1.2: Hewitt and Roberts flow maps(1969).

1.4. Pressure Drop

The pressure drop in the system is a main variable to determine the pumping capacity of a given flow, as pump ability must be corresponding suitably with the system requests. Therefore, it is significant to identify as accurately as possible the value of pressure drop. A significant part of this pressure drop happens along vertical channels, and it becomes mainly significant when the pipes are lengthy as detailed by Perez [8]. It happens because of many factors including frictional, acceleration, and gravitational drops. In case of nonboiling two-phase, the acceleration term is neglected due to the constant value of quality or the dryness fraction. Pressure drop causing from friction is considered more problematic and expressed as a function of the friction factor

1.5. Void Fraction and Liquid Hold Up

One of the main problems encountered in any study of two-phase

(gas-liquid) flow is the void fraction. It means the volumetric ratio of the channel section occupied by the gas to the volume of the channel section. Generally, it is expressed by a fraction various between zero and unity. Thome[9] concluded that it is the important physical variable for estimating many other main limitations, like the density and viscosity of two-phase, for finding the relative average velocity, and is of primary significance for guessing flow patterns transitions, pressure drop and heat transfer, while volumetric ratio of the pipe section taken by the liquid phase to pipe section is usually known as liquid hold up.

1.6. Objectives of This Work

The objectives for the present work are as follows:

Manufacturing and construct a divergence rectangular ribbed channel model for experimental examination.

To investigate the effect of water superficial velocity, air super velocity and opening angle on the pressure profile and recovery pressure across ribbed divergence section for two cases: vertical flow and inclined flow

To investigate the effect of water superficial velocity, air super velocity and opening angle on the pressure profile and drop pressure across ribbed convergence section for two cases: vertical flow and inclined flow, and draw the flow pattern map

Comparison of experimental and numerical results obtained from the program of ANSYS.

CHAPTER TWO

LITERATURE REVIEW

Literature Review

2.1. Introduction

The two-phase flow exists in many varied Practical applications. Where conducted many experiments of two-phase for understanding the flow more broadly by the researchers' .in this chapter has been mention some studies and tests conducted on the two-phase flow, especially the flow of type of gas-liquid because of their relationship with this research

2.2. Theoretical Studies

Behzadi et al. (2004) [10] the Eulerian approach for the prediction of dispersed two-phase flow at high volume fractions of the dispersed phase were modified. New relations for the effect of high volume fraction on the interphase forces were presented. They also suggested an upgraded version of k-Ɛ turbulence model; the new models were carried out in a CFD code and verified for bubbly flow through a tube sudden expansion. The turbulent kinetic energy, the phase fraction and the continuous phase velocity were counted by using the new and old models and then were compared with experimental results. The results demonstrated that the new model gives improvements of prediction better than the old model.

Cheng el at. (2008) [11] conducted a comprehensive review of previous studies Which deals with two-phase flow (gas-liquid) flow patterns and flow maps For adiabatic and non-adiabatic conditions. It was noted that the Conclusions, which obtained from different researchers were not corresponding under the same test conditions and same fluids, Because Most researchers used classical visual-only method In their studies of flow patterns. These methods mostly lead to large errors in the flow-pattern observations.

Uchiyama and Degawa (2008) [12] concerned with the two-dimensional simulation of bubbly flow (air gas) around a hydrofoil. The approach of Lagrangian was used to calculate the behavior of bubble motion. It was confirmed that the simulated distributions of pressure and air volume fraction and agree well with the trend of the measurement. These results show that the eddies method is usable to the bubbly flow analysis around a hydrofoil obstruction**.**

Naji (2009) [2] Established Explicit correlations to guess the mounts liquid holdup of two-phase (air-water) flow in the inclined pipe. The comparison was conducted with several previous studies. The comparison shows that this correlation was semi- correspondence with correlation by Taitel-Dukler model [13] and it displays that the suggested correlation had the best performance than the others. Due to it adopts the effect of the inclination. As showed also the amounts of the liquid holdup in horizontal flow was bigger those in inclined flow because of the inclination effects.

Hameed et al. (2009) [14] an analytical studied of the pressure drop that occurs due to presence the obstruction through two-phase flow in the horizontal channel was presented. Various obstruction shapes with size were examined. A mathematical relationship was established between the drop pressure and two-phase multiplier and gas superficial velocity. It was concluded also that the drop pressure rise with rising the size of the obstruction.

Zhu et al. (2009) [15] Conducted a numerical study of the effect of hydrofoil on the distribution of bubbles for the bubble flow of different ranges of attack angles and Reynolds number. It was observed that the effect of the attack angle was small at Reynolds number low, but the effect increased with the increase in Reynolds number. It was also observed that

the angle of attack on the distribution of the bubble was clearer at the angle of 20 instead of 10 degree.

Deniz and Eskin (2012) [16] two-phase flow (water-air) in the adiabatic horizontal pipe with smooth divergence were numerically studied. The commercial software, FLUENT Were employed for the modeling. The numerical results were validated and compared with the experimental results, which were previously obtained. In this study, the coalescence between the bubbles was neglected and the diameter of the bubbles was assumed constant. For numerical simulation of the two-phase flow, RSM turbulence model was selected because this model gave results were closer to the experimental results. This study showed that numerical simulation provides well agreement with the experimental results .it was also showed that Experimental and numerical profiles for local void fraction downstream the expansion are similar and Approaching each other as the flow progresses.

Kumer (2014) [17] Performed numerically simulation for water oil two-phase stratified flow in the horizontal and inclined pipes by using the volume of fraction (VOF) approach and RNG k-ε turbulence model. The angle of inclination had been ranged from ±50, 00, ±100 from the horizontal. Selected models have successfully predicted the flow pattern, local phase fraction, slip ratio, pressure drop, turbulent kinetic energy and turbulent energy dissipation rate.

Ahmadpour et al. (2015) [18] two-phase flows (air-water) were simulated in a smooth gradual divergence with three different of area ratio (0.43, 0.5, and 0.65) and five different of opening angle (5, 15, 30, 45, and 90). A turbulence model k-Ɛ was employed. The influence of Reynolds number, volumetric fraction and divergent angle on pressure profile was studied. This study showed that increasing the volumetric fraction at the entrance

and the Reynolds number of the liquid increases the recovery of pressure, while the recovery pressure decreases with increasing the area ratio and increasing the opening angle. Secondary recirculating flow with high turbulent intensity was observed for high divergent angles of the expansion due to flow separation.

2.3. Experimental Studies

Aloui and Souhar (1996) [19] experimentally investigated bubble flow in a horizontal Rectangular sudden enlargement, cross sections of upstream and downstream of the enlargement was 55 x 44 mm and 5 x 100 mm, respectively. The void fraction and the pressure of downstream of the enlargement for a semi-symmetric bubble flow were studied. The results showed that when volumetric qualities were low, the bubble flow became asymmetrical but when the void fractions more about 10%, the bubble flow became practically symmetrical. It was also observed that the highest void fraction was in the recirculation region, the local void fraction reduced gradually when one moves farther from the singularity along the axis of the enlargement in the main flow.

Xu (1999) [20] experimentally investigated an adiabatic co-current two-phase flow of water and air in vertical rectangular conduits. A test section was used with dimensions 12 mm in widths, 260 mm in lengths, by using different gaps of 0.3, 0.6 and 1 mm. Video camera was used to observe flow patterns. They found that The flow pattern in the conduits with the gaps of 1.0 and 0.6 mm were correspondent to those achieved in conduits with medium dimensions, and involved of bubbly, slug, churn and annular flow while the conduit with the gap of 0.3 mm, the flow configurations were different from the typical flow configurations in conduits with medium dimensions and in the conduits with the gaps of 0.6 and 1 mm and Bubbly flow was never detected even at very low gas flow velocity,

Ahmed et al. (2008) [21] experimentally studied characterize the development of two-phase flow (air-oil) before of a abrupt enlargements. In this experiment, the superficial the velocities used for the air and the oil ranged (0.136 3.75 m/s) and (0.02 – 0.756m/s) respectively. The results showed that as the flow about the sudden enlargement, the void fraction increased. In addition, it increased strongly across the enlargement; it then reduced to an about fixed value in the fully developed area. The reason for the sudden rise in a void fraction at the enlargement section is due to the separation of gas in the recirculation region.

Rogero (2009) [4] Performed an experimental investigation of the development of intermittent flows in horizontal tubes in order to attain a thorough physical understanding of the internal configuration of two-phase flow regimes. The differences between the slug and the plug flow were explained and effect of slug void fraction on the flow characteristics and the behavior of the dispersed bubbles in the slug body were examined.

Takashi et al. (2010) [22] studied the influence of a sudden enlargement on the flow pattern of two-phase flow (air-water) in rectangular a millimeter-scale channel. Four of different heights (0.19, 0.5, 1and 2mm) were used and the expansion ratio was 5, 2.5, 1.67 and 1.25 for every height. The superficial velocities of water were between 10.0 cm/s to 80.0 and superficial velocities of air were between 5.0 cm/s to 80.0 cm/. ` The flow regimes were classified generally into the following four types:

(1) The flow regime was not affected by a sudden enlargement. Bubbly, slug, annular flows were involved in this type. This type often occurs in small expansion ratios.

(2) The recycling area appeared immediately after the sudden enlargement. The recirculation zone was observed at high expansion ratios for h=2.00 mm, 1.00 mm and 0.50 mm at high expansion ratios

(3) The configuration of the air cavity after the sudden enlargement and a water jet enter through it. This type occurred in low water flow rate, high air discharge, and a high expansion ratio.

(4) A split occurs for each bubble toward sideways direction immediately after the sudden enlargement. This type was observed in the small channel height at h=0.19 mm.

Ansari and Arzandi (2012) [3] experimentally studied the two-phase flow (air-water) using ribbed and smooth horizontal rectangular channels to illustration the influence of ribs height on the regime boundaries, as The flow map was studied. Three ribs with heights (1, 2, and 4 mm) were used; the rib pitch and width was 50 mm and pitch 10 mm respectively. The ribs were located in the channel at three different locations: the lowest wall, the upper wall and both the lowest and upper wall. They found that position of the ribs in the channel did not influence the type of the flow regimes; however, the regime boundaries were much different. Where the boundary was shifted to lower gas velocities due to the presence of the ribs. It was concluded that the effect of the ribs when were positioned on both the lowest and upper wall was more clear than in other cases. As well was observed that increasing of the rib height started hydrodynamical instability at lower fluid velocities.

Eskin and Deniz (2012) [23] investigated experimentally the pressure drop of two-phase flow (water-air) in adiabatic Horizontal channel with smooth divergence. The smaller and larger tube diameters were 40 mm and 50 mm respectively. Flow rates of air were 30, 50 and 60 l/min while the flow rate of air was constant at 3 l/s. Measurements of the pressure were carried out at four regions: injector, upstream, expansion section and downstream pipes. In order to obtain a two-phase flow, the injector was used to inject the air into the water. Two injectors with different distribution holes were

used: an in-line injector and circular injector. In-line injector consists of 32 holes with 1 mm diameter placed on three horizontal bars while the circular injector consists of 16 holes with a diameter of 2 mm. this study showed that when the in-line injector was used, the pressure recovery caused by expansion was higher.

Anupriya and Jayanti (2014) [24] investigated vertical two-phase flow (air-water) in progressive and sudden enlargement. The divergence angles for progressive enlargement were used with 8 and 15 degrees. The area ratios were 1.5 and 2.0, a range of water and air flows rate was used so that the annular flow was predominant in the upstream section. The study showed that pressure recovery was strong at downstream of the expansion in all cases. Recovery pressure was significantly delayed if air flow rates are much lower than those Required to form an annular flow.

2.4. Experimental and Theoretical Studies

Brnkovic and Currie (1996) [25] experimentally and numerical (CFD) studied the bubbly flow through a sudden tube expansion. This study was the first attempt to perform a numerical simulation of a bubble flow through an expansion section. The experimental and numerical results for mean velocity were compared. For the experimental study, a Laser Doppler Anemometry was used to measure the bubble and liquid velocity .while for numerical study, the Lagrangian formulation was used to predict the bubble motion in the liquid flow and a Navier –Stokes equations for the liquid phase flow. The results show that the agreement of mean velocity was excellent between experimental and numerical results downstream. However, the agreement was not good near the entrance of the separation area.

Abdelall et al. (2005) [26] experimentally investigated the pressure changes caused by sudden enlargement of mini-channels. The testing were

carried out with deionized water and air. The smaller and larger tubes were 0.84 and 1.6 mm in inner diameters, respectively. The two-phase flow pressure variations produced by enlargement were significantly lesser than the estimates of the homogeneous flow model and showed a significant velocity slip at the nearness of the enlarged section. The closest acceptability obtained between experimental and theoretical results was found at the assumption of the slip ratio of S= (QL/QG) 1/3

Ahmed et al. (2007) [27] a general formula for the pressure recovery of two-phase flow through a sudden enlargement were developed.in this formula, the losses in the recirculation zone, wall shear stress and flow regime changes (void fraction) were considered. The two-phase flow was achieved by using air-oil for three different area ratios of 0.0625, 0.25 and 0.444. It was observed that this formula improved prediction of the pressure recovery because this formula took into account all relevant parameters. It was also observed that it gives a good prediction for the flow pattern map of Taitel and Dukler (1976) in the fully developed regions for upstream and downstream.

Ara (2007) [28] experimentally studied the effect of mixing ratio between the gas and the liquid in two-phase flow in a horizontal tube with and without rotating disk which makes the flow eddying. The water was used as a liquid phase and the air as the gas phase. The tube was made of glass to observe flow patterns. The experimental and theoretical results were compared. The results showed that different flow patterns could be obtained by changing the mixing ratio. It also showed that increasing of the pressure drop by 40%-60% in case of rotating disk was used. The comparison between the experimental and theoretical results showed that cannot be obtained actual results by using theoretical correlation in the two-phase flow because there is no exact mathematical correlation.

Chen et al. (2007) [29] experimentally investigated of characteristics of the two-phase flow (water-air) across the sudden enlargement. The inlet circular conduit with 3 mm diameter was used while dimensions of enlargement 3 mm by 9 mm or 3mm by 6mm. The experimental pressure change was compared with surviving correlations. But none of them gives good acceptability of this work. Amongst them, the Wadle's correlation [30] achieves the further suitable estimate for the measured data. With some adjustment of the empirical constant K of the Wadle's correlation.

Frank et al. (2007) [31] presented A new method to purpose study the two-phase flow around a half-moon obstacle in a vertical tube that gives detailed three-dimensional information for validating of the CFX code for the complicated shapes. The CFD simulation has been compared to the three-dimensional air volume fraction and water velocity fields, which were gotten from the wire—mesh sensor data, the comparison demonstrated that the agreement was very good. Therefore, CFD code validation on this type of complex three-dimensional flow shapes allows the estimation of flow solver accuracy for industrial applications

Li et al. (2008) [32] investigated super cavitation around a hydrofoil. It was demonstrated that the cavitation structure depends on the collaboration of the vapor– water mixture and the vapor among the entire super cavitation stage. While the cavitation number was gradually dropped, three super cavitating flow types were detected: (a) fluctuating cavity with frequent eddies shedding (b) water–vapor and vapor exist in the cavity with a turbulent wake (c), a cavity a great extent loaded with vapor and with a two-phase tail and clear phase boundaries in the wake region.

Kourakos et al. (2009) [33] investigated horizontal two-phase flow (air-water) in progressive and sudden enlargement. In this work, the static pressure development was measured and flow regimes visualization was

carried out. Compared to the previous survey, a deviation from Chisholm ’s model [34] and with Jannsen’s model [35] was 10% and 5% for axisymmetric sudden enlargement. For progressive enlargement, the greatest pressure recovery was in the case of the smallest the opening angle (at same surface area ratio). The lowest pressure recovery happened for sudden enlargement geometry at the same flow conditions.

Abadie et al. (2012) [36] the results showed that when the flow rate ratio of liquid and gas increases, the length of the slug and bubble increases. A numerical study of the hydrodynamic properties of the two-phase flow in the channel and small tubes was also carried out.

Al-Turaihi and Jaafer (2013) [37] experimentally and numerically studied the two-phase flow (air-water) around multi-shapes obstacles (circular cylinder, square cylinder, and triangular cylinder) through the rectangular duct. For the numerical simulation, the Eulerian multiphase model was employed and the turbulent model K-Ɛ standard was used. This study was aimed to study the pressure difference and flow behavior. The flow rate of the air was (10, 20, 30 and 40 l/min), while the flow rate of the water was (20, 25, 35 and 45 l/min). It was observed that the pressure difference increased with increasing the flow rate of water or air. It was also observed that high turbulence was appeared with increasing of air flow rate.

Noora (2013) [38] experimentally and theoretically studied the two-phase flow (water-air) through the vertical pipe with an internal diameter and length of 0.0254 m and 3.65 m respectively. Certain ranges of velocities were employed, In order to obtain bubble, slug and annular flow patterns. The superficial velocity value of water was ranged from0.0986m/s to 0.968 m/. While the air superficial velocity was ranged from 0.197m /s to 14.25 m /s., the experimental study was aimed to investigate the flow patterns by

using a camera and measured the pressure at five locations by using pressure sensors. The experimental results showed that for bubble and slug flow, pressure gradient and pressure drop were proportional with the superficial velocity of water and inversely with the superficial velocity of air. While for annular flow, pressure gradient and pressure drop are directly proportional with the superficial velocity of air and water. The experimental results were compared with several theoretical correlations and observed that the correlation of Lockhart and Martinelli[39] was the closest to the results of the pressure drop for the bubble flow. While Steinhagen and Heck correlation [40] gave a good prediction of the results of slug and annular flow.

2.5. The scope of This Work

Two-phase flow characteristics have been studied in different ways as presented in this chapter. The pressure profile and pressure drop were studied by measuring them directly using devices such as a pressure transducer or theoretically using a mathematical model or CFD models. Other characteristics such as the two-phase flow behavior were studied mostly theoretically. Most of the materials used by other researchers were water and air.

In this work, two-phase flow in ribbed divergent rectangular ducts was studied and the working fluid used was air and water. The experimental test channel was photographed to show the flow behavior. The results were compared with the results found by a CFD model. The pressure was measured from the test channel experimental rig using four pressure sensors at four different points along the test channel and the values were compared with the pressure values of a CFD model that was modeled with the experimental boundary conditions.

2.6. Relation of Present Work with the Previous Survey

After reviewing the previous research, it was noticed that there is no comprehensive study of the effect of the ribs in the two-phase flow.Therefore; the present work is aimed to study the effect the addition of ribs in the divergence\contraction section and study the behavior of the flow

2.7. Summary

The literature presented in this chapter are brief in Table (2.1)

Table (2.1): Summary for the Previous Literature

Author(s), Year	Subject	finding
Behzadi et al 2004	Theoretical study for two-phase flow at high volume fractions	the new model gives improvements of prediction better than the old model
Cheng el at 2008	a comprehensive review of flow patterns and flow maps	the conclusions which obtained from different researchers were not corresponding
Uchiyama and Degawa2008	two-dimensional simulation of bubbly flow around a hydrofoil	simulated distributions of pressure and air volume fraction were agreed good
Naji 2009	presented correlation for inclined stratified flow	The correlation was semi-correspondence with correlation by Taitel-Dukler model

Hameed et al 2009	Study of the influence of obstacle in horizontal flow.	the drop pressure increased with increasing the size of the obstruction
Zhu et al 2009	a numerical study of the effect of hydrofoil	The angle of attack was clearer at the angle of 20 instead of 10 degree.
Deniz and Eskin 2012	Numerically study for flow in smooth divergence horizontal.	the experimental and numerical profiles for local void fraction downstream the divergence are similar
Kumar 2014	numerically simulation for water oil in the horizontal and inclined pipes	Low Reynolds number flow becomes stratified at all inclinations (±50, 0, ±100).
Ahmadpour et al 2015	numerically simulated flow through a smooth gradual divergence	increasing the volumetric quality increases the recovery of pressure,
Aloui and Souhar 1996	An experimental study for flow in of horizontal channel	the highest void fraction was in the recirculation region
Xu 1999	An experimental study for flow in mini vertical rectangular channels	The bubbly flow was never detected at a very low gas velocity
Ahmed et al 2008	Experimental study of (air-oil) downstream in sudden enlargements	As the flow approached the sudden enlargement, the void fraction increased.
Rogero 2009	Experimental study	Explained effect of slug void

	flow in horizontal tubes.	fraction on the flow characteristics
Takashi et al 2010	Experimental Study for flow in rectangular a millimeter-scale sudden divergence channel	There was no influence of an abrupt divergence on the flow pattern when the expansion ratio was close to unity.
Ansari and Arzandi 2012	An experimental study for flow in smooth and ribbed horizontal rectangular ducts.	The ribs effect of regime boundaries
Deniz and Eskin 2012	An experimental study for flow in horizontal smooth expansion channel.	Influence of volumetric void fraction on pressure drop at the injector was more than the other regions
Anupriya and Jayanti 2014	Experimentally study of vertical gradual and sudden divergence.	The pressure recovery was strong at downstream of the divergence in all cases
Brnkovic and Currie 1996	experimentally and numerically for sudden divergence tube	The agreement of mean velocity was excellent between experimental and numerical results.
Abdelall et al 2005	Experimental and theoretical study for flow in sudden divergence mini channels	The slip ratio of $S=(QL/QG)^{1/3}$ given closest acceptability between experimental and theoretical

		results
Ahmed et al 2007	Experimental and theoretical study for flow in a sudden divergence.	A new formula improved prediction of the pressure recovery.
Ara and Khilkhal 2007	Experimental and theoretical study for flow in a horizontal tube with and without rotating disk	Increasing of the pressure drop by 40%-60% in case of rotating disk was used.
Chen et al 2007	Experimental and theoretical study for flow in sudden divergence channel.	A new liquid-jet flow regime for the very low-quality region.
Frank et al 2007	Experimentally and numerically, study of flow around a half-moon obstacle in a vertical tube.	The numerical and experimental results were in good agreement.
Li et al 2008	Experimentally and numerically, study for cavitation around a hydrofoil.	Found three super cavitating flow types.
Kourakos et al 2009	Experimental and theoretical study for flow in gradual and sudden divergence channel.	The greatest pressure recovery was in the case of the smallest the opening angle.

Abadie et el 2012	Experimentally and numerically for flow in microchannels.	When the flow rate ratio of liquid and gas increases, the length of the slug and bubble increases.
Al-Turaihi and Jaafer 2013	Experimental and numerical study for flow around multi-shapes obstacles in a rectangular channel.	When the discharge of air or water increases, great turbulence was appearing.
Noora and Adil 2013	Experimentally and theoretically, study for flow in the vertical pipe.	For annular flow, the pressure drop is directly proportional with the superficial velocity of air and water.
Present work	Experimental and numerical study for flow in ribs divergent/convergent vertical and inclined duct	

CHAPTER THREE

NUMERICAL ANALYSIS

Numerical Analysis

3.1. Introduction

Ansys FLUENT 18.0 is used in this work to simulate and analyze the flow characteristics of two-phase flow (water-air) through the test channel. The effect of water and air discharge and opening angle on the pressure profile and difference pressure are studied, As air volume fraction simulation of the two-phase flow was also performed. To understand such a system, computational fluid dynamics can be used which is an effective tool in predicting the behavior of the flow. The simulation is run down similar conditions in the experiments .Solution by CFD problem divides to four parts; Physical model geometry, Mesh Generated, Set- up physical model, solve it and post processing the computed data [41]. In ANSYS FLUENT 18, the Euler-Euler models of multiphase are classified into three models: (VOF), mixture, and Eulerian. In the present work, two-phase flow through ribs divergent/convergent rectangular duct were modeled using VOF model with several parameters depending on variables of experiments and results experiments for comparison with results CFD.

3.2. Geometry Model

3.2.1. The Geometry

The software SOLIDWORKS 2013 is used to draw and construct the geometry of test section as a 3D, by drawing the front view of test channel on the X-Y plane. then, the extrude cut order was given for geometry to obtain the 3D structure. A circle with diameter 0.00126 m was drawn inside a rectangle in the bottom surface of the structure .so that circle represents entry of air into the test channel and the remaining area represents the entry of water, as shown in Figure (3.1). All sides of the structure were set to be adiabatic walls. The lowest surface of test channel was drawn so represents entry of air and water into the test section, while

the top surface represents outlet flow. The geometry (surface body) was fixed as fluid.

Description of two-phase flow geometry can be observed from the figure (3.2 a) to (3.2 l) of test channel for all cases.

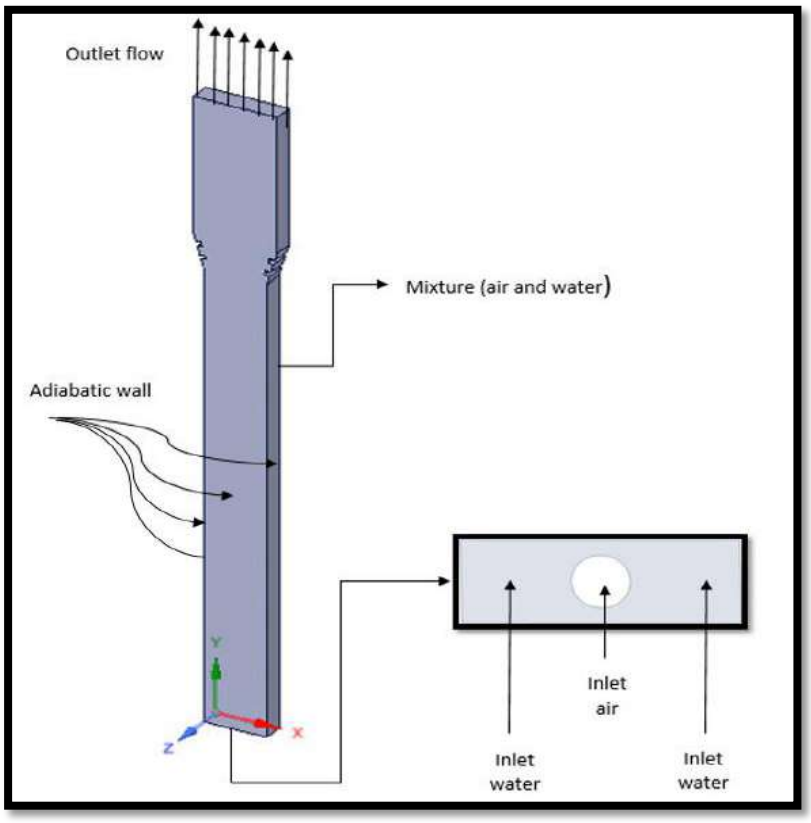

Figure (3.1): Problem Description

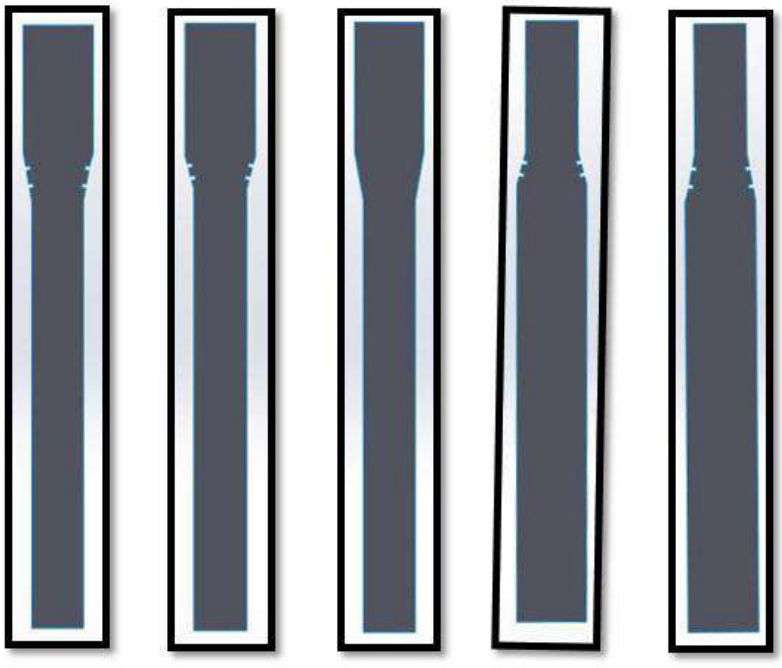

(a) (b) (c) (d) (e)

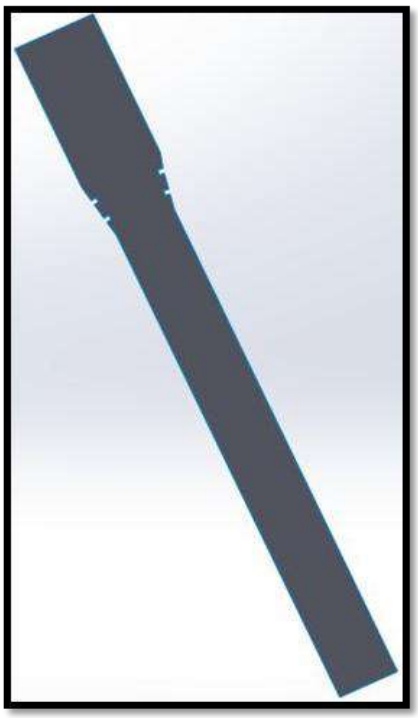

(f)

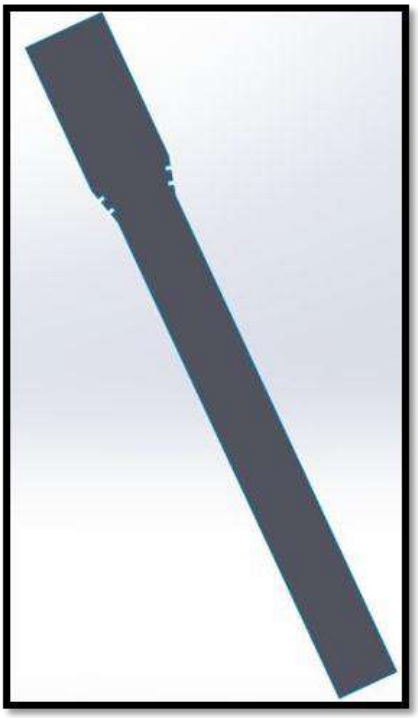

(g)

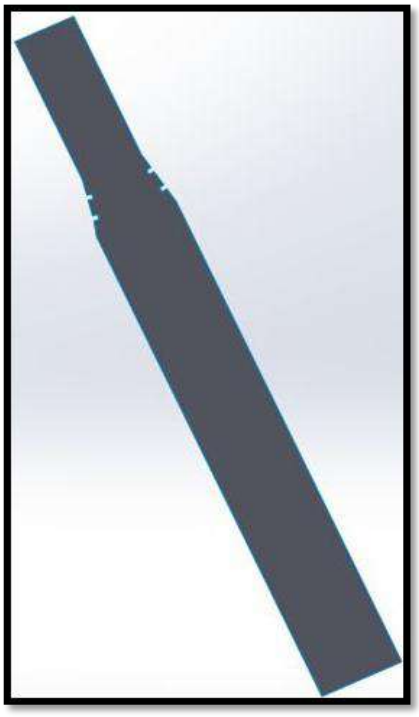

(k)

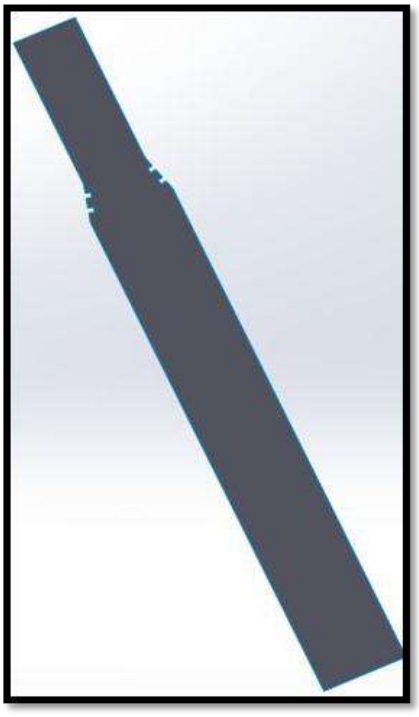

(l)

Figure (3.2): Geometry of test channel for all cases

3.2.2. The Mesh

After sketching the geometry, many attempts were made using the ANSYS meshing to mesh the domain. There are so many types of meshes, choosing the type of mesh depends on parameters such as flow field, geometry, and complexity. The size and type of mesh have a main important on the CPU (center processing unit) time requisite, accuracy of solution, and convergence rate [42]. In this work, a geometries of the test pipe were divided into element as A Quadrilateral grid type was chosen by employed ANSYS workbench 18, bigger and lesser size of elements was (1mm). The numbers of elements and nodes as shown in Table (3.1). Figures from (3.3a) and (3.3b) show the mesh of the two-phase flow in divergence section with 10 and 15 degrees, respectively.

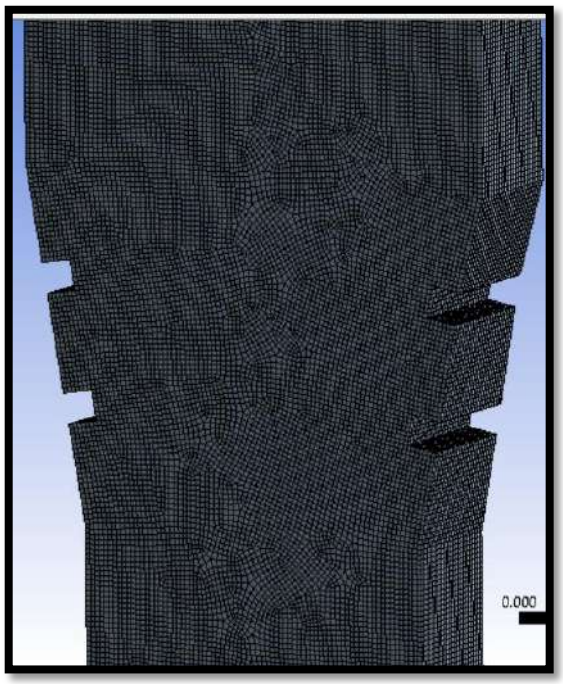

Figure (3.3a): The mesh of divergence with 10

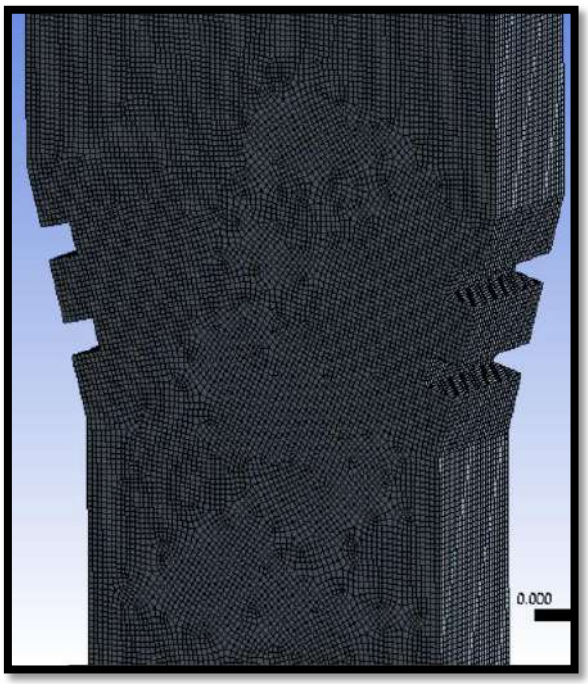

Figure (3.3b): The mesh of divergence with 15

cases	Nodes No.	Elements No.

Table (3.1): The number of elements and nodes used in mesh independent study

without ribs		
Diverge vertical 15 degree	1013502	949600
Diverge inclined 10 degree	1044162	978420
Diverge inclined 15 degree	1013502	949600
Converge vertical 10 degree	1080912	1013420
Converge vertical 15 degree	1042902	977600
Converge inclined 10 degree	1080912	1013420
Converge inclined 15 degree	1042902	977600

3.3. The Boundary Condition

The fluids that used in this study are water and air designed as the primary and secondary phase, respectively. Boundary condition used for this model are explained as follows:

3.3.1. Inlet B.C.

The used inlet boundary condition was the superficial velocity of the air and the water entering the test channel from the lowest surface of the channel, which was taken from the experimental work. With values (0.0777-0.3108 m/s) and (0.761-2.1756m/s), respectively.

3.3.2. Wall B.C.

All the portion of the channel wall was set to be an adiabatic wall

3.3.3. Outlet B.C.

The upper surface of the channel represented the exit of it and to be set as outlet flow. The under relaxation factors are see in Table (3. 2).

Table (3.2): Model Relaxation

Variable	Relaxation Factor
Pressure	0.3
momentum	0. 5
Volume Fraction	0.5
Energy	0.1

3.4. Problem Assumption

Due to simulate the flow in duct in geometry model, the following assumptions are made as turbulent flow, planer, three-dimensional space, unsteady flow, pressure-based solver, incompressible flow ,(-9.81 m/s^2) gravity in Y-direction .

3.5. Properties of Two-Phase

The properties of working fluid of two-phase flow are shown in Table (3.3)

Table (3.3): Properties Two-phase

Property at temperature (19-23) c°	**Water (Ansys Fluent 18.0 Database)**	**Air (Ansys Fluent 18.0 Database)**
Density (kg/m^3)	998.49-997.63	1.204-1.194
Viscosity (kg/m.s)	0.001028-0.000933	1.825e-05 – 1.873e-05

3.6. Simulation Model

Eulerian-Eulerian multiphase model was used with a volume of the fluid model where the viscous model was RNG k-epsilon (ε), to simulate the two-phase flow in the test channel. Monitoring a high amount of bubbles in the flow field was the way to solve the dispersed phase; it also exchanged the mass and momentum among phases [43].

3.7. Governing Equation

The volume of Fluid model solves the volume fraction and conservation of momentum equations for each phase. This model is more suitable and accurate for present work. Value the domain is modeled as 3-D, according to boundary conditions of mixture internal flow and by pressure -based solver calculated a solution. The momentum equation is solved by depending on variables such as phases volume fractions, and properties: density (ρ), and viscosity (μ) [44].

1. The Volume Fraction Equation

The evolution of the q-th fluid in a system on (n) fluids is governed by the transport equation

$$\frac{\partial \alpha_q}{\partial t} + \overrightarrow{v} \cdot \nabla \alpha_q = \frac{S_{\alpha_q}}{\rho_q} \qquad \text{..... (3-1)}$$

With the following constraint

$$\sum_{q=1}^{n} \alpha_q = 1 \qquad \text{..... (3-2)}$$

In each cell, the properties of the mixture like mixture density and dynamic viscosity are depended on the volume fraction of all phases as given by equation (3.3).

$$\rho = \sum \alpha_n \rho_n \; ; \; \mu = \frac{\sum \alpha_n \rho_n \mu_n}{\sum \alpha_n \rho_n} \qquad \text{..... (3-3)}$$

2. The Momentum Equation

One momentum equation is resolved everywhere the field, and the velocity field is participated between the phases. The momentum equation is based on the volume fractions of every phases out of the properties: density (ρ) and dynamic viscosity (μ)

$$\frac{\partial}{\partial t}(\rho\vec{v}) + \nabla\cdot(\rho\vec{v}\vec{v}) = -\nabla p + \nabla\cdot[\mu(\nabla\vec{v} + \nabla\vec{v}^{T})] + \rho\vec{g} + \vec{F} \quad \ldots\ldots (3\text{-}4)$$

Where $\vec{v}$ is velocity field and $\vec{F}$ is a body force.

3.8. Turbulence Model

In this work, the turbulence RNG mixture model was used to simulate the two-phase flow, which is used with swirl flow. The two-equation for RNG model, first equation for kinetic energy, k (3.5), and second for dissipation, ϵ (3.6), which is the rate of dissipation of k

$$\frac{\partial}{\partial t}(\rho_m K) + \nabla\cdot(\rho_m\vec{V}_m K) = \nabla\cdot\left(\frac{\mu_{t.m}}{\sigma K}\nabla K\right) + G_{K.m} - \rho_m \in \quad \ldots\ldots\ldots (3\text{-}5)$$

$$\frac{\partial}{\partial t}(\rho_m \epsilon) + \nabla\cdot(\rho_m\vec{V}_m\epsilon) = \nabla\cdot\left(\frac{\mu_{t.m}}{\sigma\epsilon}\nabla\epsilon\right) + \frac{\epsilon}{K}(C_{1\epsilon}G_{K.m} - C_{2\epsilon}\rho_m \in \quad \ldots (3\text{-}6)$$

Where k is turbulent kinetic energy, $\in$ is rate of turbulent dissipation, G is energy, σ and is number of turbulent Prandtl for K and $\in$.

The density and the velocity of the mixture can be found by using Eqs. (3.6) & (3.7), respectively.

$$\rho_m = \sum_{i=1}^{N}\alpha_i\rho_i \quad \ldots\ldots\ldots\ldots (3\text{-}٧)$$

$$\vec{v}_m = \frac{\sum_{i=1}^{N}\alpha_i\rho_i\vec{v}_i}{\sum_{i=1}^{N}\alpha_i\rho_i} \quad \ldots\ldots\ldots\ldots (3\text{-}٨)$$

As can be calculated turbulent viscosity ($\mu_{t,m}$) and kinetic energy ($G_{k,m)}$ of the mixture (air-water) from the equations (3.8) & (3.9), respectively.

$$\mu_{t,m} = \rho_m C_m \frac{k^2}{\epsilon} \quad \text{.. ..... (3-٩)}$$

$$G_{K.m} = \mu_{t.m} \left(\nabla \vec{V}_m + \left(\nabla \vec{V}_m \right)^T \right) : \vec{V}_m \quad \text{..... (3-١٠)}$$

The model constants is show in Table (3.4).

Table (3.4): Model Constants

Model constant	**Value**
C_m	0.09
$C_1 - \epsilon$	1.44
$C_2 - \varepsilon\epsilon$	1.92
σ_k	1
σ_ϵ	1.3

3.9. Simulation Steps

For two-phase flow modeling by using a dynamic computer fluid model, the following steps were implemented:

1- SOLIDWORK used to configuration the geometry.

2-ANSYS Workbench 18 used to generation mesh of two-phase field.

3- Choosing a model (VOF).

4- The definition of material.

5- Choosing phases and boundary conditions.

6- The solution initialization.

7- The solution was run with a maximum iteration (5000) and time step was 0.001 sec.

8- The results of the pressure and the air volume fraction were extracted.

3.10. Convergent Criteria

Every numerical basis solution contains errors. The key is to know how those errors are big and whether the numerical results are acceptable in the engineering applications. In the present numerical Convergence was accepted as being completed when the residual curve reached 10^{-4}. Table (3.5) shows the residual error.

Table (3.5): Residual error for the tested case.

Equations	**Continuity**	**X-Velocity**	**Y-Velocity**	**energy**	**k**	**E**	**Volume Fraction**
Residual Error	10^{-5}	10^{-4}	10^{-4}	10^{-6}	10^{-4}	10^{-4}	10^{-4}

CHAPTER FOUR

THE EXPERIMENTAL WORK

The Experimental Work

4.1. Introduction

A detailed description for experimental system to study two-phase flow in ribs divergent/convergent duct. It is configured in the fluid laboratory of the Mechanical Engineering Department in Babylon University. A schematic diagram for system is shown in Figure (4.1). There are a rigid frame to support the test pipe and prevent vibration in figure (4.2). All experiments are carried out at conditions of ambient laboratory (19-23) C^o and 1bar) temperature and pressure.

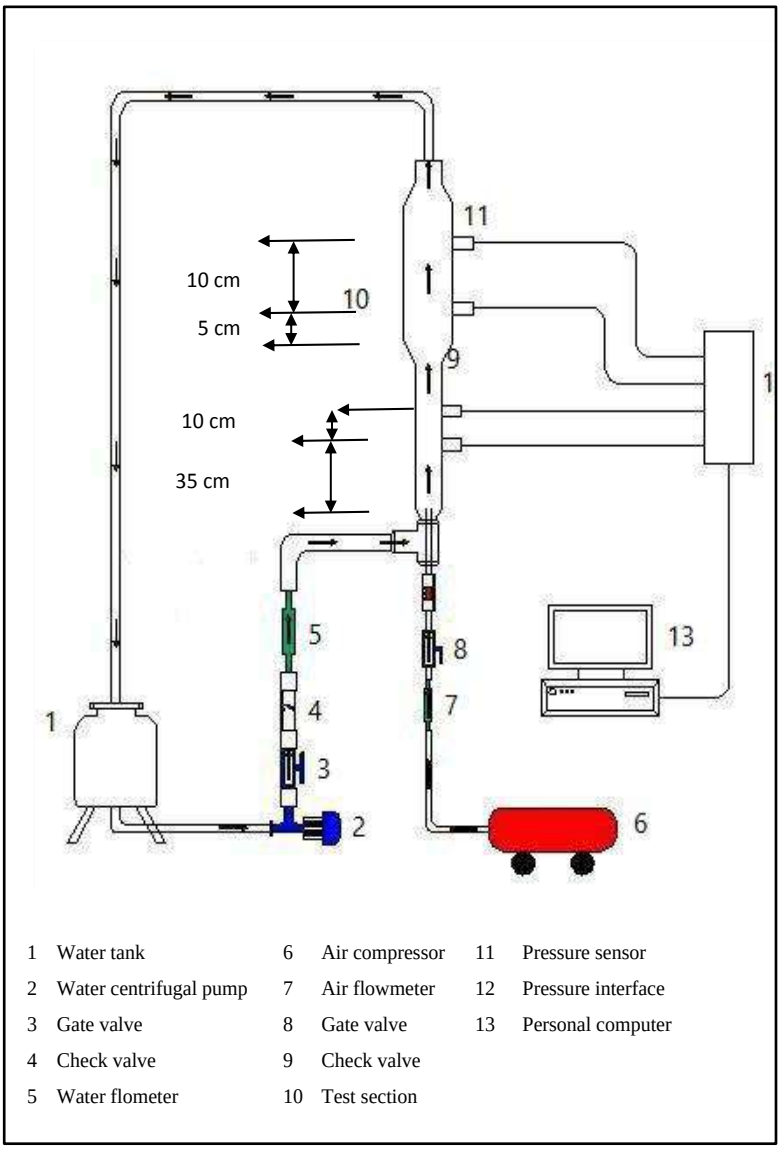

1	Water tank	6	Air compressor	11	Pressure sensor
2	Water centrifugal pump	7	Air flowmeter	12	Pressure interface
3	Gate valve	8	Gate valve	13	Personal computer
4	Check valve	9	Check valve		
5	Water flometer	10	Test section		

Figure (4.1): Schematic of Experimental system

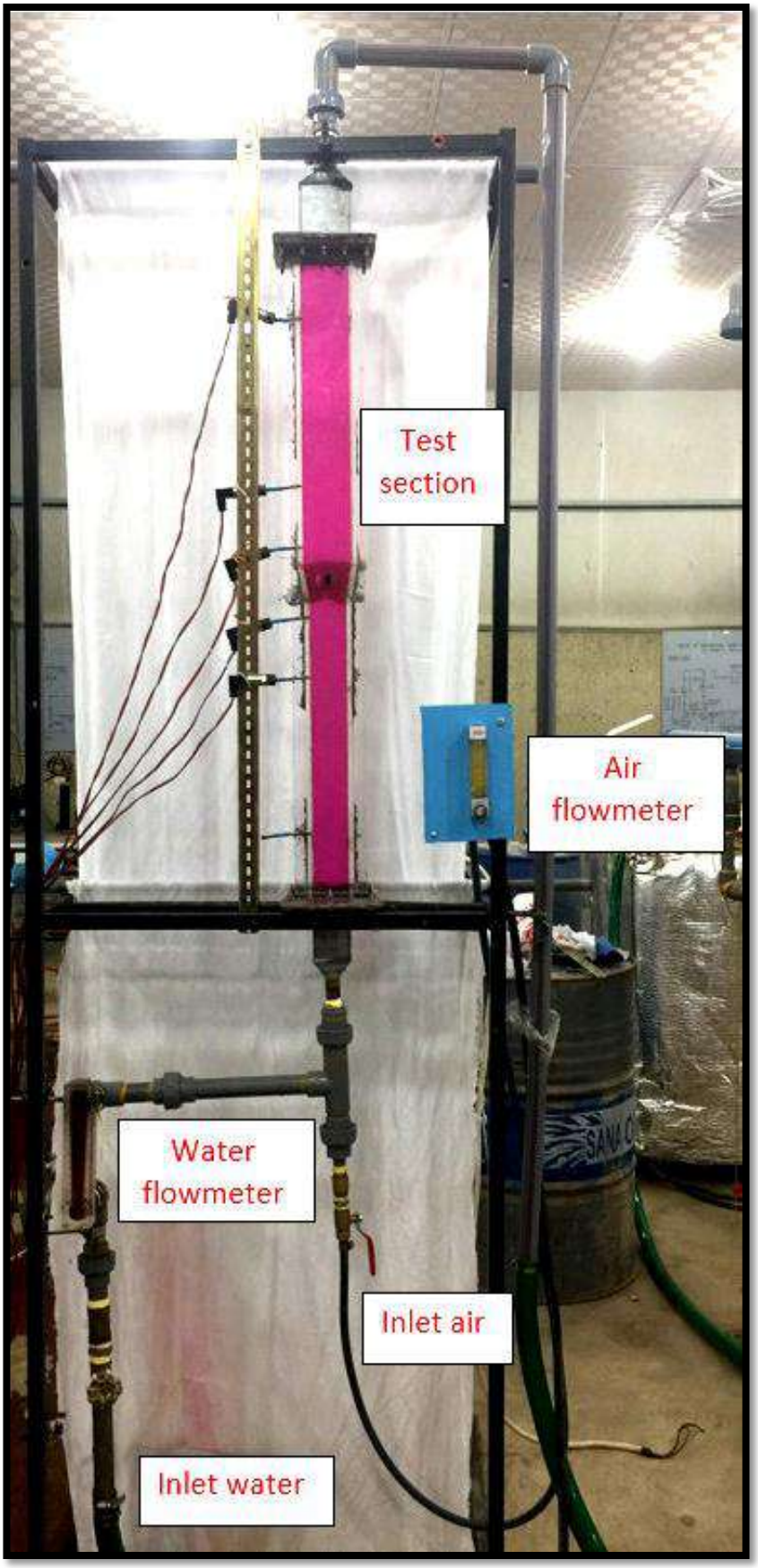

Figure (4.2): Experimental Rig for the two-phase flow

4.2. Two-Phase Flow Experiment Setup Components

The experimental rig, which utilized to do the experiment tests of the two-phase flow in a divergence/convergence rectangular channel comprises of the subsequent sections:

Water tank
Water centrifugal pump
Water flow meter
Air compressor
Reservoir
Air flow meter
Test section
Pressure sensors
Interface device
Personal computer
Normal video camera

4.2.1. Water tank

The water reservoir has a capacity of (500) litters, with dimension (1m x 1m x 0.5m). It made of stainless steel metal and covered with rock wool to keep the temperature of the water.

4.2.2. Water pump

A centrifugal pump utilized to provide water into the test. It is used because the case required a large discharge with a small head. The pump makes is Stream with specifications as Centrifugal type, model NO. SHFM5AM, quantities (5-480) L/min, head (5-20) m, Power (1.5 KW) and 1410 rpm.

4.2.3 Flow meter for water

A flow meter used to control and measure by Litters /minute water

quantity that entered into the test section. It has values of flow rate range from (5 to35) L/min. Figure (4.3) shows the water flow meter.

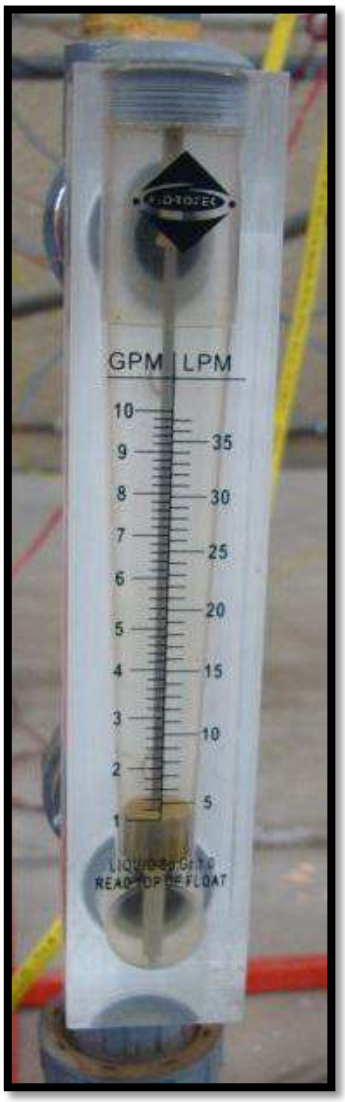

Figure (4.3): water flow meter

The water flow meter was calibrated by using a scaled container filled with the water coming out of the test pipe at a specific flow rate; the time for the water to reach a specific point on the container was recorded. This process was repeated for five times and the values are represented in a curve with the flow meter values as shown in figure (4.4).

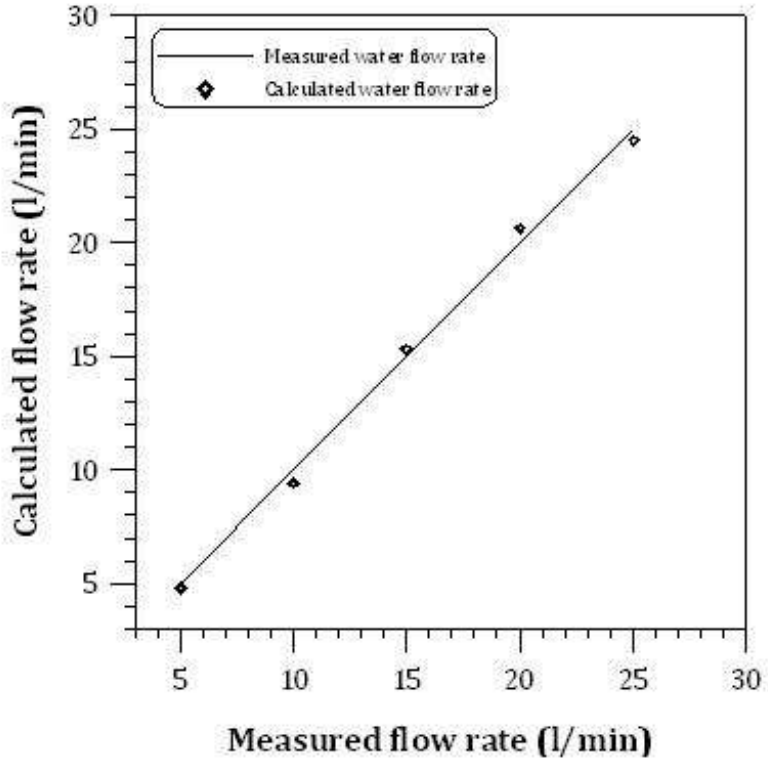

Figure (4.4): Calibration of the Water Flow Meter

4.2.4 Air Compressor

It used to raise the air pressure, which used as a gas in two-phase flow. It is designed by Ingersoll-Rand company type (WELDED AIR RECIVER –BS 5169 IIIE). This compressor is the type of a Positive displacement machine. It contains crankshaft that moves the piston for supplying gases at high pressure with a connecting rod

4.2.5 Air Flow Meter

It has a flow rate range from (350 to 3500) L/hr as shown in figure (4.5). It is utilized to governor the discharge of air that enters the test channel. A flow meter consists of a tube, made of a clear material with a float that is exerted by a drag force of the flow and gravity.

Figure (4.5): air flow meter

4.2.6. Test section

In this work, two test sections are used for opening angles 15 and 10 degrees. The cross-section area for each test sections was (2 * 6) cm before the divergence section with length were 0.5 m long, while the section area was (2 * 8) cm after the divergence section with length were 0.5 m too, as shown in figure (4.6). The test sections were manufactured of transparent glass with thickness is 1 cm. The expansion section of both test sections has four ribs, two ribs on each side with dimensions (0.5*0.5*2) cm as shown in figure (4.7). The test sections it consists of four holes in different locations, pressure sensors are fixed inside it, to measure the pressure of two-phase flow inside the channels.

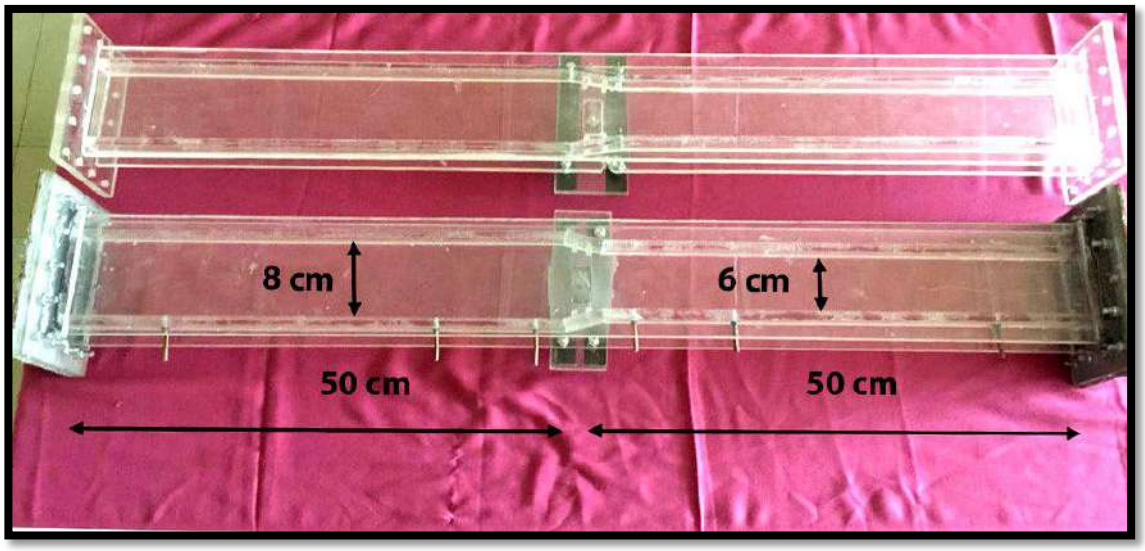

Figure (4.6): Test section

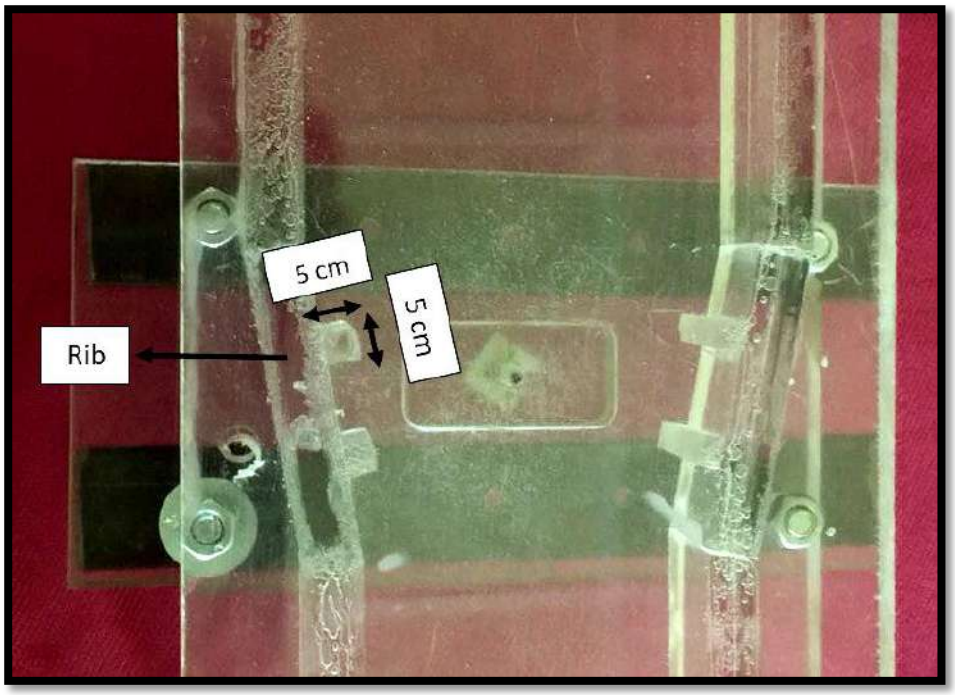

Figure(4.7): Ribs with dimensions

4.2.7. Pressure Sensors

There is four-pressure transducer sensors are mounted along the pipe to measure pressure with a range from 0 to 1 bar as shown in figure (4.8). The specifications pressure sensors as shown in Table (4.1).

Figure (4.8): a pressure sensor

Table (4.1): Specification of the pressure sensor

Operating pressure range	**(0 to 1) bar**
Sensor Output	Current (4 to 20 mA)
Hysteresis	0.5%
Body Material	Stainless Steel
Pressure Sensor Type	Piezo resistive Transmitter
Operating Temperature	(-20°C to +80°C)
External Diameter	17mm
External Length	Height = 76mm

A U-tube manometer was used to calibrate the pressure measuring system. The difference in the pressure between the first and the last tap was measured with the pressure sensor and with the manometer at the same time and for the same values of flow rate. The comparison between the values is shown in figure (4.9).

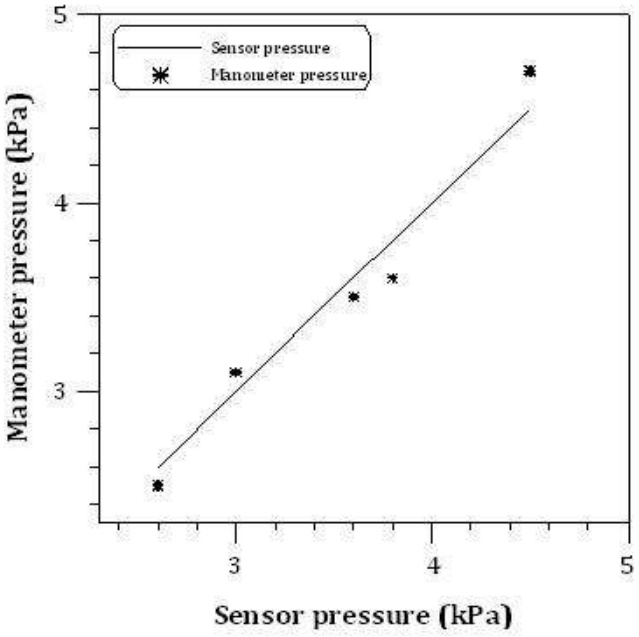

Figure (4.9): Calibration of the Pressure Sensor

4.2.8. Pressure Interface

An interface was used to connect the pressure sensor a personal computer, see figure (4.10). The voltage signal (analog) from a pressure sensor is converted to a digital signal via the interface that can be read through the DaLi08 program that is run on the PC. A universal data logger (UDL100) was used. It has high accuracy and resolution, the sampling period (750 ms), and channels isolation voltage of (400 volts). The data logger interface technical has specification shown in Table (4.2).

Figure (4.10): pressure interface

Table (4.2): Data logger Interface technical Specification

Supply Voltage	**5 V AC ± 5%**		
Environmental temperature	Operation range(-10 to 50)Cº		
	Storage range (-20 to 65) Cº		
Accuracy	±2%		
Weight	87gr		
Dimensions	Width:72m	Height:112m	Depth:26m
Power consumption	1W		

4.3. Cases of the study of experimental work

Two-test section was used with opening angles are 15 and 10 degrees as shown in figure (4.11). Each test section has been fixed in two positions: vertical position and an inclined position with an angle of 60 degrees with horizontal. Each position has been studied in the case of diverging and converge as a show of figure (4.12) to figure (4.19).

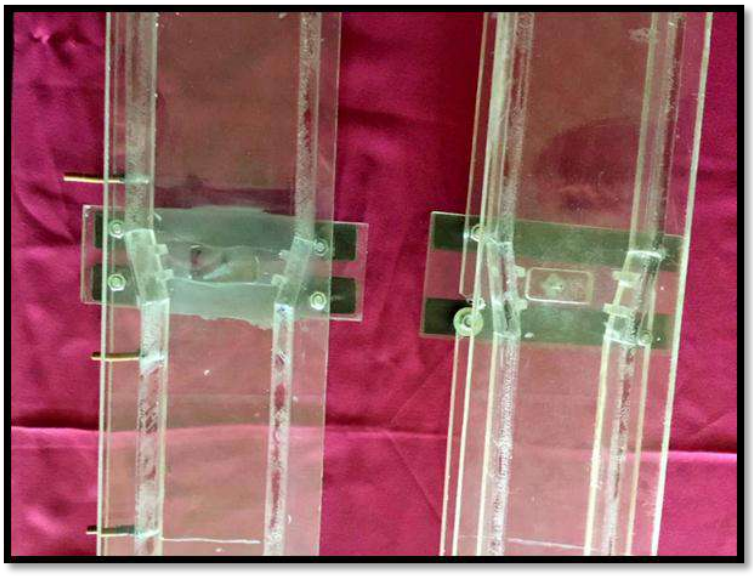

Figure (4.11): Divergence sections with different opening angle

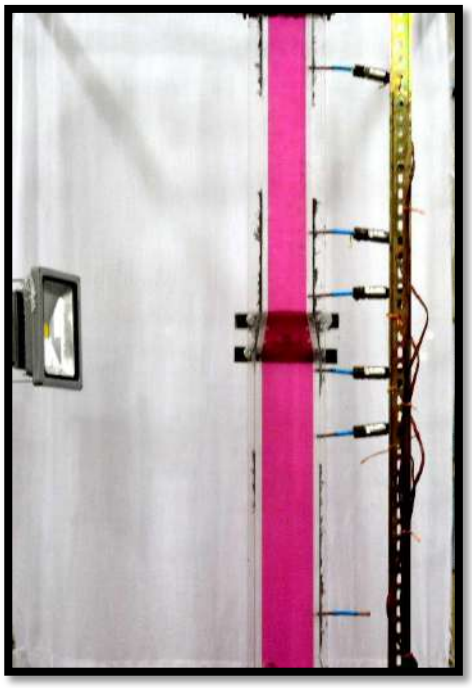

Figure (4.12) vertical converge

Test Section with angle 10

Figure (4.13) vertical diverge

test section with angle 10

Figure (4.14) vertical converge

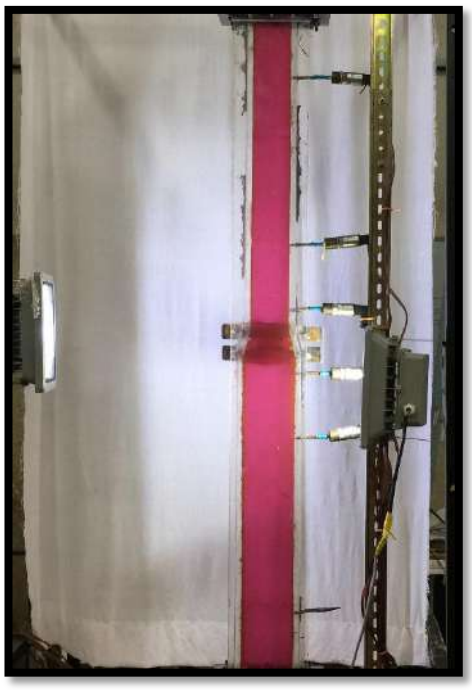

diverge

test Section with angle 15

Figure (4.15) vertical

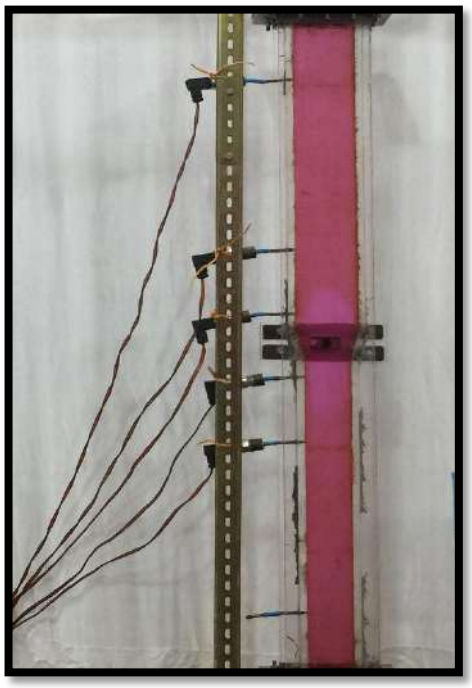

test section with angle 15

Figure(4.16)inclined converge test Section with angle 10

Figure(4.17)inclined diverge test section with angle 10

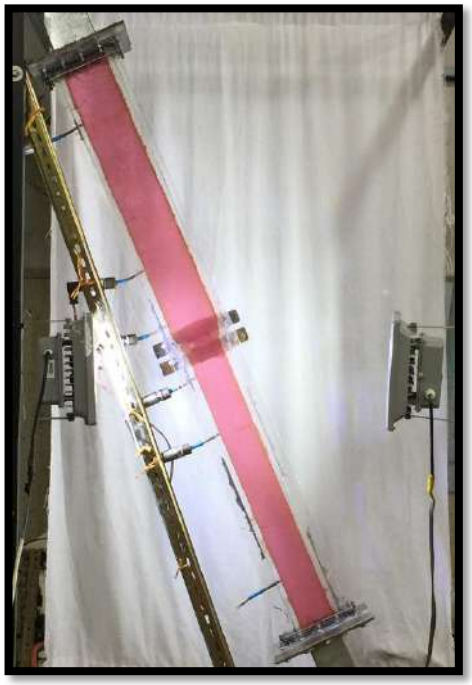

Figure(4.18)inclined converge test Section with angle 15

Figure(4.19)inclined diverge test section with angle 15

4.4. Phases Used in the Experimental Work

4.4.1. Continuous Phase

The continuous phase utilized for the experimental work was liquid water, at ambient conditions; it is pumped to the test channel from the tank by the water pump and regulated by water flow meter.

4.4.2. Dispersed Phase

The air was the dispersed phase at ambient conditions. The air is pumped by an air compressor and regulated by using an air flow meter and then mixed with water from the bottom of the test channel.

4.5. Experimental procedure

After building the system and installing all the measuring devices, the system was operated several once to ensure that there were no leak or any mistake in operating. In this work, One hundred and eighteen

experiments were performed. All the tests carried out by taken different amounts of discharge of water and different amounts of discharge of air, as shown in Table (4.3) and Table (4.4).

Run the water centrifugal pump to push the water from the water tank. Then the water valve was opened until the volume flow rate in the flow meter reached the first valve of the water flow rate

Turn on the air compressor and then air valve was opened until the volume rate in the flow meter reached the first value
The water and air mixture entered from the bottom of the test channel

The pressure begging measured by the pressure sensors, where it can be read through computer software. and image of the motion of two-phase flow was taken by the normal digital camera

5. Repeat above procedure with new discharges of water until to complete the entire water discharges.

Table (4.3): Values of work conditions used in experiments for diverge and converge vertical cases

Water discharge (L/min)	**Air discharge (L/min)**
5	5.833
10	8.333
15	10.833
20	13.333
	16.666

Table (4.4): Values of work conditions used in experiments for diverge and converge inclined cases

Water discharge (L/min)	Air discharge (L/min)
5	5.833
15	10.833
20	16.666

4.6. The Physics parameter of the Experiment work

4.6.1. Superficial Velocity

Superficial velocities were estimated for water and air to know the range of velocities which used. The discharge was read immediately from the flow meter and employed to compute the superficial velocity according to Eq. (4.1) [3], which gives the values as shown in Table (4.5).

$$Q = UA \quad \text{..... (4.1)}$$

Where

U = Liquid superficial velocity (m/s).

Q = discharge (m^3/s).

A = Cross-sectional area (m^2).

$$A_{air} = \pi/4 \ D^2_{pipe} \quad \text{..... (4.2)}$$

$$A_{water} = (w*h) - A_{air} \quad \text{..... (4.3)}$$

Where

w = width of the duct

h = height of the duct

Table (4.5): Superficial Velocities

Water flow rate (L/min)	**Water velocity Superficial (divergence case)(m/s)**	**Water velocity Superficial (convergence case) (m/s)**	**Air flow rate (L/min)**	**Air superficial velocity (m/s)**
5	0.0777	0.04448	5.833	0.761
10	0.1554	0.088968	8.333	1.088
15	0.2331	0.13335	10.833	1.414
20	0.3108	0.17792	13.333	1.7409
			16.666	2.1756

4.6.2. Mass flux (G)

Mass flux for water and air was calculated for the purpose of calculating the term ($\frac{G^2}{\rho}$) which using for drawing the flow map as shown in Table (4.6)

Table (4.6): Superficial Velocities

$\frac{G^2}{\rho}$ **air**	**Air flow rate (L/min)**	$\frac{G^2}{\rho}$ **water**	**Water flow rate (L/min)**
0.706	5.833	6.015	5
1.44	8.333	24.0447	10
2.4377	10.833	54.1439	15

3.6921	13.333	96	20
5.762	16.666		

4.6.3. Reynolds Number

Reynolds number can be found by the Eq. (4.4), which gives the values as shown in Table (4.7).

$$Re = \frac{\rho U D_h}{\mu} \quad \text{..... (4-4)}$$

Where (for water)

$$D_h = \frac{4A}{P} \quad \text{..... (4-5)}$$

Where

P is wetted perimeter = $\pi D_{pipe} + (w + h)$

Table (4.7): Reynolds Number

Q_{water} L/min	**Re_{water} (divergence case)**	**Re_{water} (convergence case)**	**Q_{air} L/min**	**Re_{air}**
5	1855	1181	5.833	661

10	3711	2362	8.333	945
15	5567	3540	10.833	1229
20	7423	4724	13.333	1513
			16.666	1891

4.7. Design Consideration

Considerations of this present study were depending on the previous study. Applications of two-phase flow are in chemical or mechanical engineering applications for that was selected two-phase water and air. The cross-section area of the duct and opening angle were chosen to depend on Ahmedpour 2016[19]. Where the hydraulic diameter equivalent of the circular pipe diameter, which used in the work of Ahmedpour 2016 was calculated. A wide range of water and air discharges were selected, only the values of the discharges which make the dominant flow are slug flow were selected. The discharge that makes the flow of a type of churn flow are not selected because high fluctuation occurs in the flow.

4.8. The error analysis

The error analysis is necessary for find out if the result is acceptable for its intentional aim and to achieve whether it is proportionate with other comparable results. A more precise method of error analysis in experimental results has been presented by Ronald and Richard 2011[45]. (Appendix A)

Results and Discussion

5.1. Introduction

Description the experimental results and the numerical results that extract from a system of two-phase flow (water and air) in ribs divergence/convergence rectangular duct. Comparison between experimental results and computational fluid dynamics results has been made in order to study and investigate the two-phase flow.

The effect of increasing water discharge from (5 L/min to 20 L/min), air discharge from (5.833 L/min to 16.666) for two opening angles (10, 15) degree on the pressure distribution and difference pressure were studied. The experimental and numerical pressure results were drawn together for comparing between them. Furthermore, the two-phase flow was recorded by video camera, converted it into a series of images, and compared with images for the corresponding contours, which found numerically.

5.2. Program validation

For verifying the numerical code , the calculated axial profile of pressure is compared with numerical results previously studied. By Ahmedpour 2016[19] for two-phase flow (water and air) through sudden and graduation smooth divergence rectangular vertical channel. The case was for $Re_L=1.8*10^5$, $\beta=20$ %, $\sigma=0.43$ and different opening divergence angle 90, 15 and 5 degrees as shown in figure (5.1). A good agreement is detected between the numerical results of pressure and numerical results of Ahmedpour 2016[9] with average percentage error was (12.8) %. Which validates the accuracy of the numerical code.

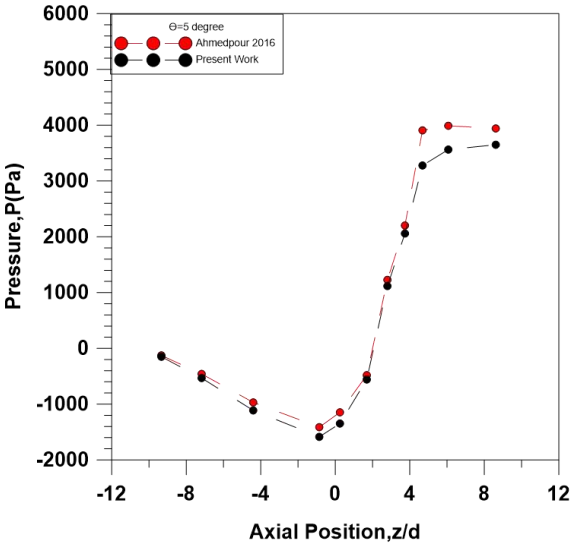

(a

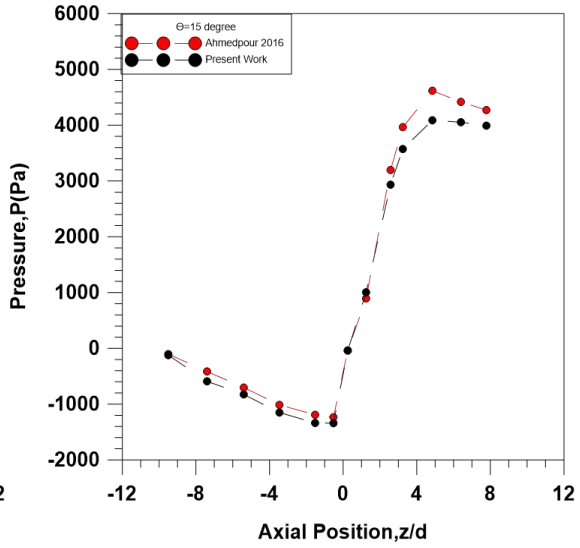

(b

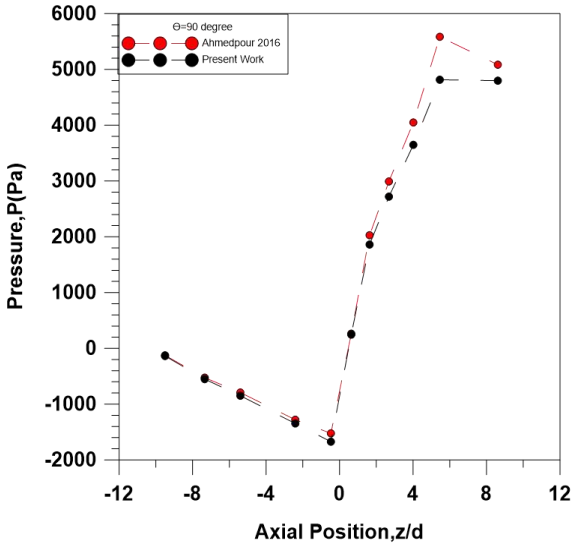

(c

Figure 5.1: The validation of numerical code with numerical results of Ahmedpour

5.3. Two-phase flow through divergence section for vertical and inclined position

5.3.1. Experimental results

5.3.1. A. Influence of water and air discharge on the pressure profile

Figure (5.2) to (5.5) show the effect of increasing water and air discharge on the experimental results of the pressure profile at four different points along the test channel. Note from these figures that the value of the pressure mixture is decreases as progress the flow. When the mixture reaches the divergence section, the pressure value begins to increase. At the upstream of the divergence section, the pressure value will decrease again. It can be seen that the pressure profile increased with increasing water or air discharge because to the volume of the test channel was constant, so any increase in the amount of water or air would increase the pressure over the walls of the channel.

Figure (5.2), offers the experimental results of the pressure profile for vertical test channel with opening angle 10 degrees, with different air discharge (5.833,8.333,10.833,13.333 and 16.666 L/min) for water discharge (5,10,15,20 L/min. as the water discharge increased from (5 L/min to 20 L/min) at the same location of the pressure transducer and constant air discharge (0.35 m and 5.833 L/min), respectively, the value of pressure increase from (14.6 kpa to 16.7 kpa).

Figure (5.3), offers the experimental results of the pressure profile for vertical test channel with opening angle 15 degrees, with different air discharge (5.833,8.333,10.833,13.333 and 16.666 L/min) for water discharge (5,10,15,20 L/ min. As the water discharge increased from (5 L/min to 20 L/min) at the same location of the pressure transducer and constant air discharge (0.35 m and 5.833 L/min), respectively, the value of pressure increase from (14.9 kpa to 17.2).

Figure (5.4), offers the experimental results of the pressure profile for vertical test channel with opening angle 10 degrees, with different air discharge (5.833,10.833 and 16.666 L/min) for water discharge (5,10,15,20 L/min. As the water discharge increased from (5 L/min to 20 L/min) at the same location of the pressure transducer and constant air discharge (0.35 m and 5.833 L/min), respectively, the value of pressure increase from (16.1 kpa to 17.6 kpa).

Figure (5.5), offers the experimental results of the pressure profile for vertical test channel with opening angle 10 degrees, with different air discharge (5.833,8.333,10.833,13.333 and 16.666 L/min) for water discharge (5,10,15,20 L/ min. As the water discharge increased from (5 L/min to 20 L/min) at the same location of the pressure transducer and constant air discharge (0.35 m and 5.833 L/min), respectively, the value of pressure increase from (15.8 kpa to 18.3).

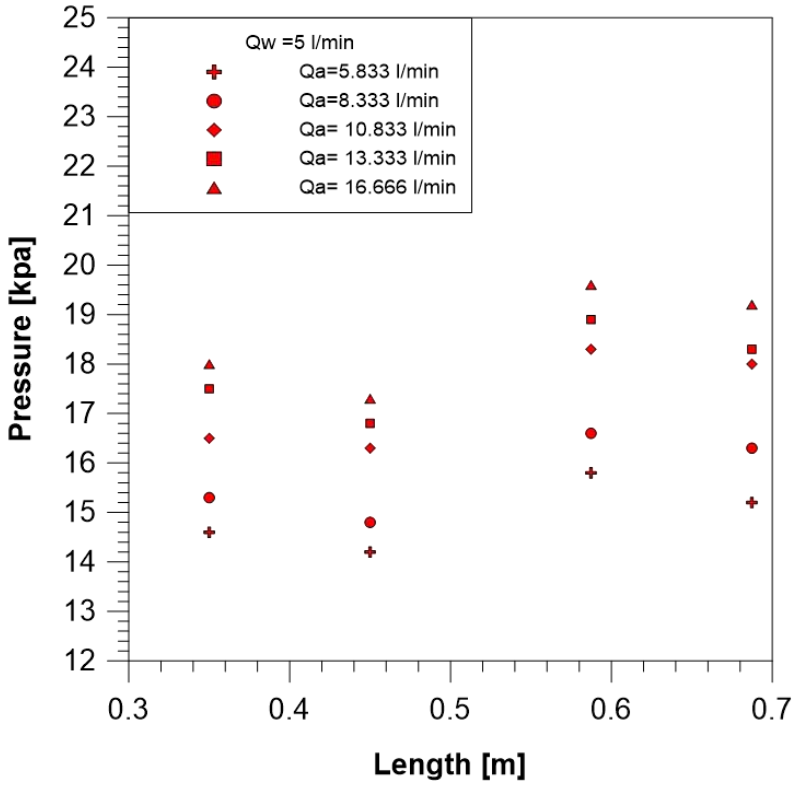

Figure (5.2a)

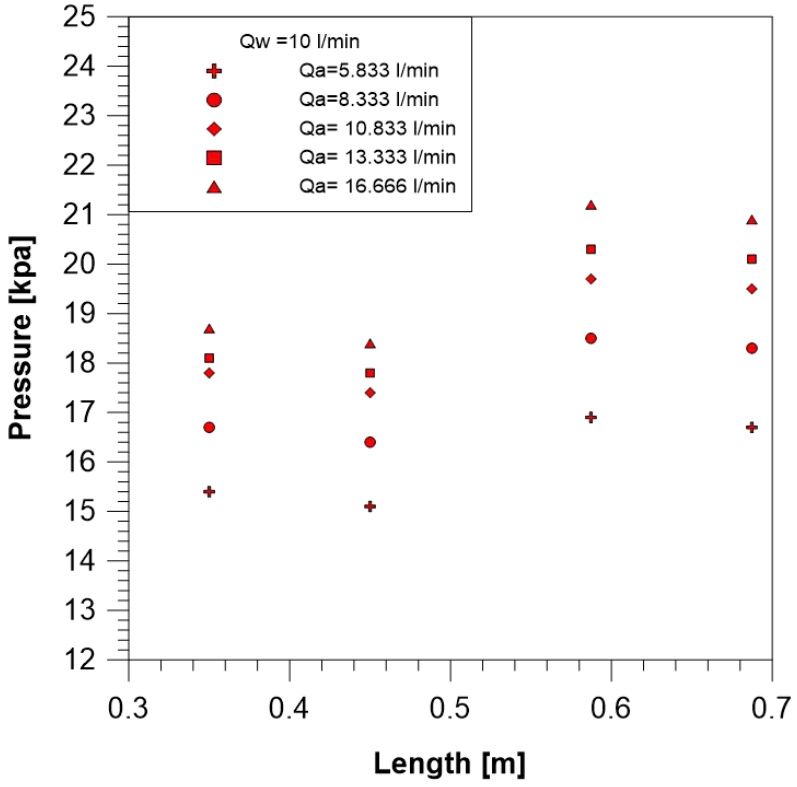

Figure (5.2b)

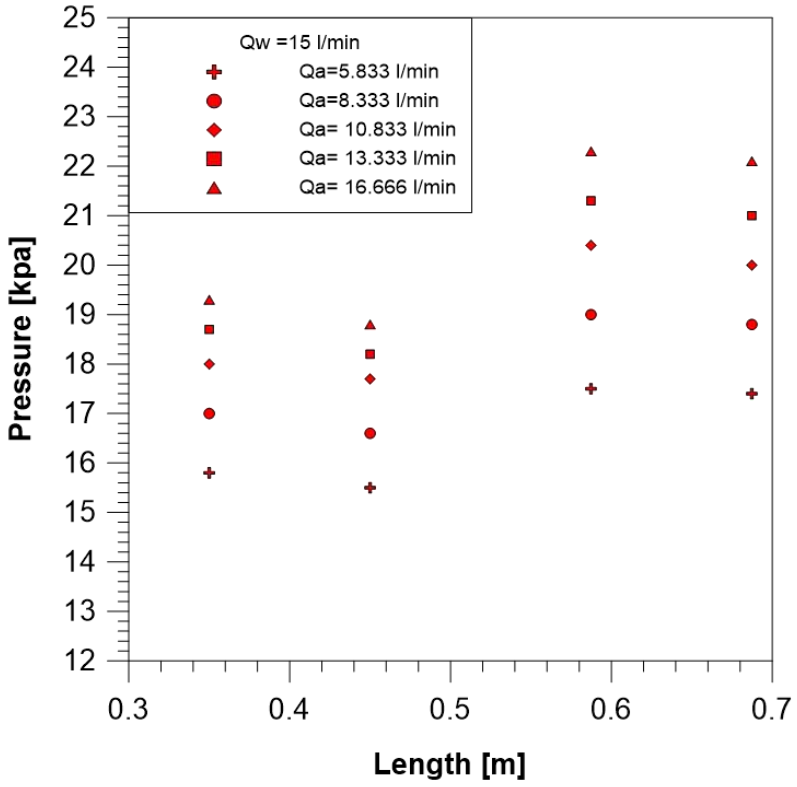

Figure (5.2c)

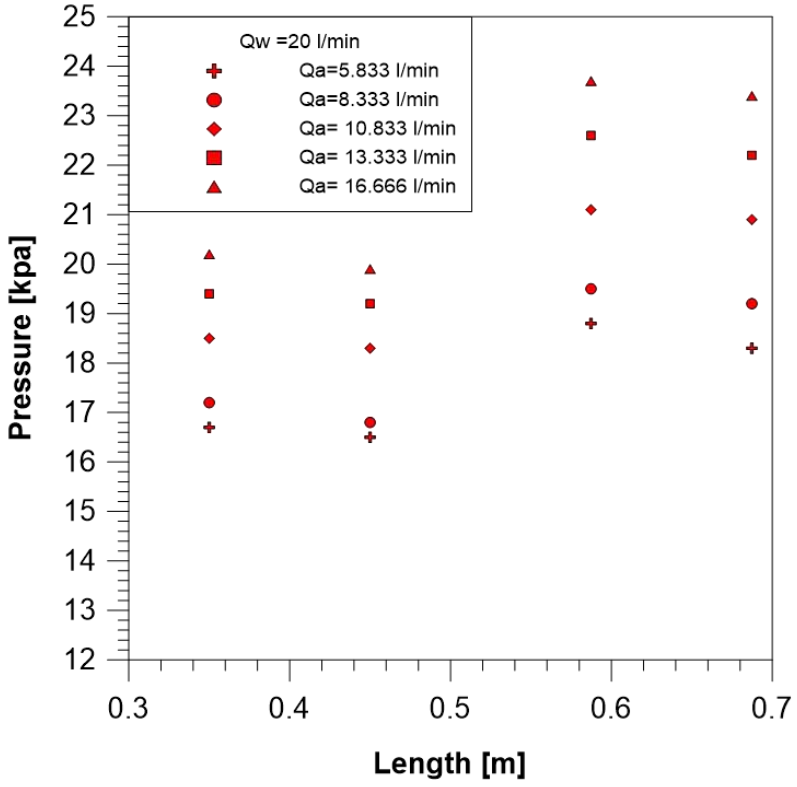

Figure (5.2d)

Figure (5.2): Effect water discharge on
Pressure profile for opening angle 10 degree (vertical)

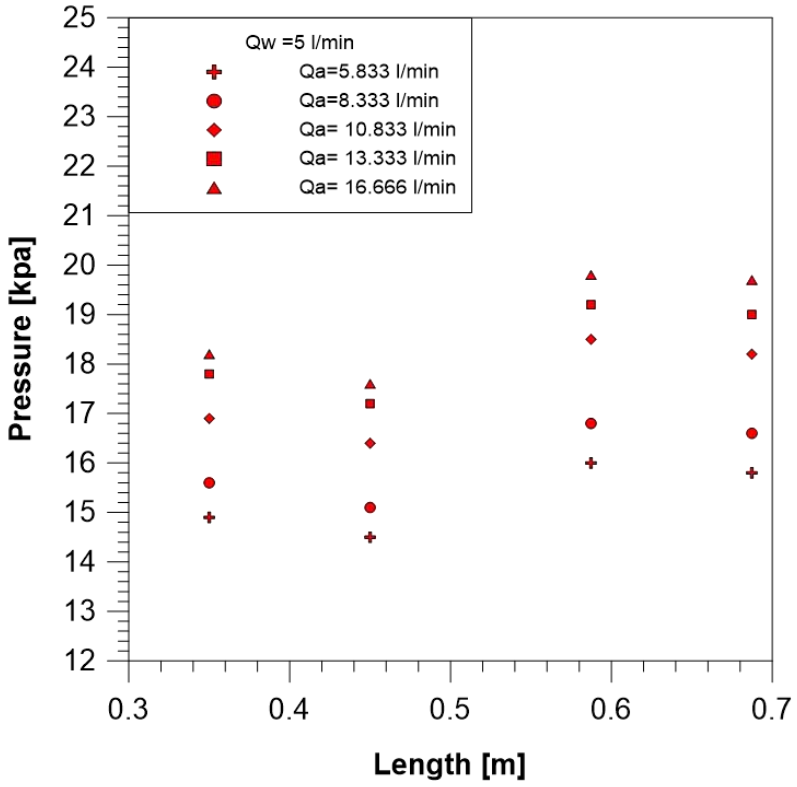

Figure (5.3a)

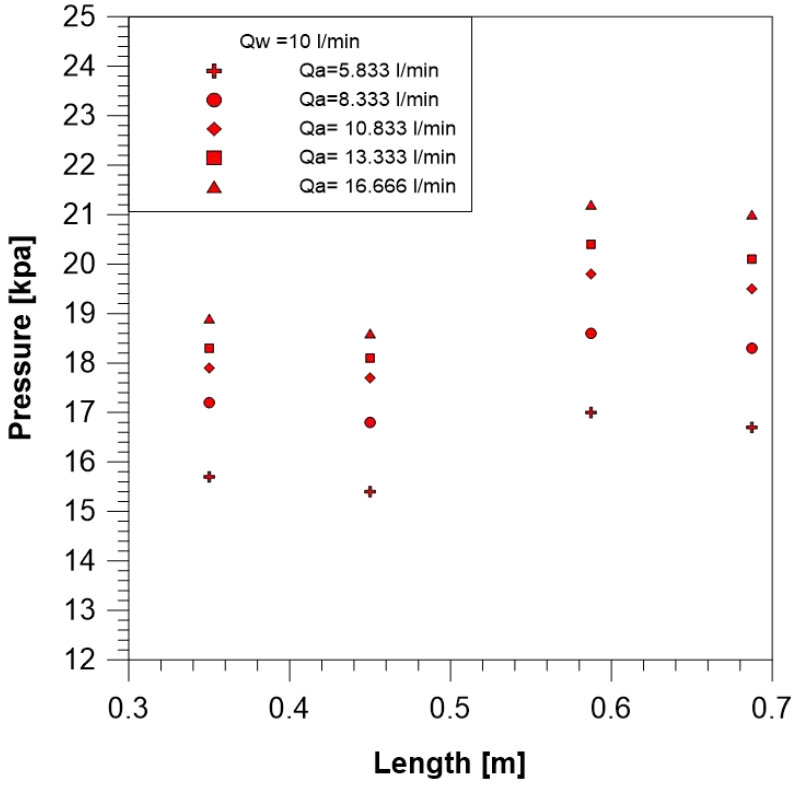

Figure (5.3b)

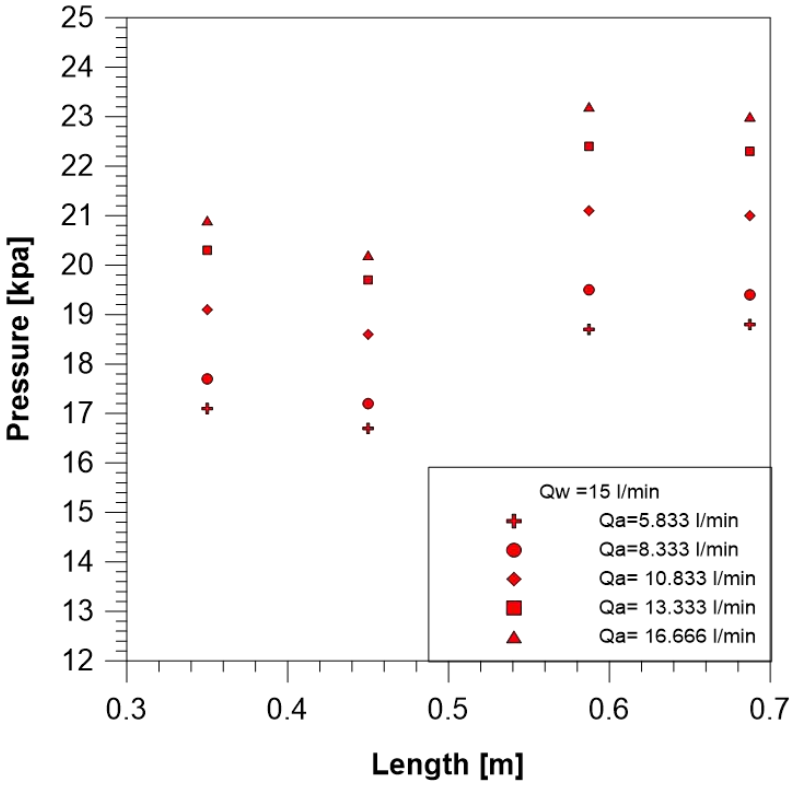

Figure (5.3c)

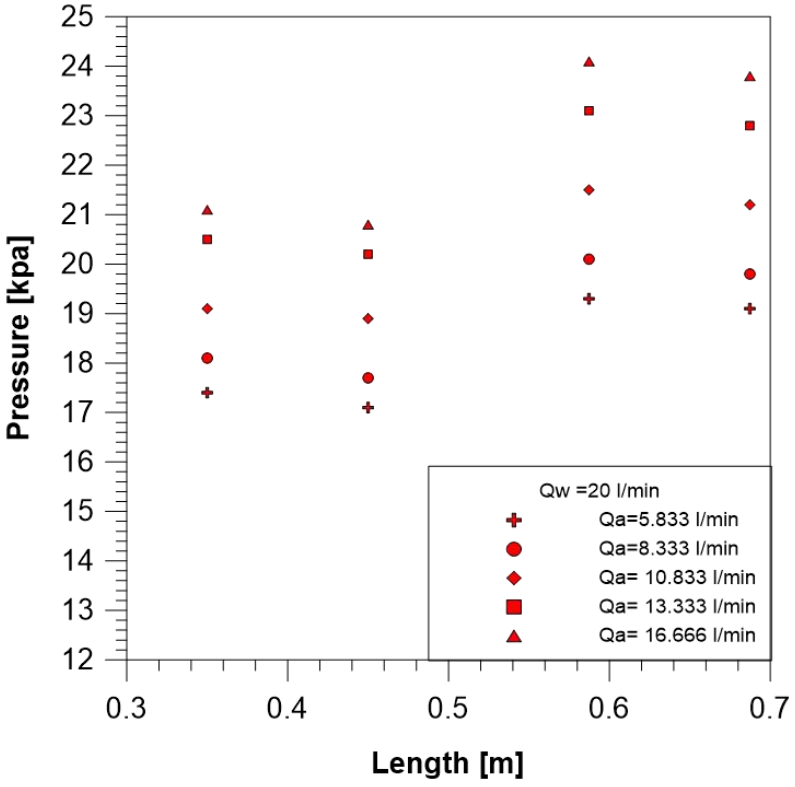

Figure (5.3d)

Figure (5.3): Effect water discharge on
Pressure profile for opening angle 15 degree (vertical)

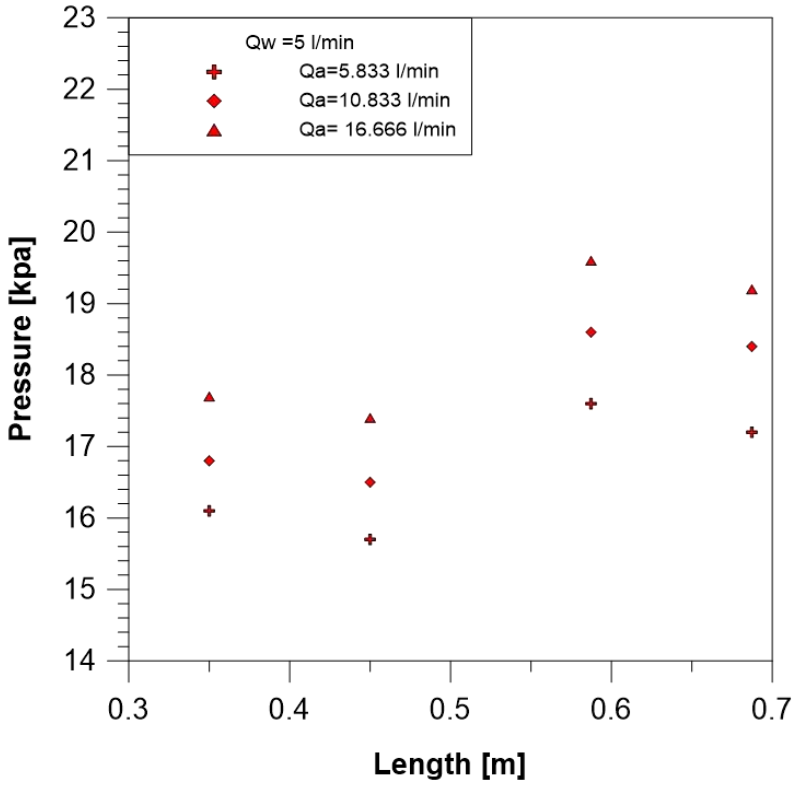

Figure (5.4a)

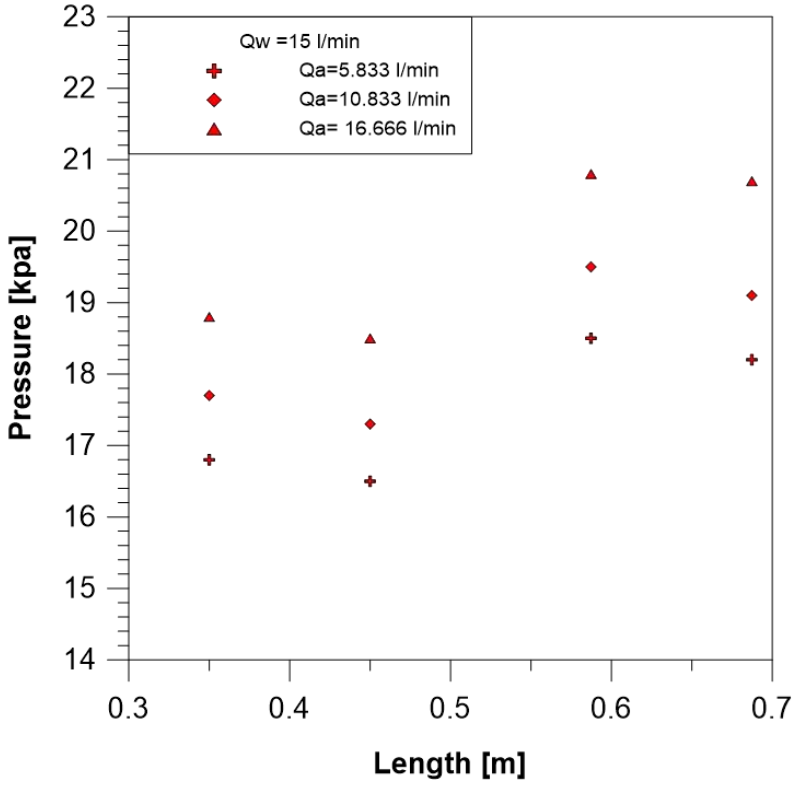

Figure (5.4b)

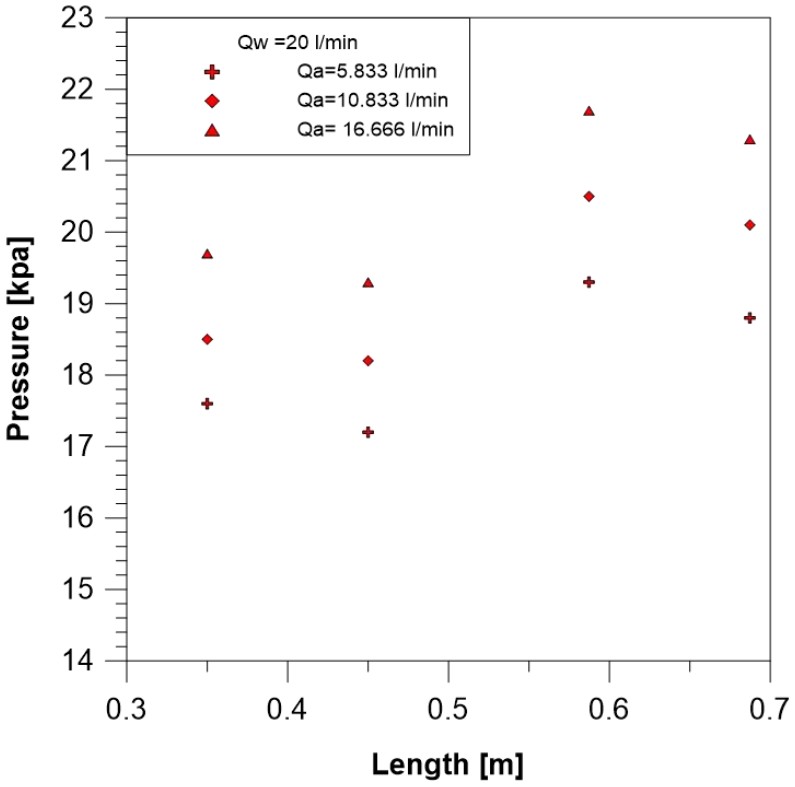

Figure (5.4c)

Figure (5.4): Effect water discharge on Pressure profile for opening angle 10 degree (inclined)

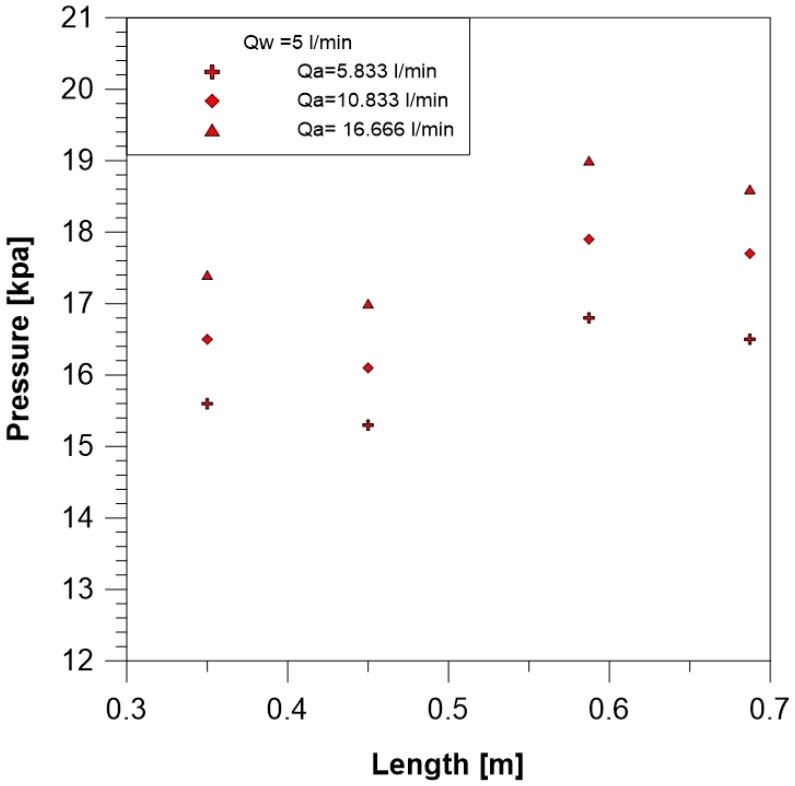

Figure (5.5a)

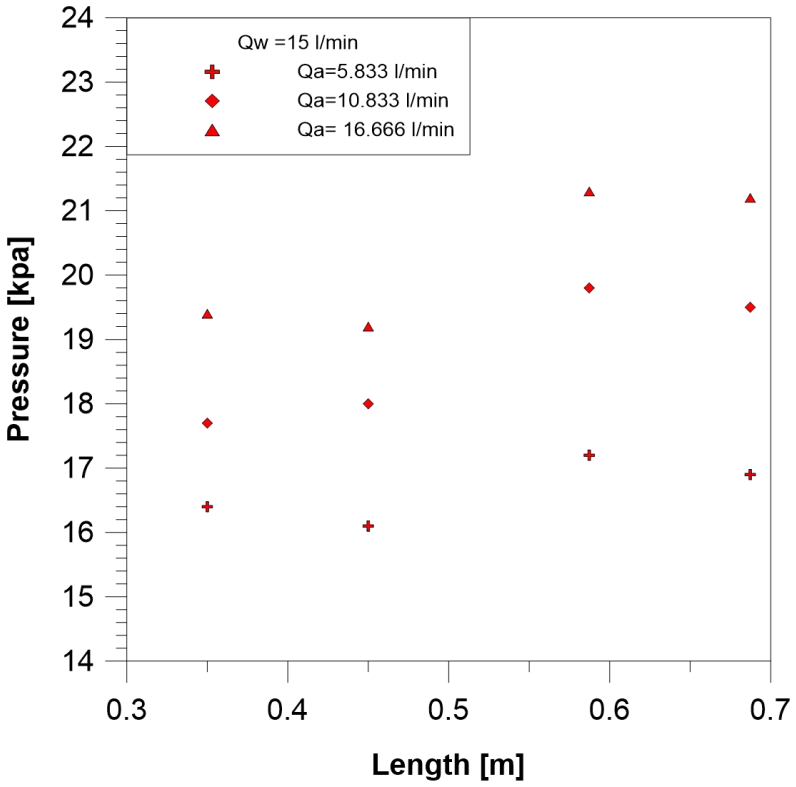

Figure (5.5b)

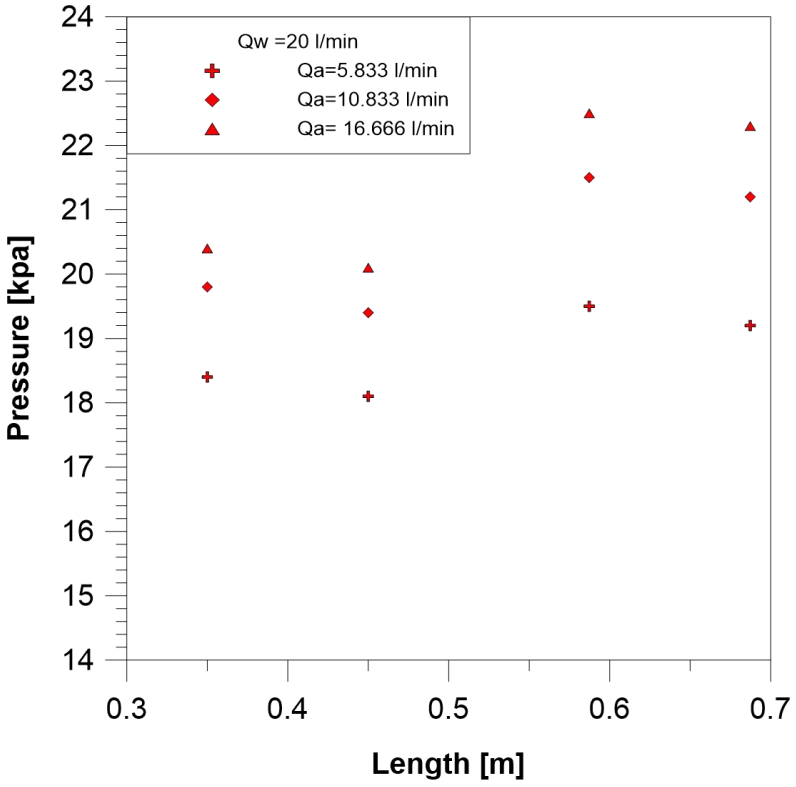

Figure (5.5c)

Figure (5.5): Effect water discharge on
Pressure profile for opening angle 15 degree (inclined)

5.3.1. B. Effect of water and air discharge and opening angle on the recovery pressure

Figure (5.6) to (5.9) show the experimental results for the mean recovery pressure through the vertical divergence section with different air and water discharge. It can be seen from these figures that the recovery pressure increases with increasing discharge of air or water for both the 10 and 15 opening angles. It was observed, too, that the recovery pressure for the opening angle 15 is less than the recovery pressure at the opening angle 10 at the same air and water discharge because of the presence of the additional flow area for case of angle 15 degree which production more turbulence wherefore more eddies are generated, leading to make the recovery pressure less than the case of opening angle of 10 degrees.

Figure (5.6) and (5.7) shows the experimental recovery pressure through the vertical divergence section for opening angle 10 and 15 degree, respectively, with different air discharge (5.833,8.333,10.833,13.333 and 16.666 L/min) for water discharge (5,10,15,20 L/min).as the air discharge increased from (5.833 to 16.666 L/min) at constant water discharge (5 L/min),the value recovery pressure increase from (1.6 kpa to 2.3 kpa) for opening angle 10 . for opening angle 15,the value recovery pressure increase from (1.5 kpa to 2.1 kpa).

Figure (5.8) and (5.9) shows the experimental recovery pressure through the inclined divergence section for opening angle 10 and 15 degrees respectively with different air discharge (5.833, 10.833 and 16.666 L/min) for water discharge (5, 15 and 20 L/min). as the air discharge increased from (5.833 to 16.666 L/min) at constant water discharge (5 L/min),the value recovery pressure increase from (1.9 kpa to 2.2 kpa) for opening angle 10 degree, while the value recovery pressure increase from (1.9 kpa to 2.2 kpa) for opening angle 15 degree.

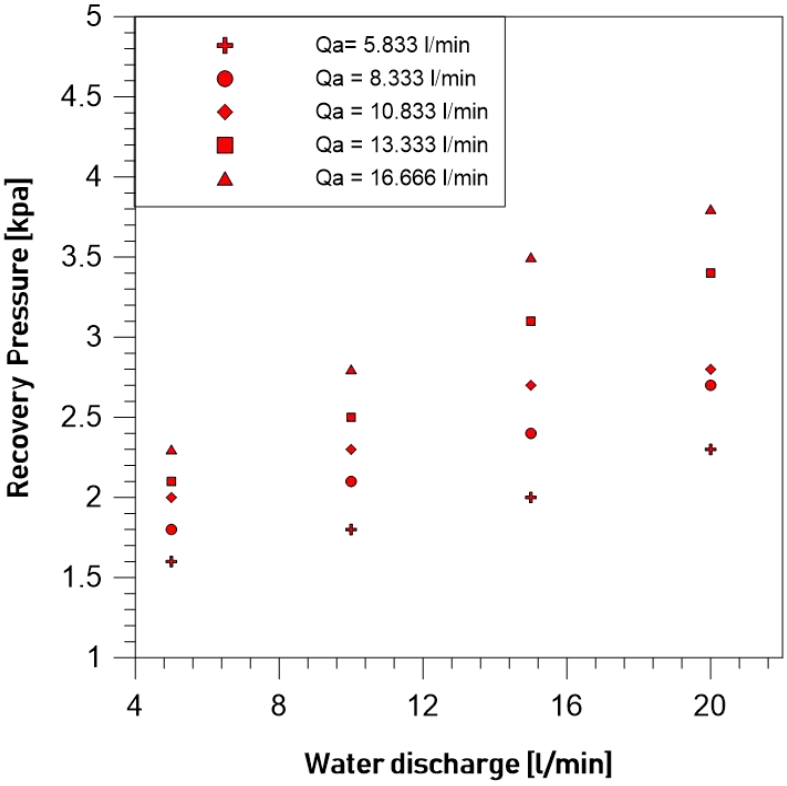

Figure (5.6): Recovery pressure for different values of water discharge at opening angle 10 degree (vertical)

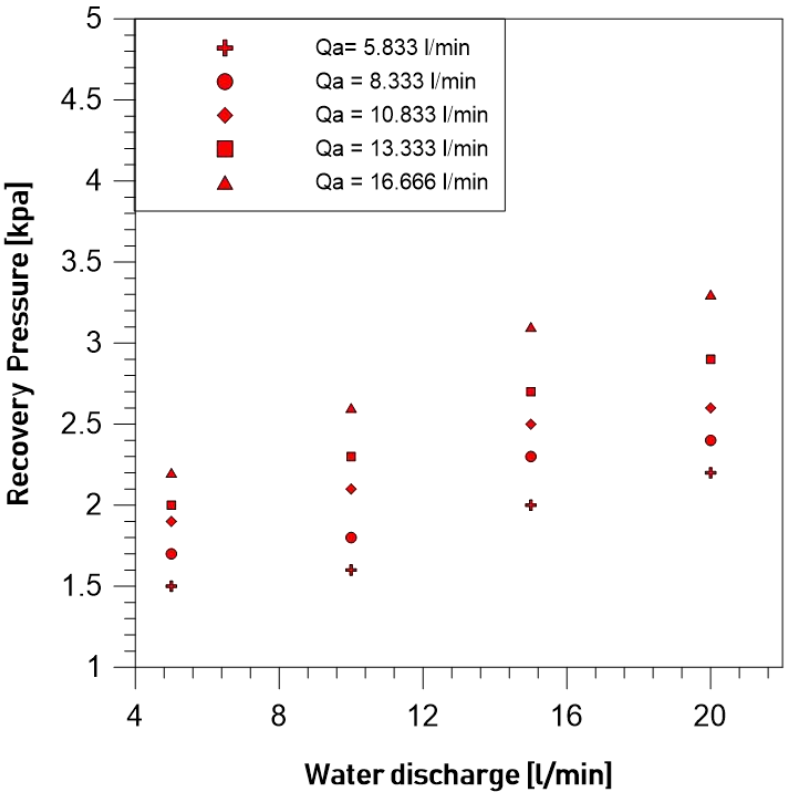

Figure (5.7): Recovery pressure for different values of water discharge at opening angle 15 degree (vertical)

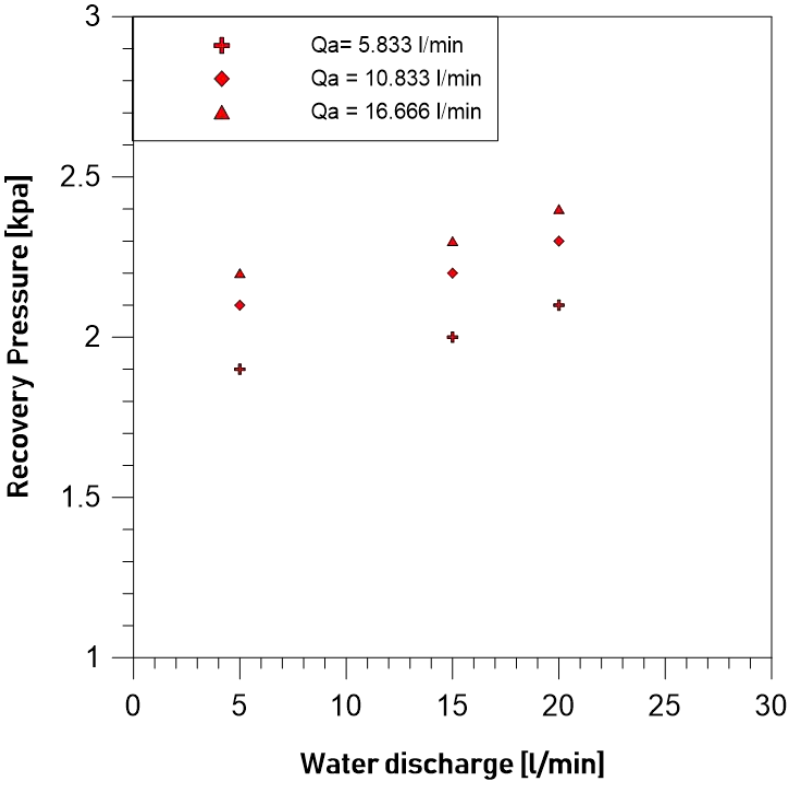

Figure (5.8): Recovery pressure for different values of water discharge at opening angle 10 degree (inclined)

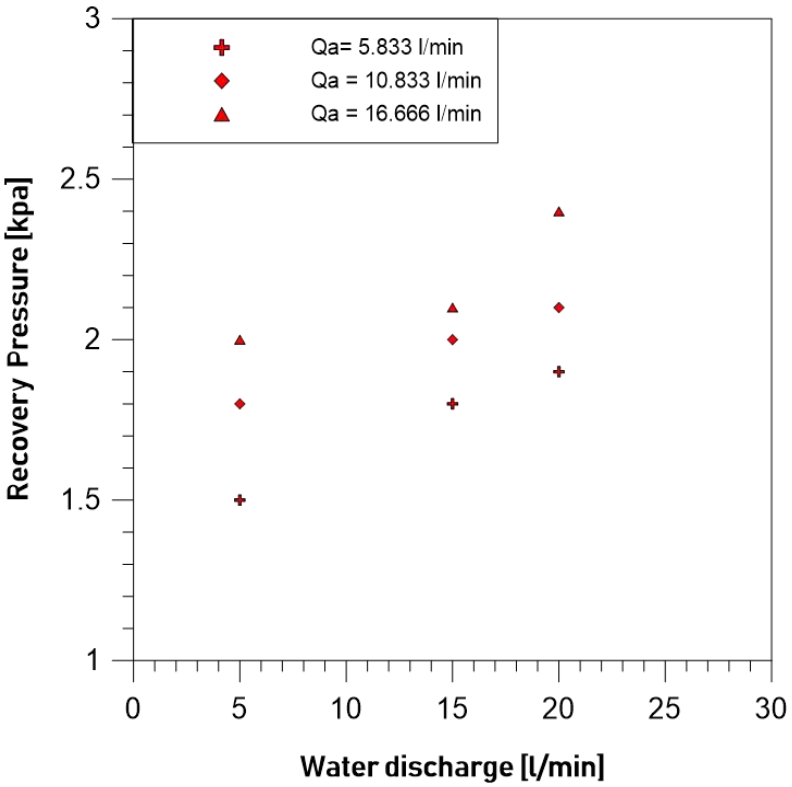

Figure (5.9): Recovery pressure for different values of water discharge at opening angle 15 degree (inclined)

5.3.2. Numerical results

5.3.2. A. Pressure contour

The purpose of the numerical CFD to study the pressure distribution and air volume fraction distribution through ribs divergence section for the vertical and inclined position**.** As like as the experimental study, a region of the test is in between sensor (1) and sensor (4).

Figures (5.10) to (5.16), show the contours of pressure distribution for two-phase flow through vertical ribs divergence test channel with opening angle 10 and 15 degrees, at various values of water (5,10,15 and 20 L/min). Each figure is five values of air discharge (5.833, 8.333, 10.833, 13.333 and 16.666 L/min)**.**

Figures (5.17) to (5.23), show the contours of pressure distribution for two-phase flow through vertical ribs divergence test channel with opening angle 10 and 15 degrees, at various values of water (5,10,15 and 20 L/min). Each figure is five values of air discharge (5.833, 8.333, 10.833, 13.333 and 16.666 L/min).

These figures describe the contour of the pressure values ,where note that the descending gradient of the value of the pressure before the divergence section, and at the divergence section, observe an ascending gradient of the pressure values due to the increase of the flow area leading to reducing the velocity thus increasing the pressure values. After divergence section, Descending gradient of pressure values beginning again**.**

Can be noted also that the value of the pressure increases with increasing values of air or water discharge due to the increased amount of flow mixture and thus increase pressure on the walls of the channel**.**

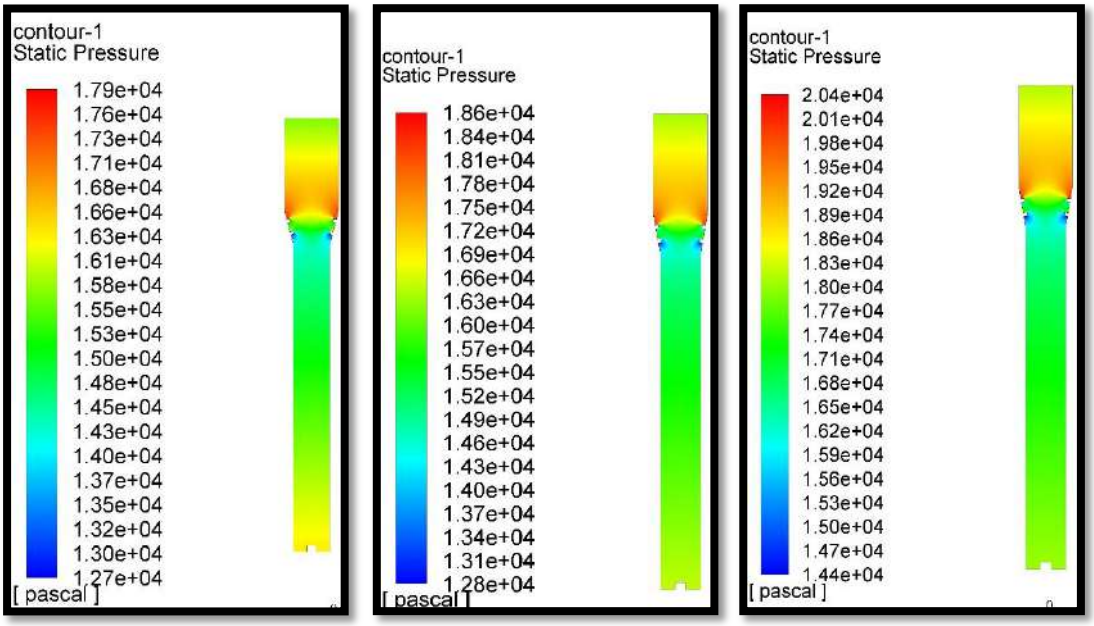

(a) Q $_{air}$ =5.833 (b) Q $_{air}$ =8.333 (c) Q air =10.833

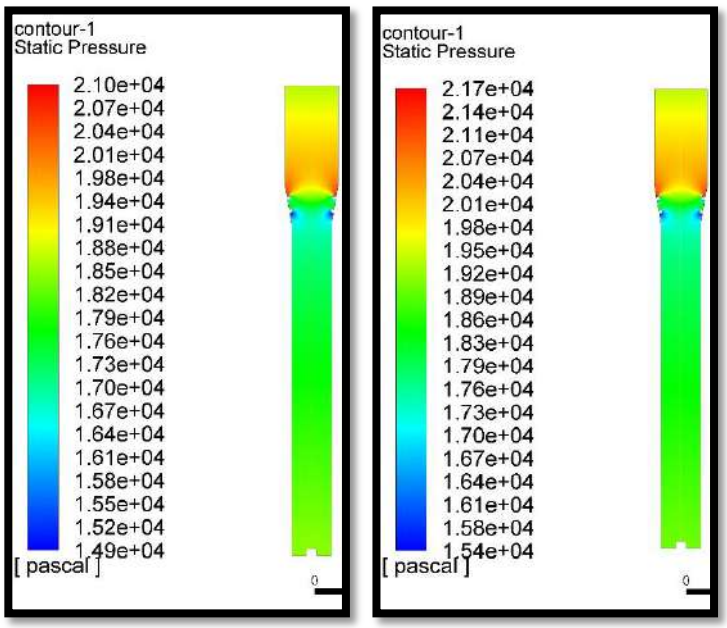

(d) Q air =13.333 (e) Q air =16.666

Figure (5.10): Influence of air discharge on pressure distribution at 5 l/min water discharge (opening

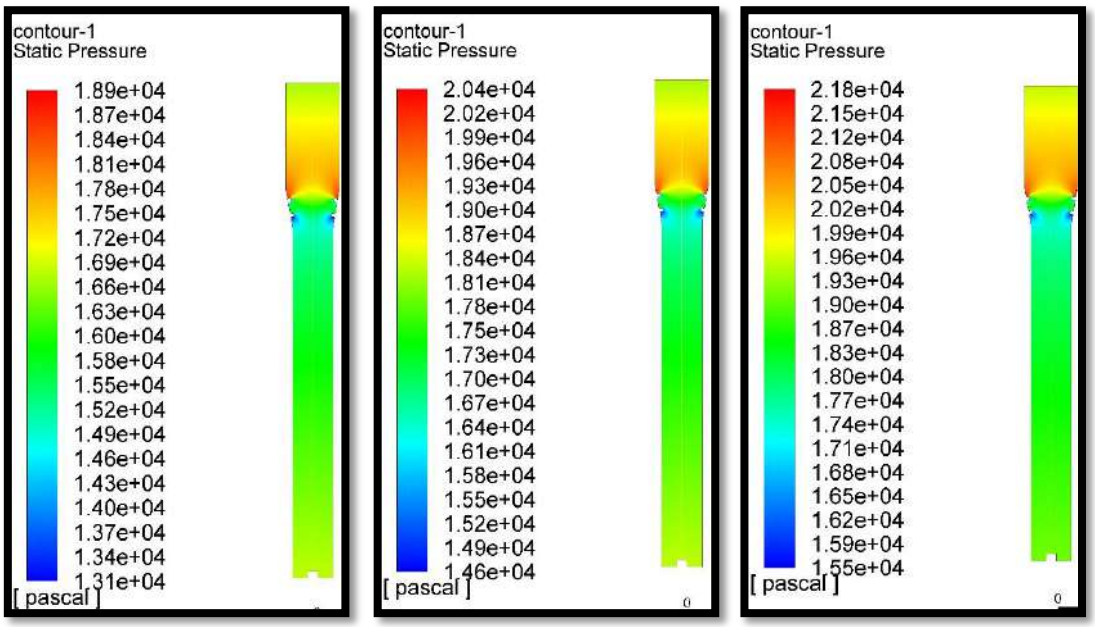

(a) Q air =5.833 (b) Q air =8.333 (c) Q air =10.8333

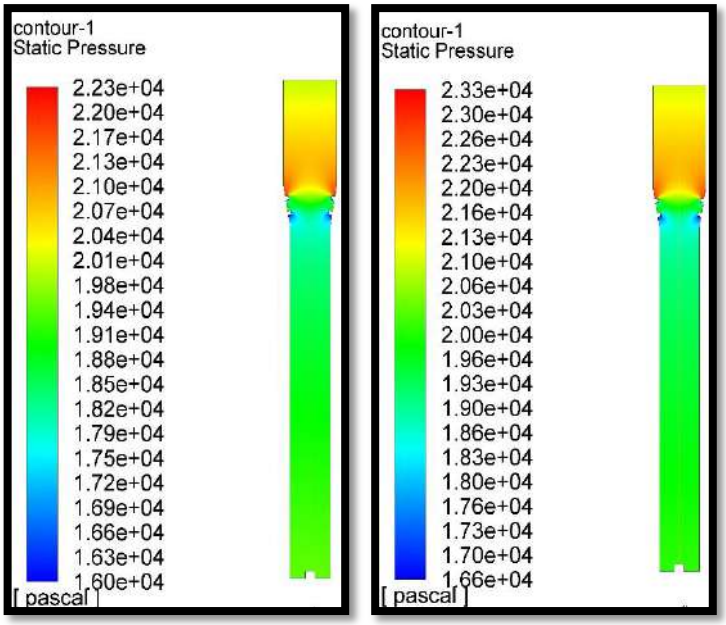

(d) Q air =13.333 (e) Q air =16.666

Figure (5.11): Effect of air discharge on pressure distribution at 10 l/min water discharge (opening

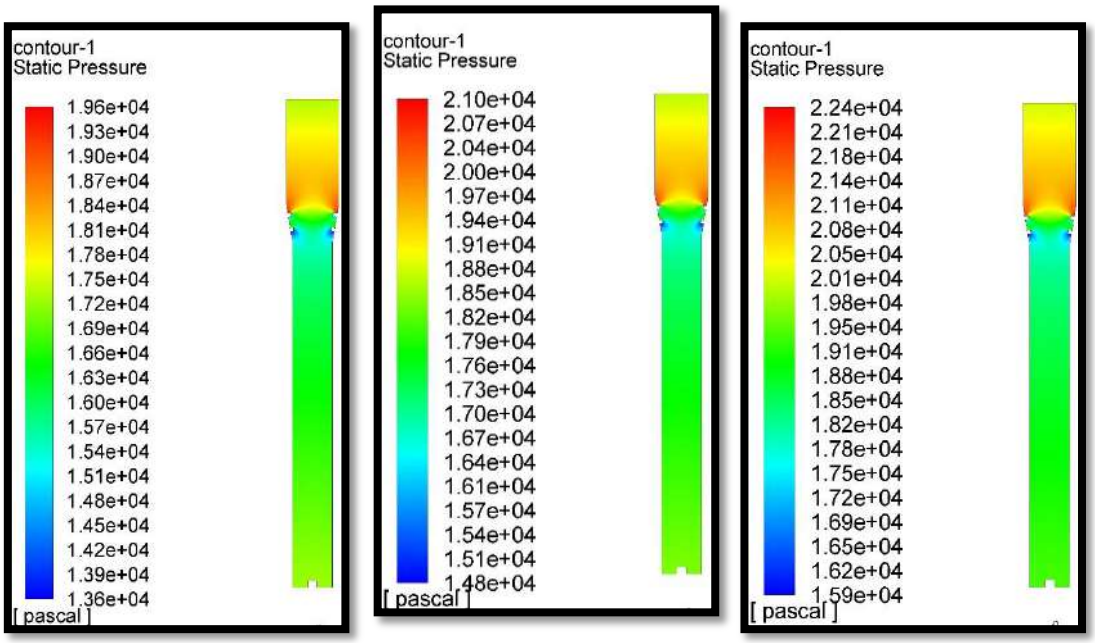

(a) Q air =5.833 (b) Q air =8.333 (c) Q air =10.8333

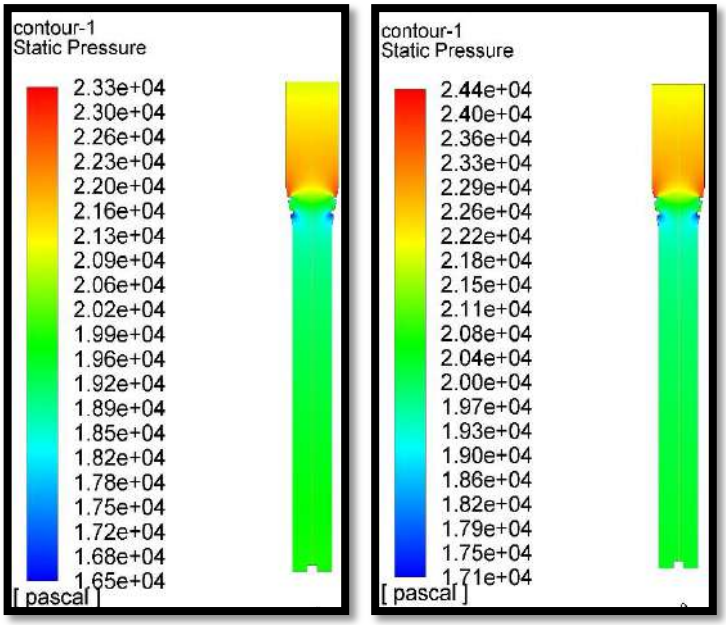

(d) Q air =13.333 (e) Q air =16.666

Figure (5.12): Effect of air discharge on pressure distribution at 15 l/min water discharge (opening

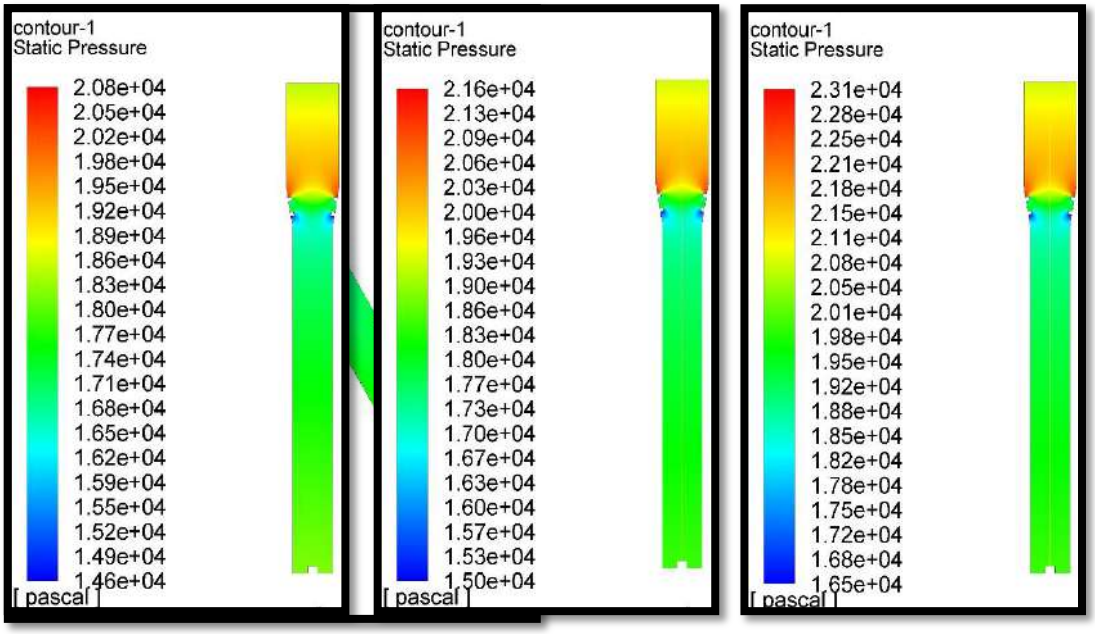

(a) Q air =5.833 (b) Q air =8.333 (c) Q air =10.833

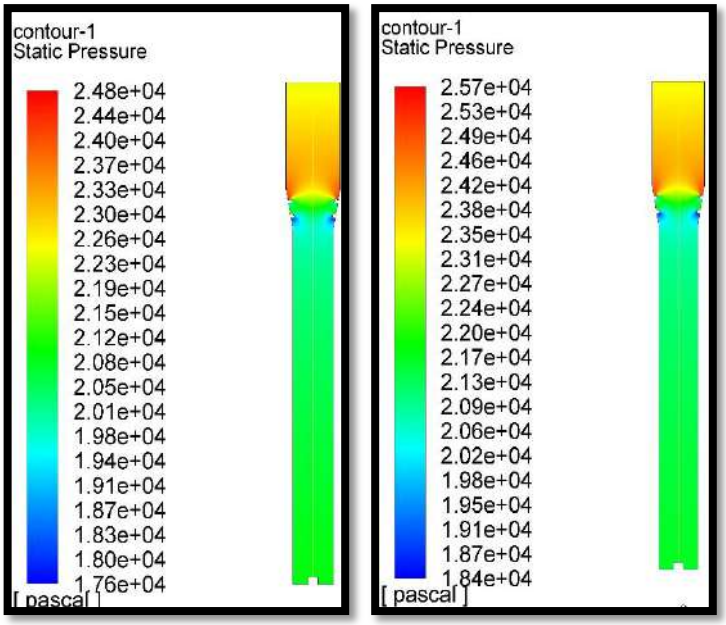

(d) Q air =13.333 (e) Q air =16.666

Figure (5.13): Effect of air discharge on pressure distribution at 20 l/min water discharge (opening

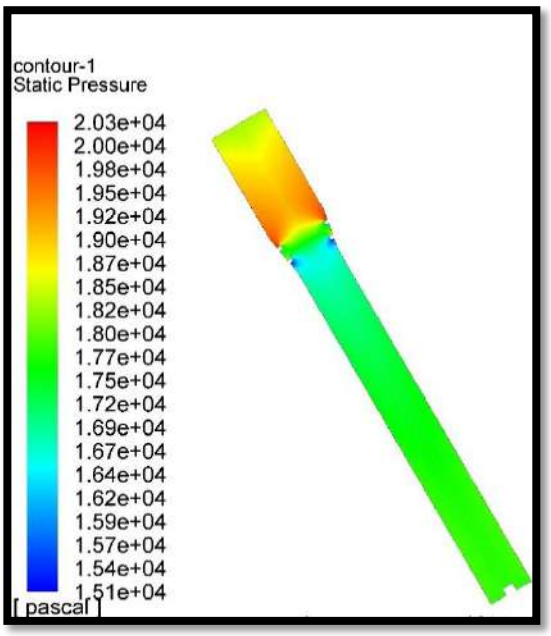

(a) Q air =5.833 (b) Q air =10.833

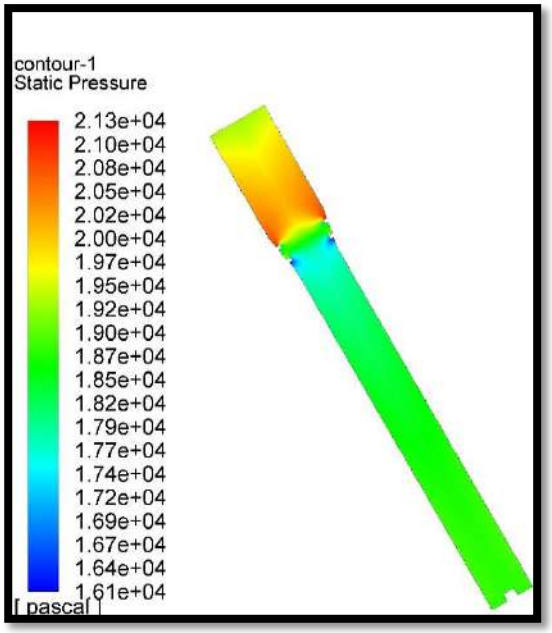

(c) Q air =16.666

Figure (5.14): Effect of air discharge on pressure distribution at 5 l/min water discharge (opening

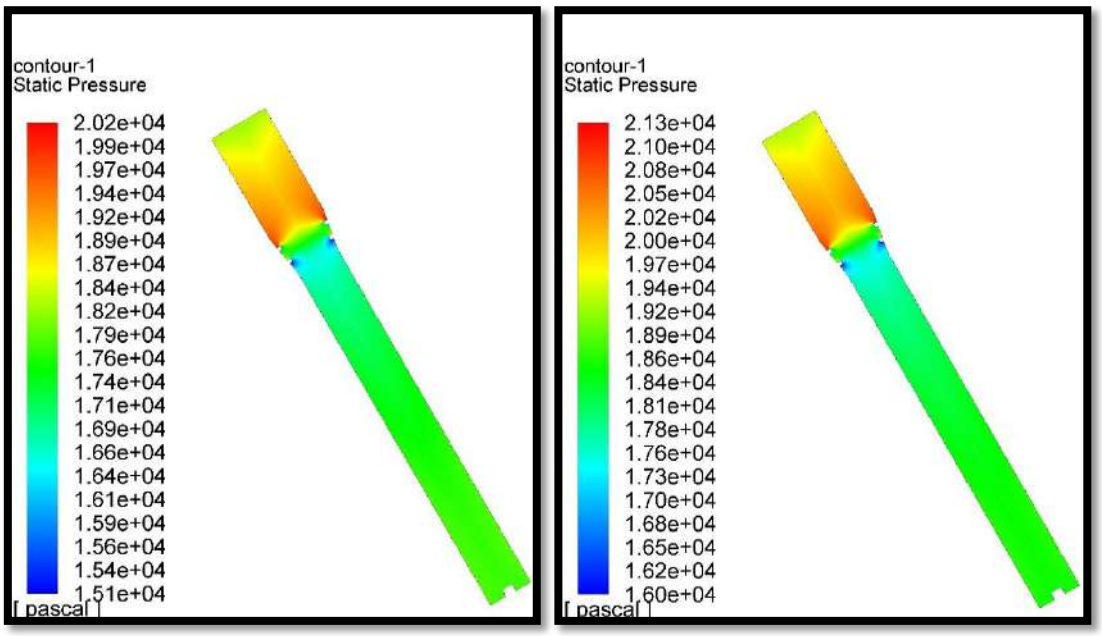

(a) Q air =5 l/min (b) Q air =10.833

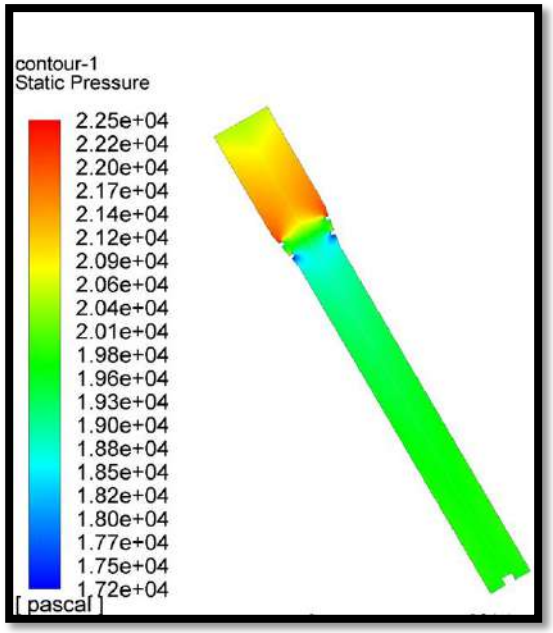

(c) Q air =16.666

Figure (5.15): Effect of air discharge on pressure distribution at 15 l/min water discharge (opening

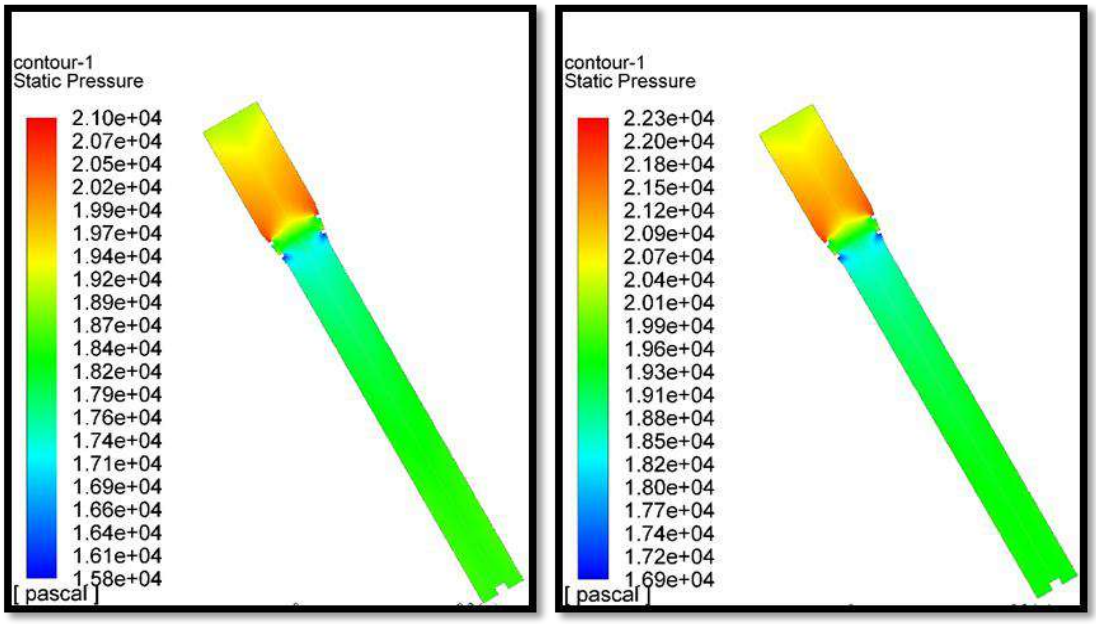

(a) Q air =5 l/min (b) Q air =10.833

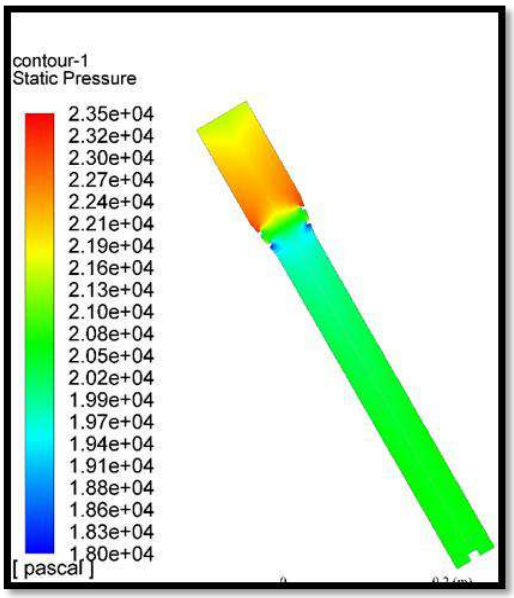

(c) Q air =16.666

Figure (5.16): Effect of air discharge on pressure distribution at 20 l/min water discharge (opening

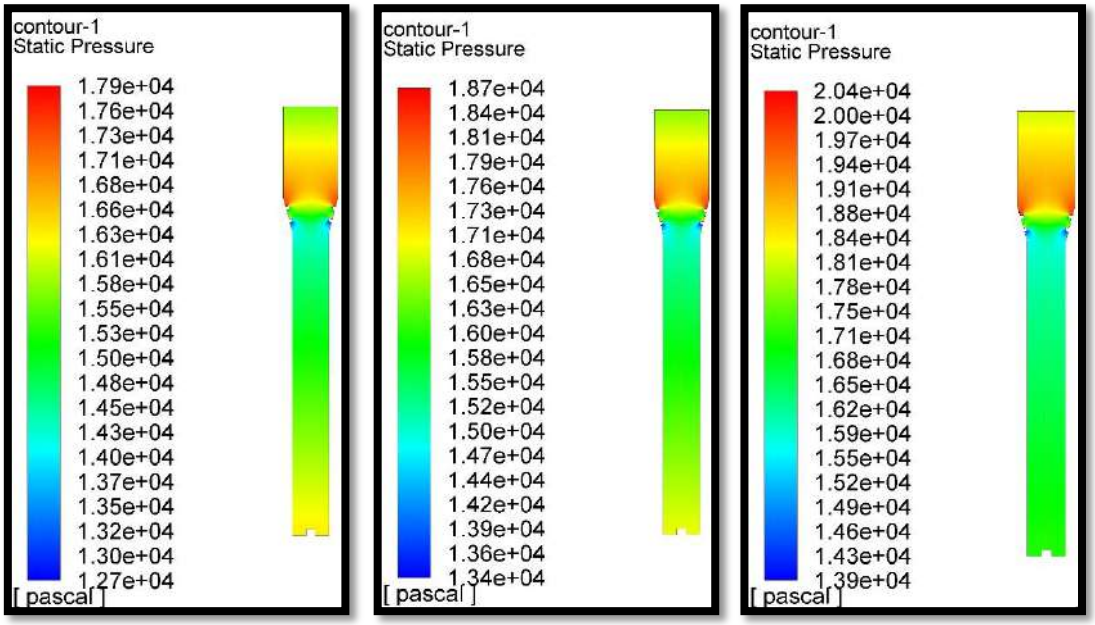

(a) Q air =5.833 (b) Q air =8.333 (c) Q air =10.833

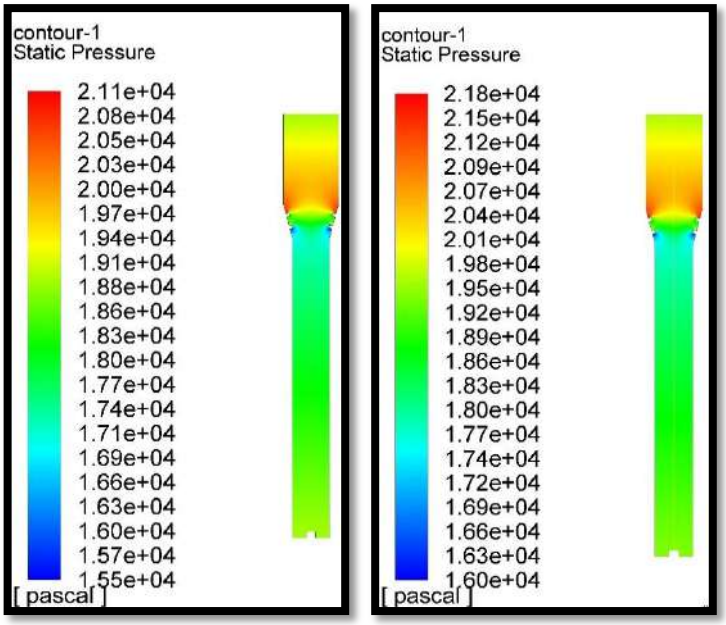

(d) Q air =13.333 (e) Q air =16.666

Figure (5.17): Effect of air discharge on pressure distribution at 5 l/min water discharge (opening

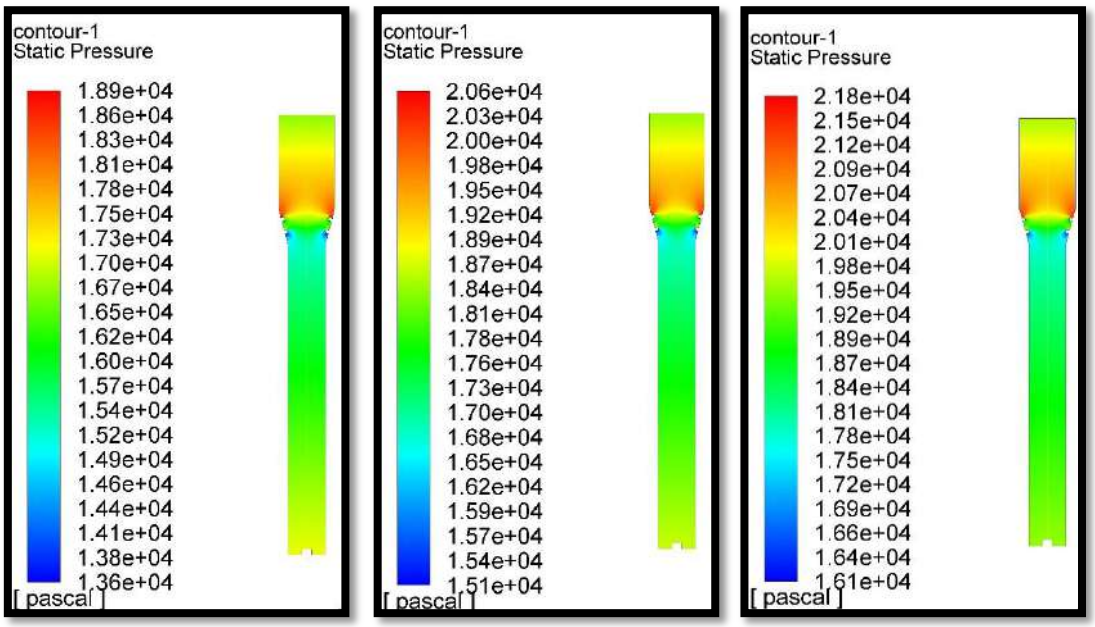

(a) Q air =5.833 (b) Q air =8.333 (c) Q air =10.833

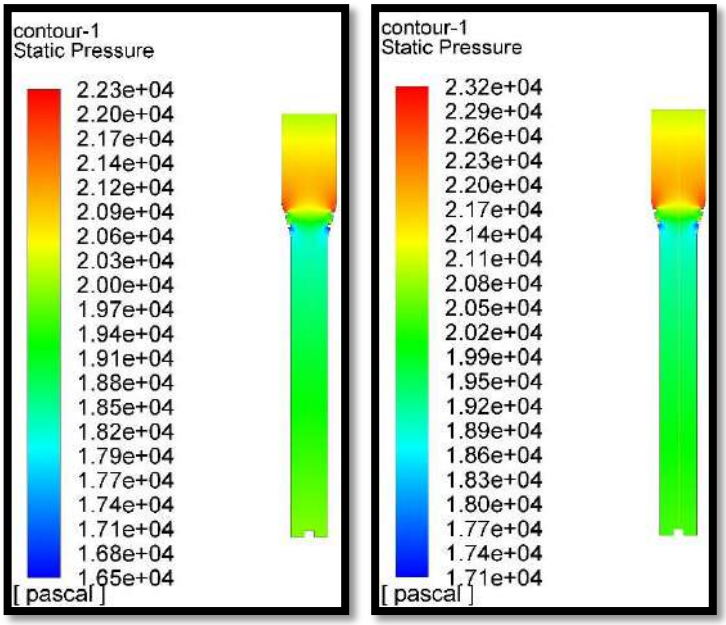

(d) Q air =13.333 (e) Q air =16.666

Figure (5.18): Effect of air discharge on pressure distribution at 10 l/min water discharge (opening

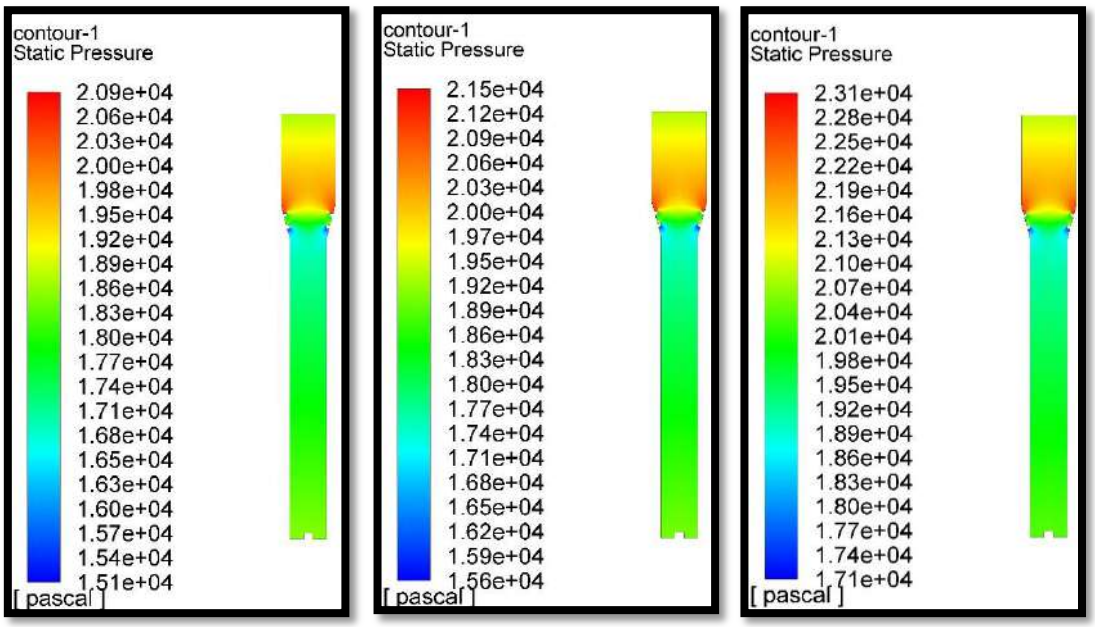

(a) Q air =5.833 (b) Q air =8.333 (c) Q air =10.833

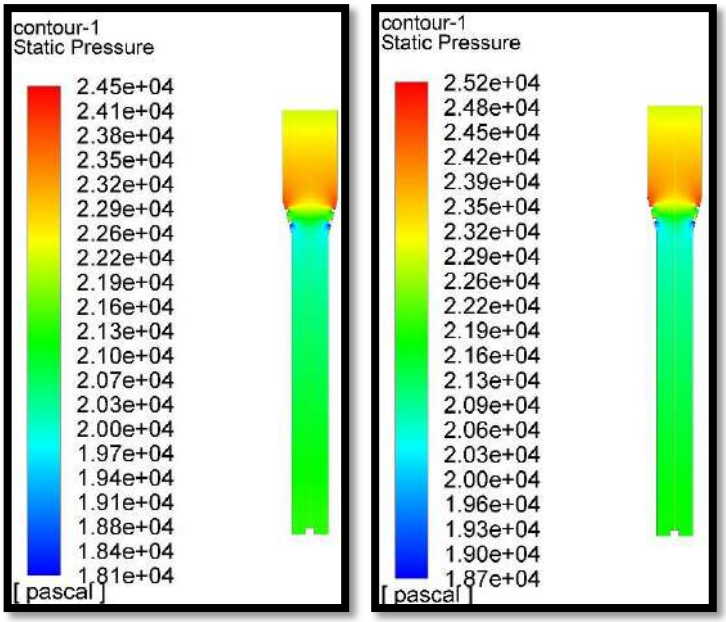

(d) Q air =13.333 (e) Q air =16.666

Figure (5.19): Effect of air discharge on pressure distribution at 15 l/min water discharge (opening

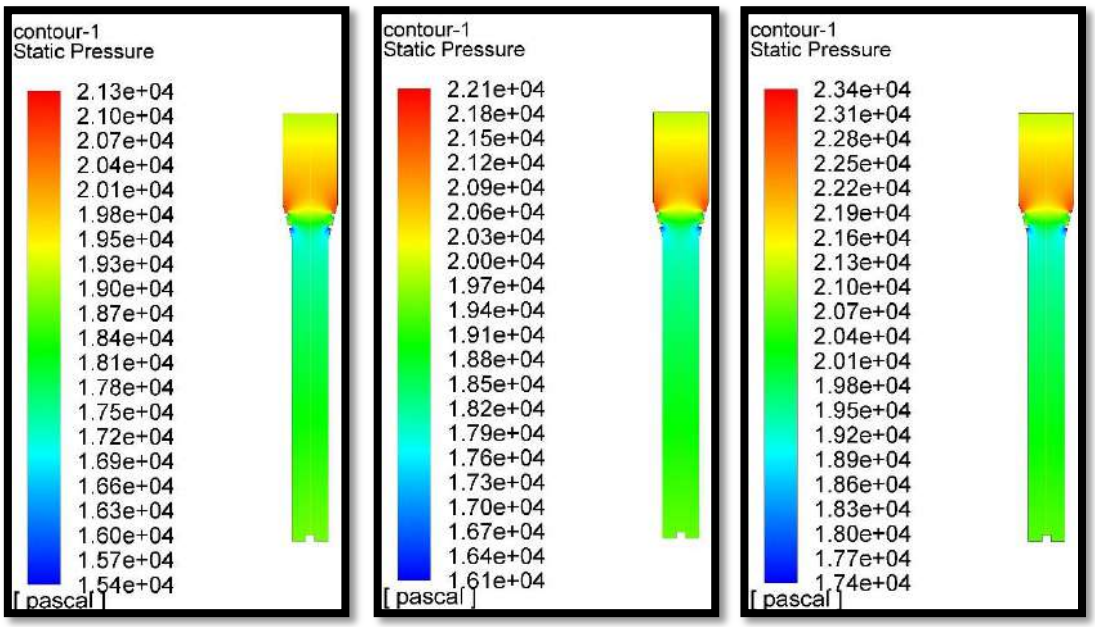

(a) Q air =5.833 (b) Q air =8.333 (c) Q air =10.833

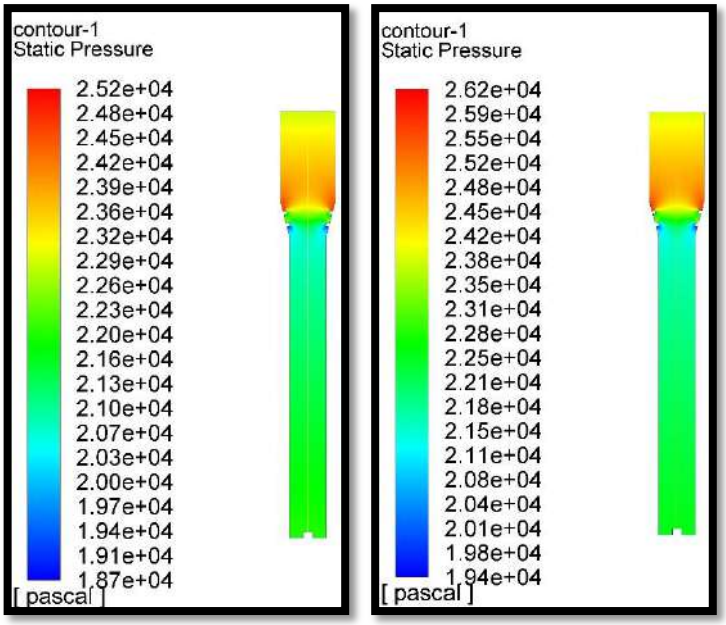

(d) Q air =13.333 (e) Q air =16.666

Figure (5.20): Effect of air discharge on pressure distribution at 20 l/min water discharge (opening

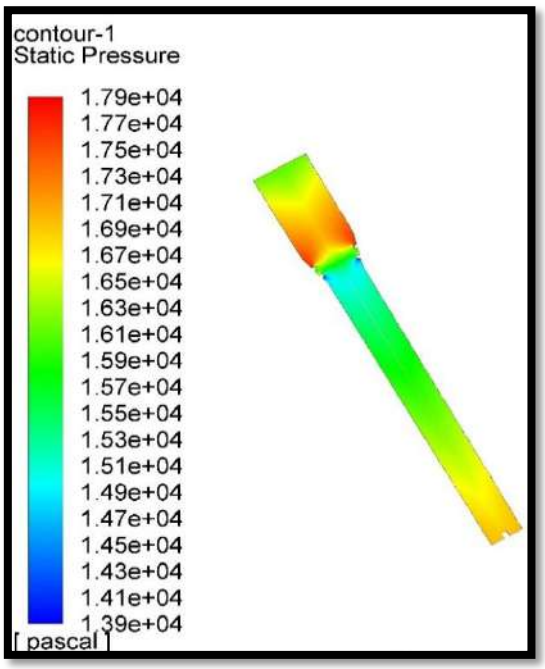

(a) Q air =5.833

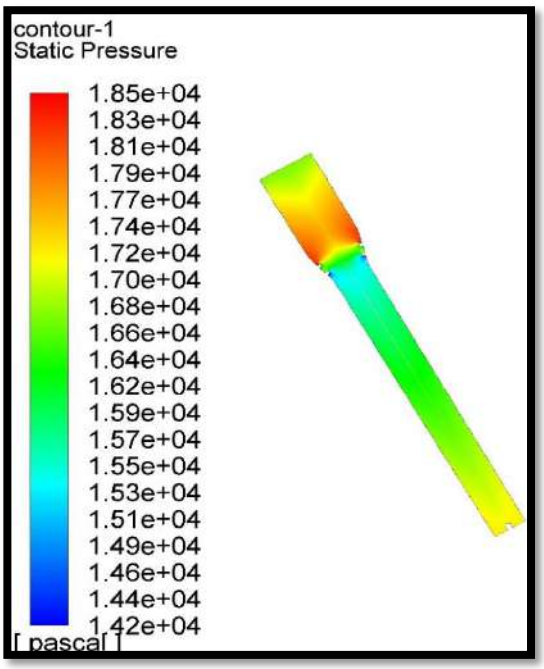

(b) Q air =10.833

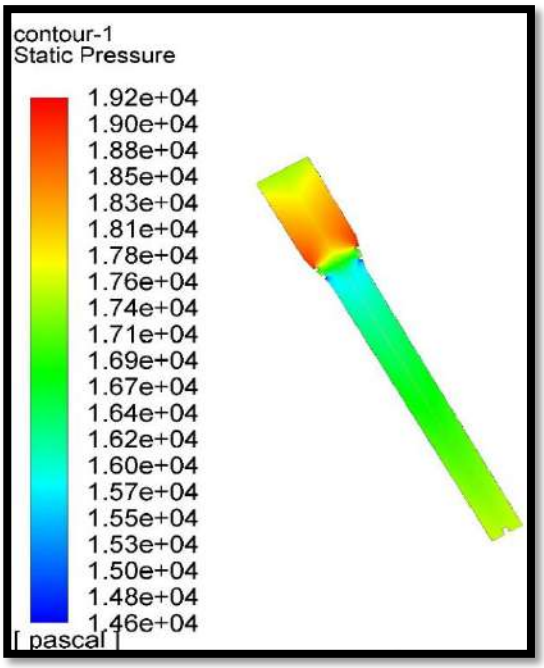

(c) Q air =16.666

Figure (5.21): Effect of air discharge on pressure distribution at 5 l/min water discharge (opening

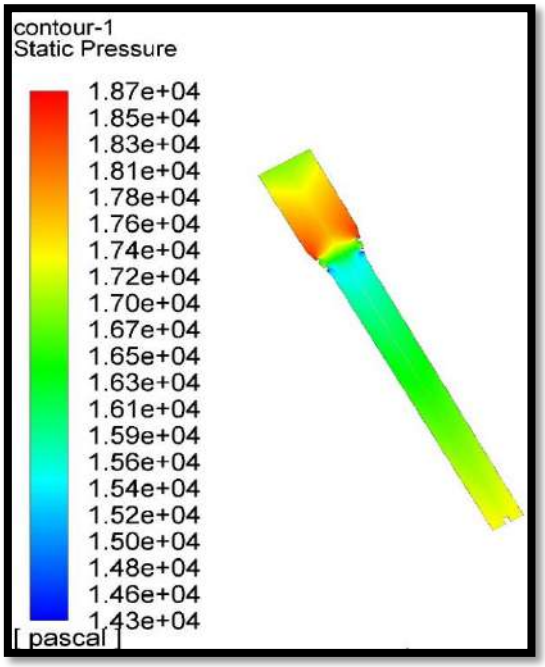

(a) Q air =5.833

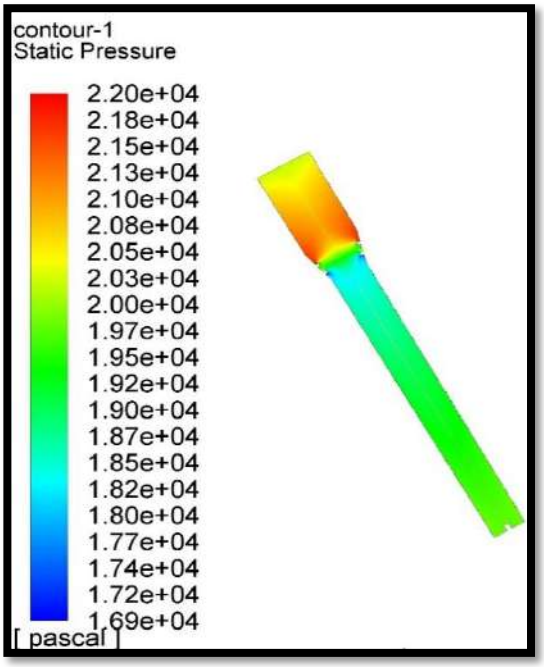

(b) Q air =10.833

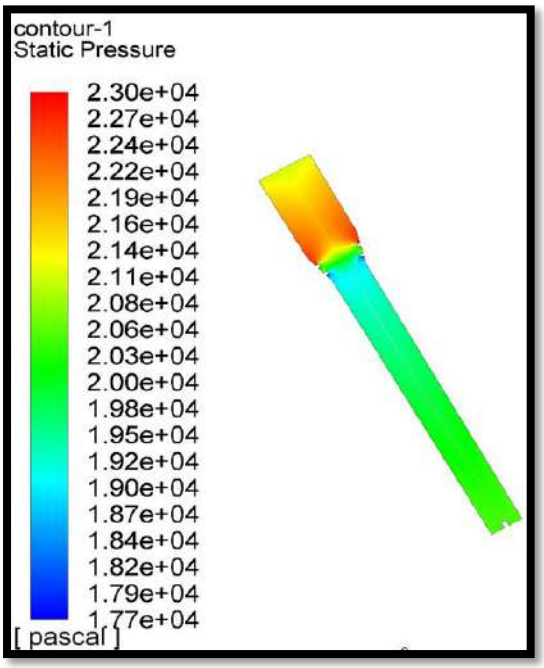

(c) Q air =16.666

Figure (5.22): Effect of air discharge on pressure distribution at 15 l/min water discharge (opening

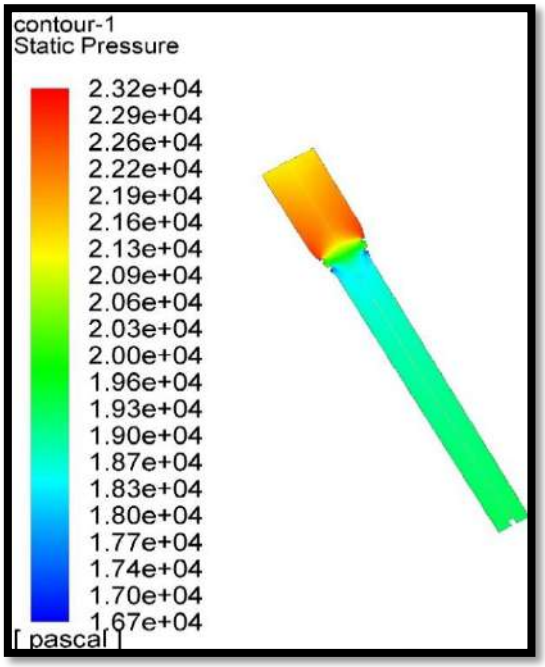

(a) Q air =5.833

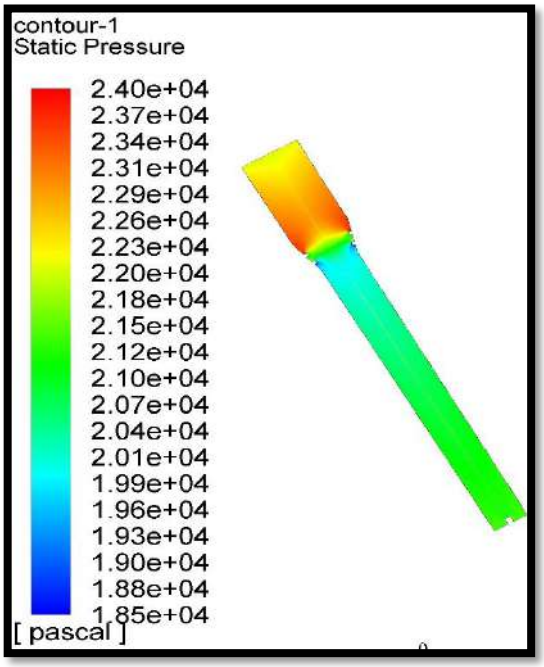

(b) Q air =10.833

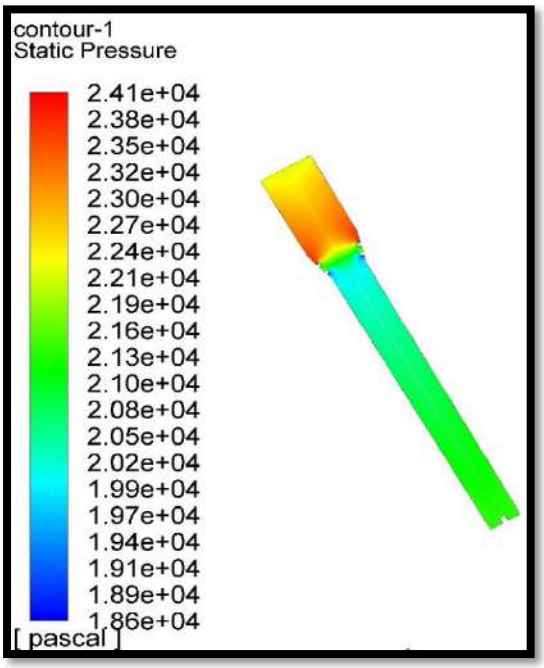

(c) Q air =16.666

Figure (5.23): Effect of air discharge on pressure distribution at 20 l/min water discharge

5.3.2. B. Velocity Vector

The figures from (5.24) to (5.27) represent the velocity vector for different cases, which indicates the direction of velocity. Can be noted from these figures that the velocity vector is affected by the turbulence of flow where it is formed as vortices, where the number and size of vortices increases with the increased turbulence of flow,

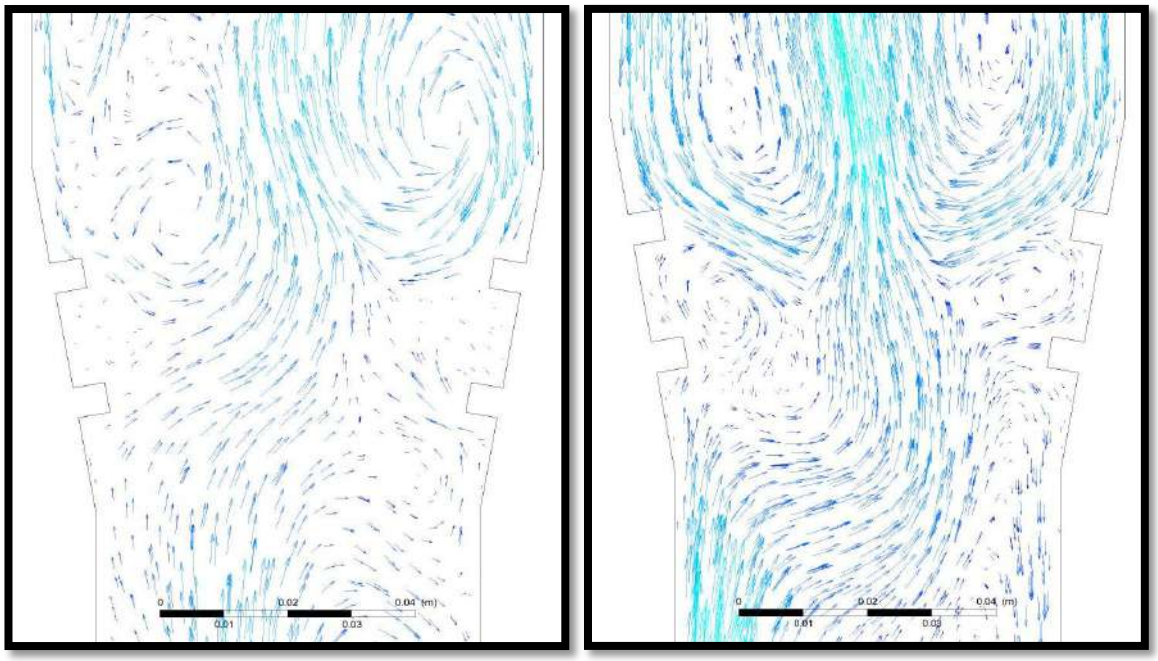

(a) Qair=5.883 L/min (b) Qair=16.66 L/min

Figure (5.24): velocity vector at 5 L/min water discharge (opening angle10 degree)

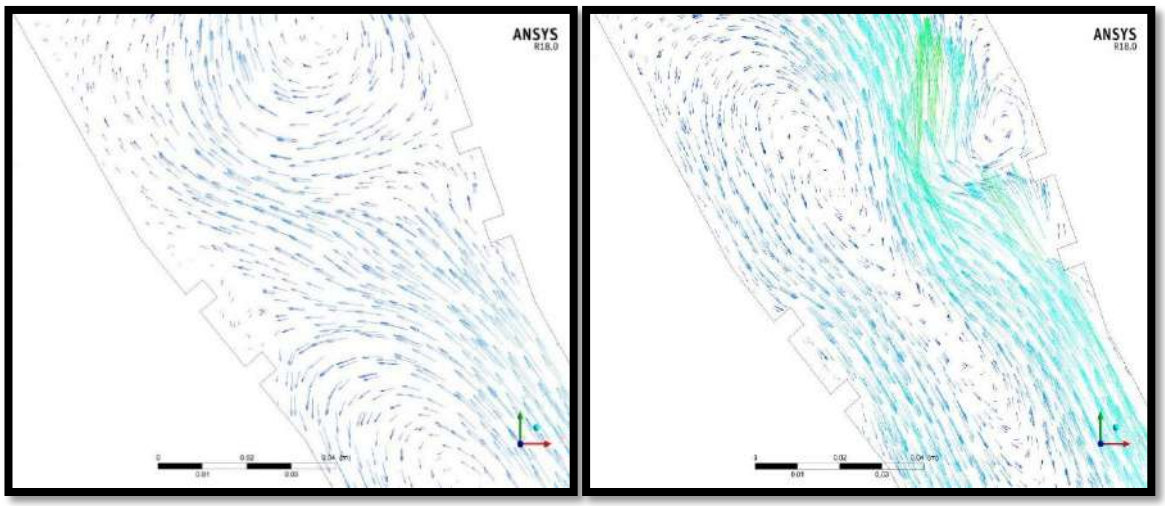

(a) Qair=5.883 L/min (b) Qair=16.66 L/min

Figure (5.25): velocity vector at 5 L/min water discharge (opening angle10 degree)

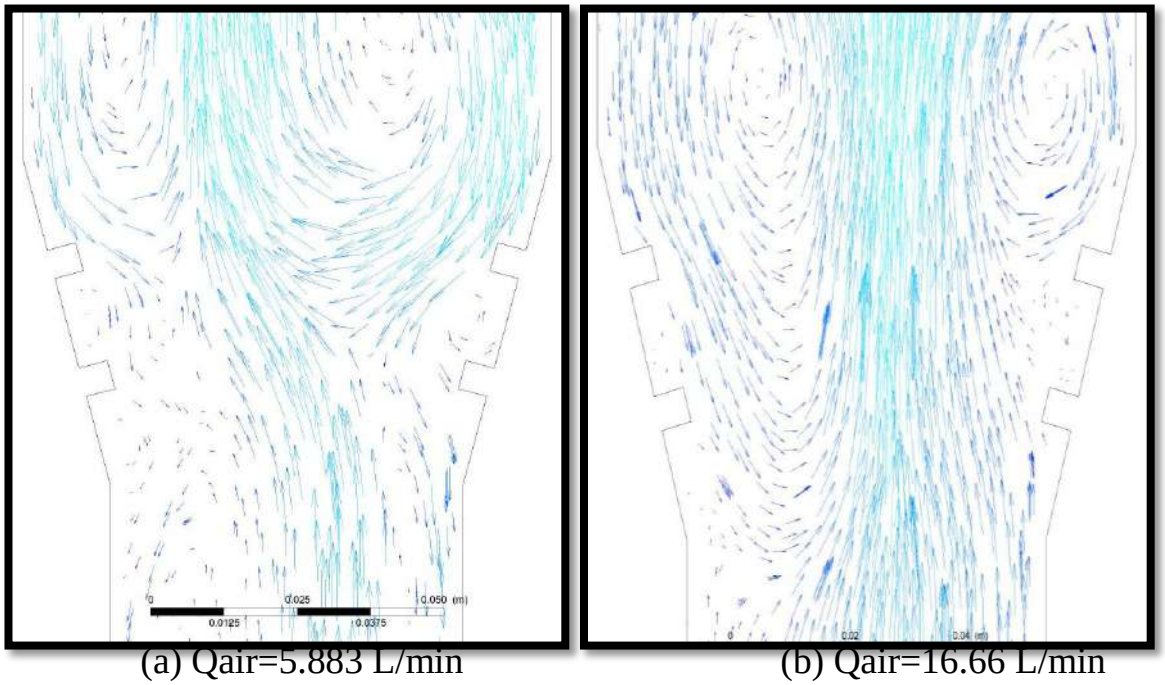

(a) Qair=5.883 L/min (b) Qair=16.66 L/min

Figure (5.26): velocity vector at 5 L/min water discharge (opening angle15 degree)

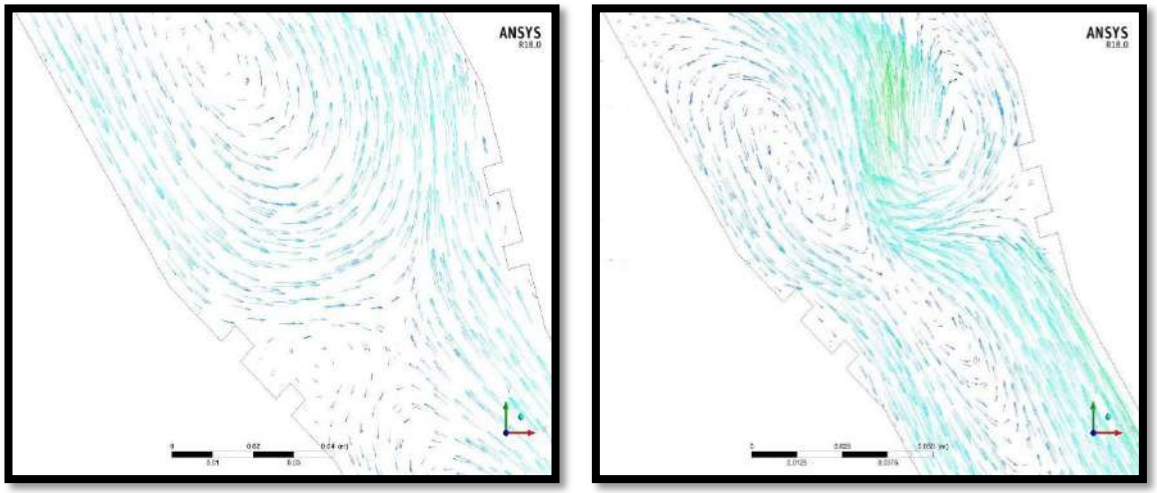

(a) Qair=5.883 L/min (b) Qair=16.66 L/min

Figure (5.27): velocity vector at 5 L/min water discharge (opening angle10 degree)

5.3.3. Comparison between experimental and numerical results

5.3.3. A. Effect of water and air discharge on the pressure profile

Observed that behavior of effect of increasing the discharge of air or water on pressure distribution was similar for experimental and numerical work. as observed that the values of experimental and numerical results were close and the maximum deviation was (7%).It was also observed that the numerical results were greater than the results of the experimental result due to neglect of several effects such as neglect of the turbulence caused by the pump and neglect of the effect of sharp edges of enter the air and water on the pressure and also neglect friction between the mixture and the walls of the channel.

Figure (5.28) to (5.31) demonstrate the compression between Effect of increasing water discharge on the experimental and numerical results of the pressure profile at four different points along the vertical test channel with opening angle 10 and 15 degrees for various values of air discharges

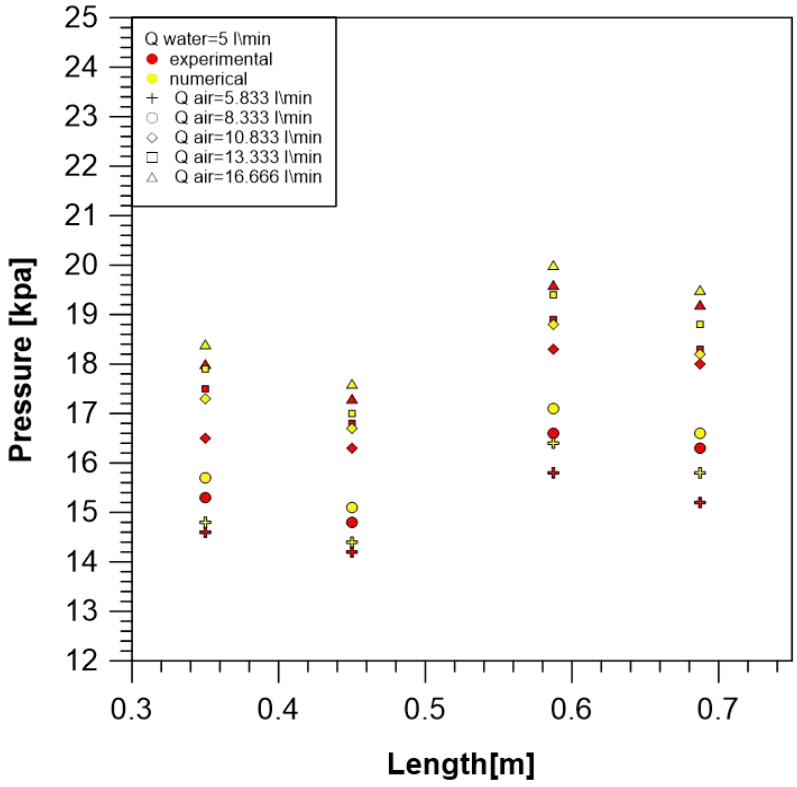

Figure (5.28a)

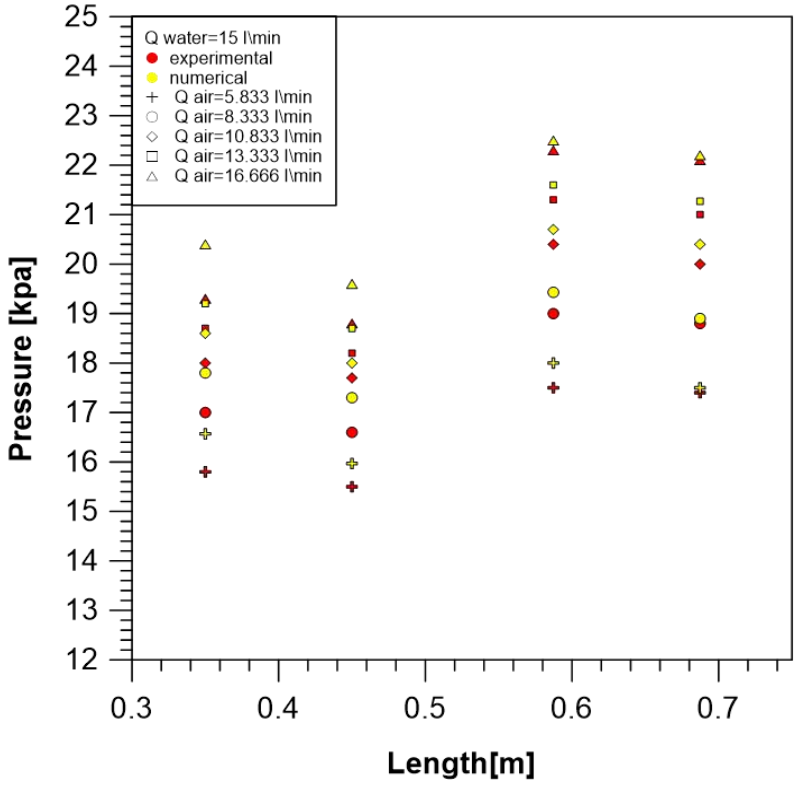

Figure (5.28b)

Figure (5.28): compression between Effect water discharge on Experimental and numerical pressure profile for opening angle 10 degree (vertical)

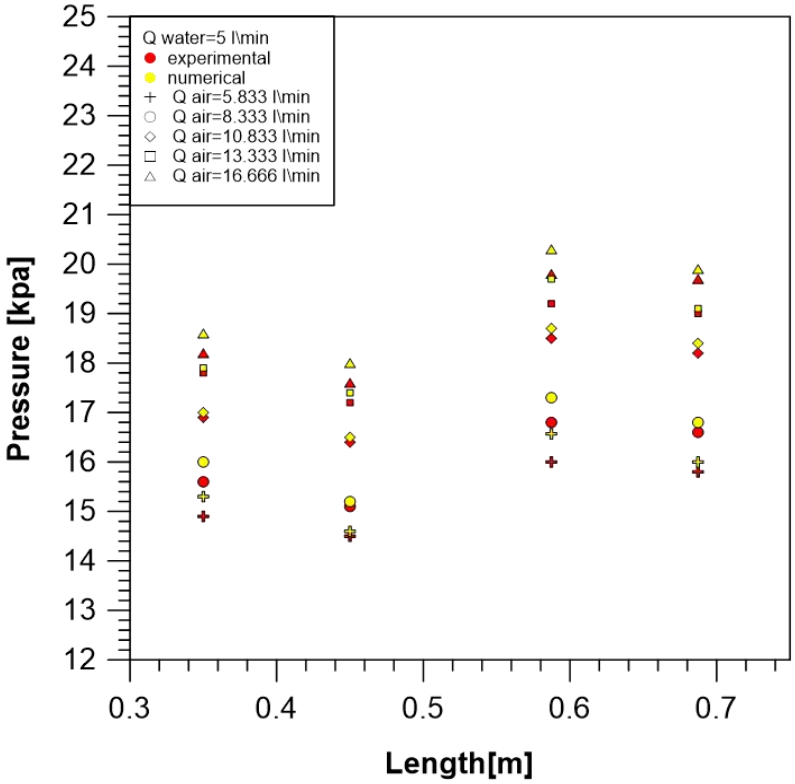

Figure (5.29a)

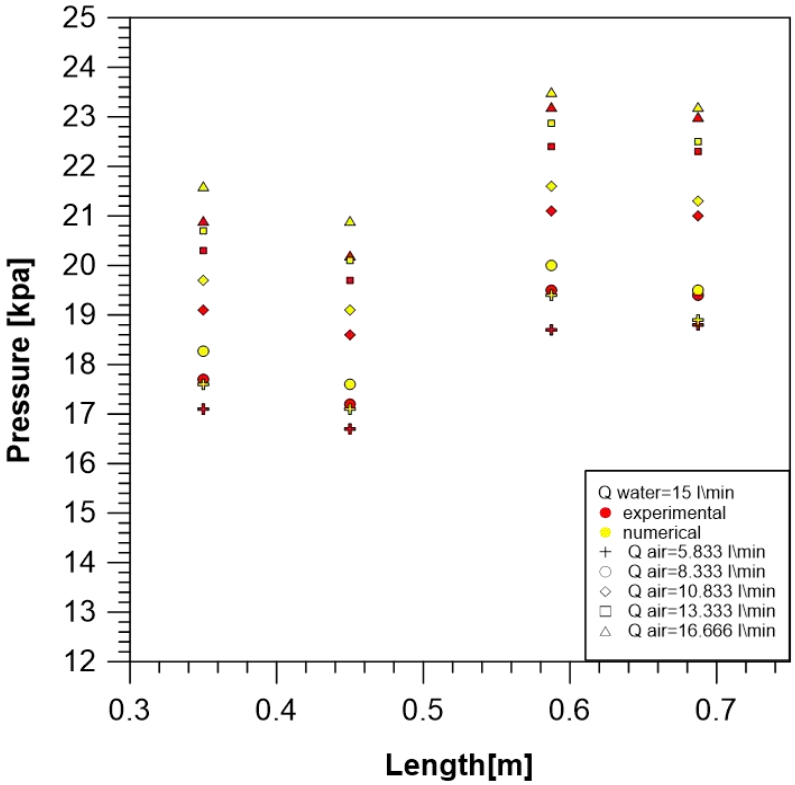

Figure (5.29b)

Figure (5.29): compression between Effect water discharge on Experimental and numerical pressure profile for opening angle 15 degree (vertical)

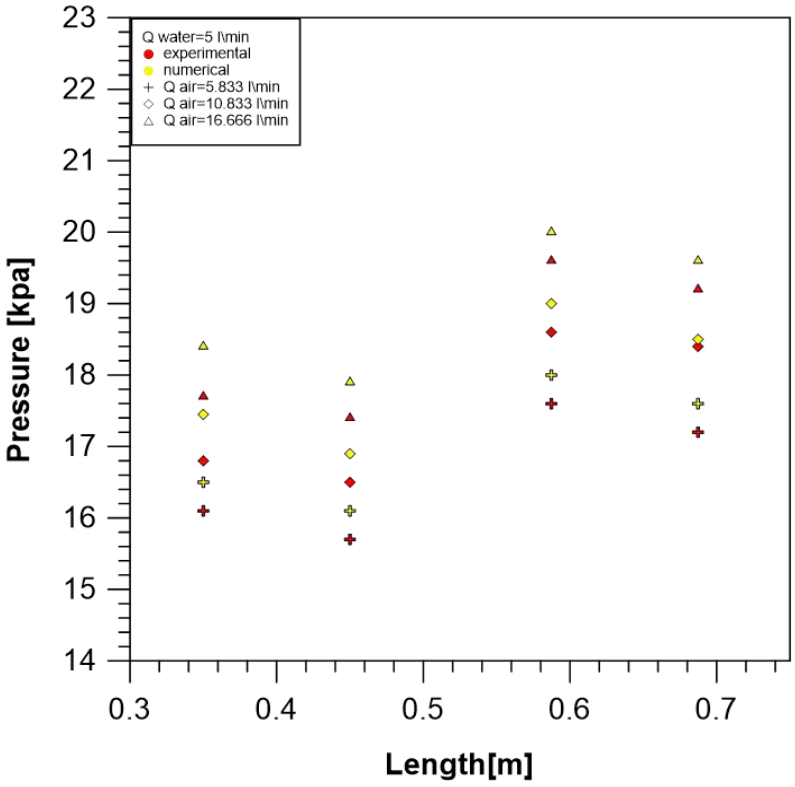

Figure (5.30a)

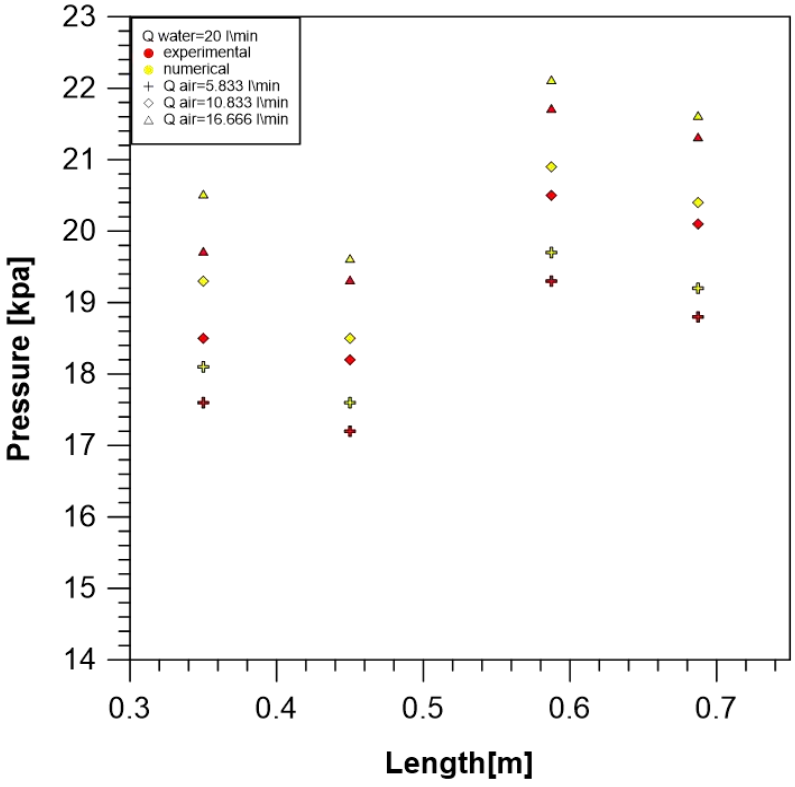

Figure (5.30b)

Figure (5.30): compression between Effect water discharge on Experimental and numerical pressure profile for opening angle 10 degree (inclined)

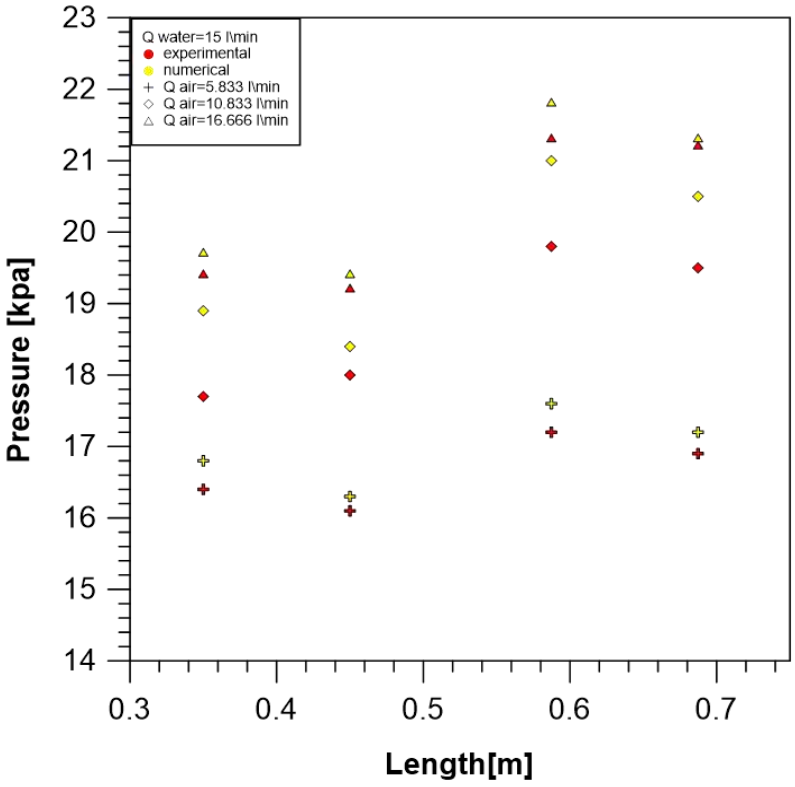

Figure (5.31a)

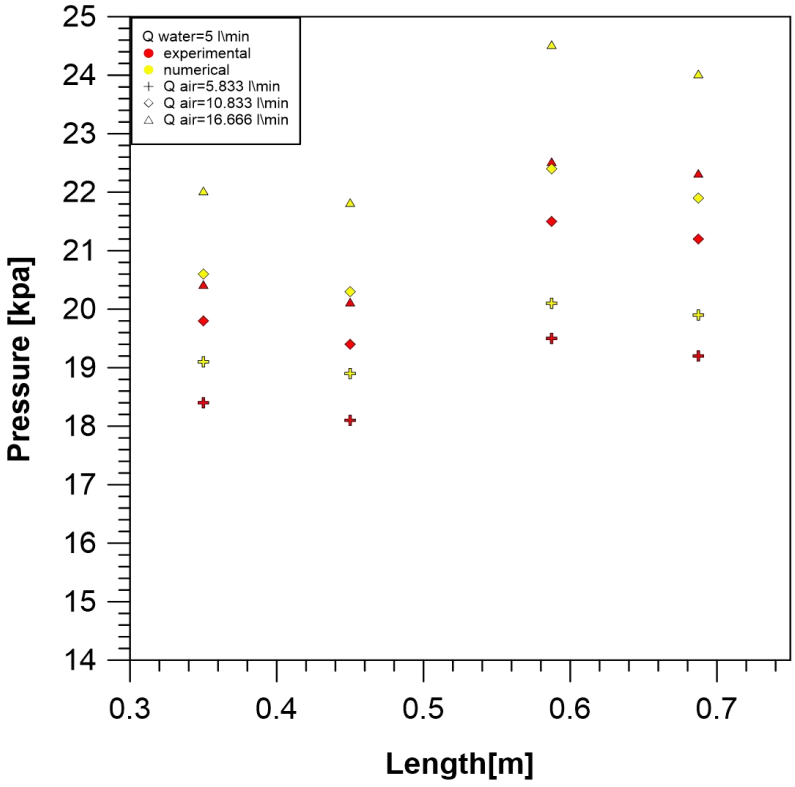

Figure (5.31b)

Figure (5.31): compression between Effect water discharge on Experimental and numerical pressure profile for opening angle 15 degree (inclined)

5.3.3. B. The influence of water and air discharge on the flow behavior

Effect of the water and air on the flow behavior are shown a figure (5.32 to 5.35). These figures show the experimental two-phase flow behavior through the photographs that were taken for the test channel and compared them with the air volume fraction found numerically with Ansys fluent 18. A close similarity was seen between the experimental and numerical image. Figure (5.32) represent the experimental and numerical images for the two-phase flow behavior in the divergence ribs rectangular vertical duct for water discharge (Qw=5 L/min) and air discharges (Qa=5.833, 10.833 and 16.666 L/min), for the opening angle of divergence 10 degrees. The figure (5.32a), Qa=5.833 shows that the number of bubbles is less and the volume of the bubble is small due to the air and water discharges being low. Also, with the increase in air discharge, the volume and number of bubbles increases, as at Qa=10.833 as shown in figure (5.32b) ,With the continuing increase of air discharge, the turbulence in flow and velocity of the vortex in the divergence section is higher compared with low air discharge cases, as shown in Figure (5.32c) at Qa=16.666 . Figure (5.33) represent images of water discharge (Qw=10 L/min) and air discharges (5.833, 10.833 and 16.666 L/min), for the opening angle of expansion of 10 degrees. These figures explain that the volume of the bubbles is smaller compared to the case of Qw=5 l/ min at the same discharge of the air with an increase in the velocity of bubbles. Figure 5.30 show images for the two-phase flow at Qw=15 L/min) and air discharges (5.833, 10.833 and 16.666 L/min). Figure (5.35) show images for the two-phase flow at Qw=20 L/min) and air discharges (5.833, 10.833 and 16.666 L/min), These figures show that the increase in discharge of the water makes the flow unstable and increases in disturbance; as also observed, eddies in the divergence section are stronger. Generally, increased discharge of air or water leads to increased velocity of the bubbles and causes more turbulence in the flow and, thus, leads to the configuration of more of the bubbles. It was also observed that the

increased water discharge has a greater effect on the turbulence of flow than the increased discharge of air.

As for the inclined flow, the effect of a discharge of air and water on the flow is similar to the vertical flow cases as shown in the form figure (5.36) to (5.38). Note that the bubbles tend to move towards the far channel wall from the inclination angle due to the influence of buoyancy force, which pushes the bubble to the far side of the channel.

Experimental Q air (a) 5.833 (b) 10.833 (c) 16.666

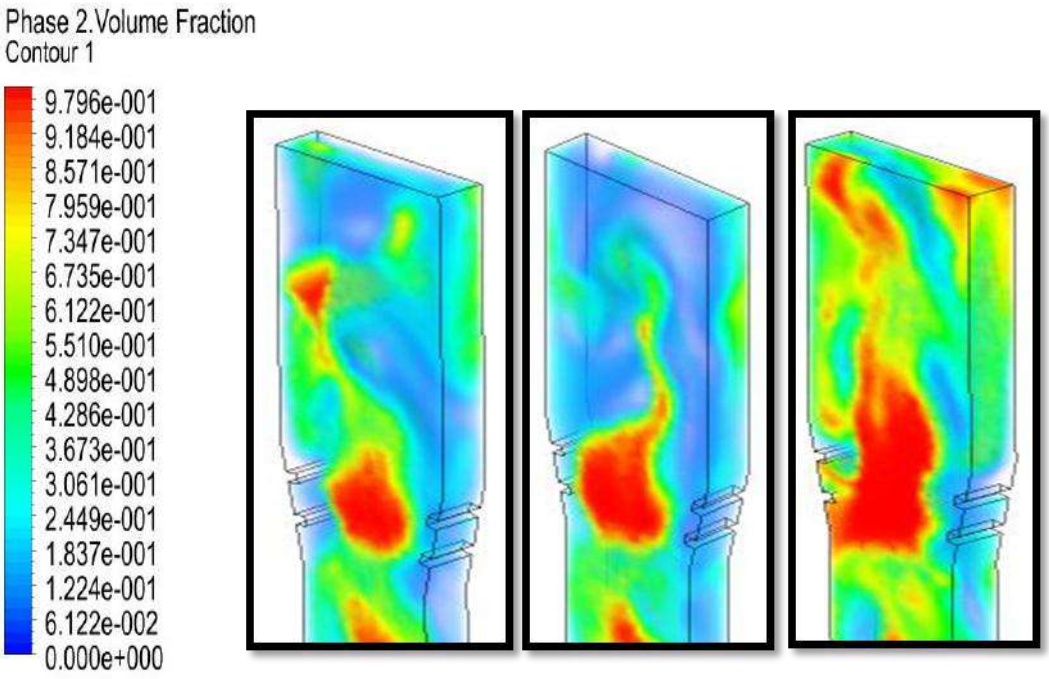

Numerical Q air (a) 5.833 (b) 10.833 (c) 16.666

Figure (5.32) compression between the experimental and numerical of effect of water and air discharge on the flow behavior at Q water =5 L/min

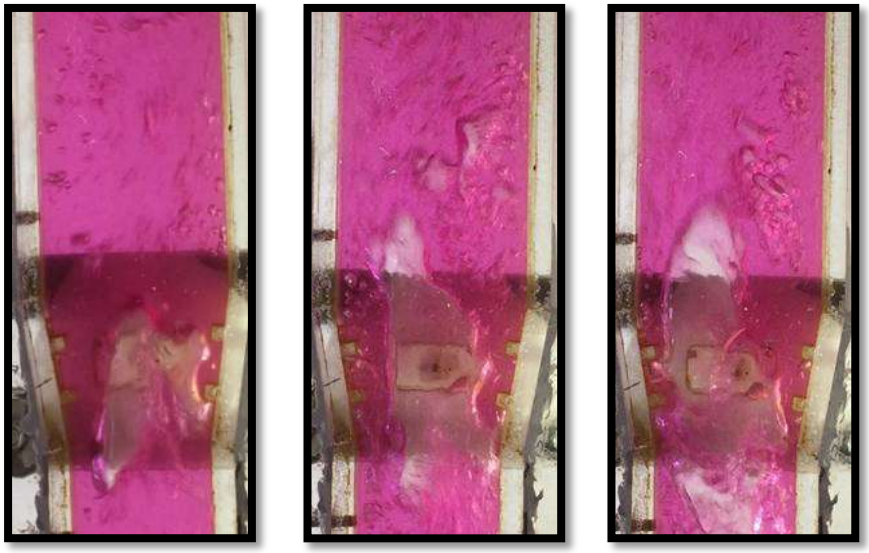

Experimental Q air (a) 5.833 (b) 10.833 (c) 16.666

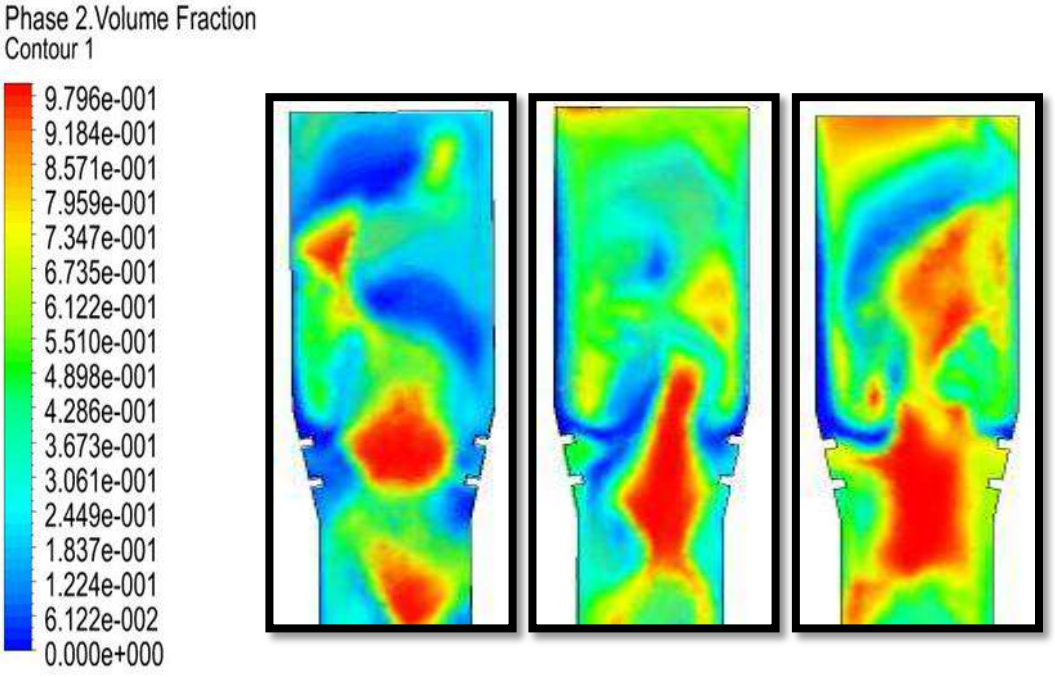

Numerical Q air (a) 5.833 (b) 10.833 (c) 16.666

Figure (5.33) compression between the experimental and numerical of effect of water and air discharge on the flow behavior at Q water =10 L/min

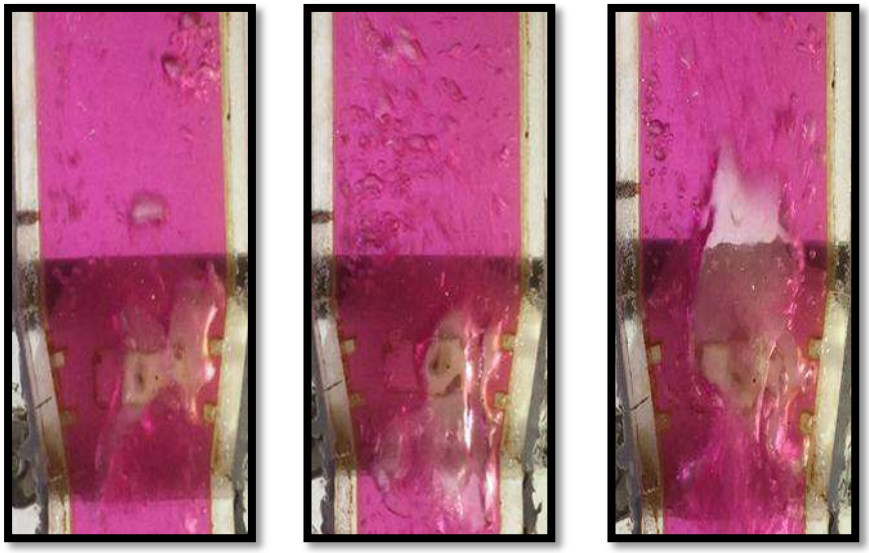

Experimental Q air (a) 5.833 (b) 10.833 (c) 16.666

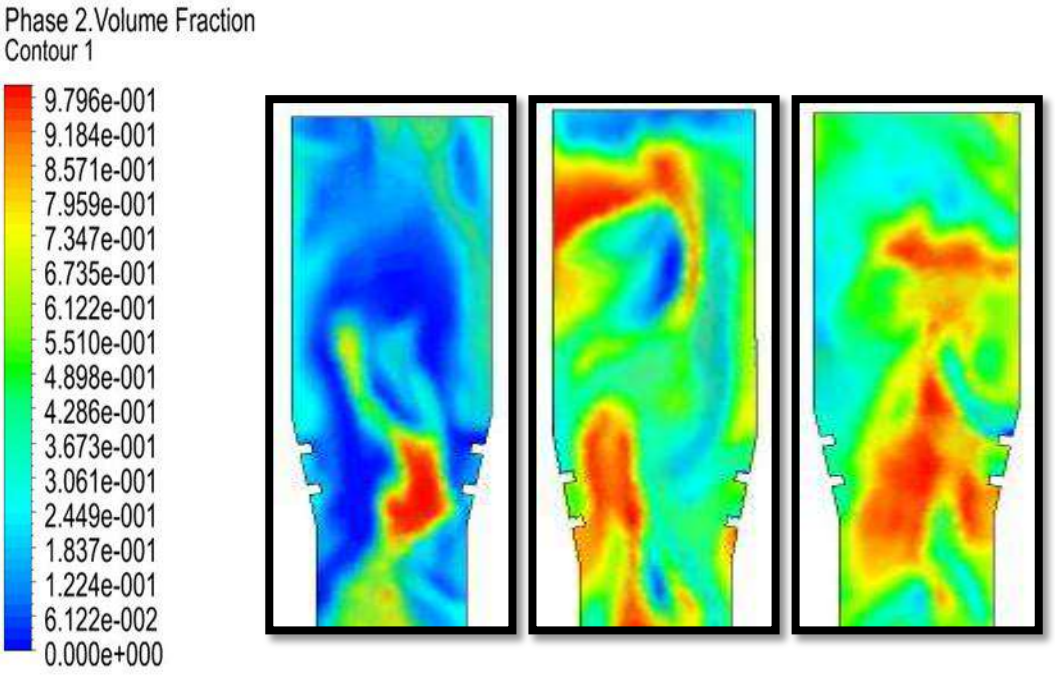

Numerical Q air (a) 5.833 (b) 10.833 (c) 16.666

Figure (5.34) compression between the experimental and numerical of effect of air discharge on the flow behavior at Q water =15 L/min

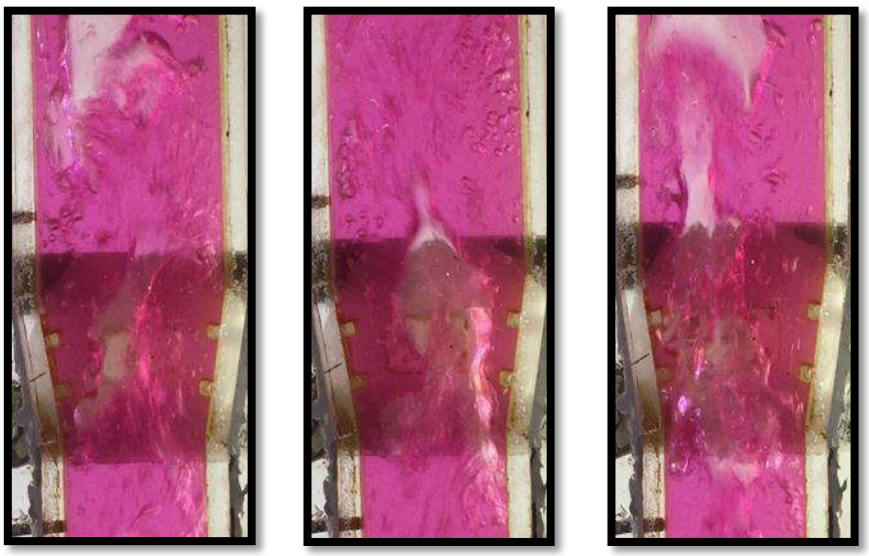

Experimental Q air (a) 5.833 (b) 10.833 (c) 16.666

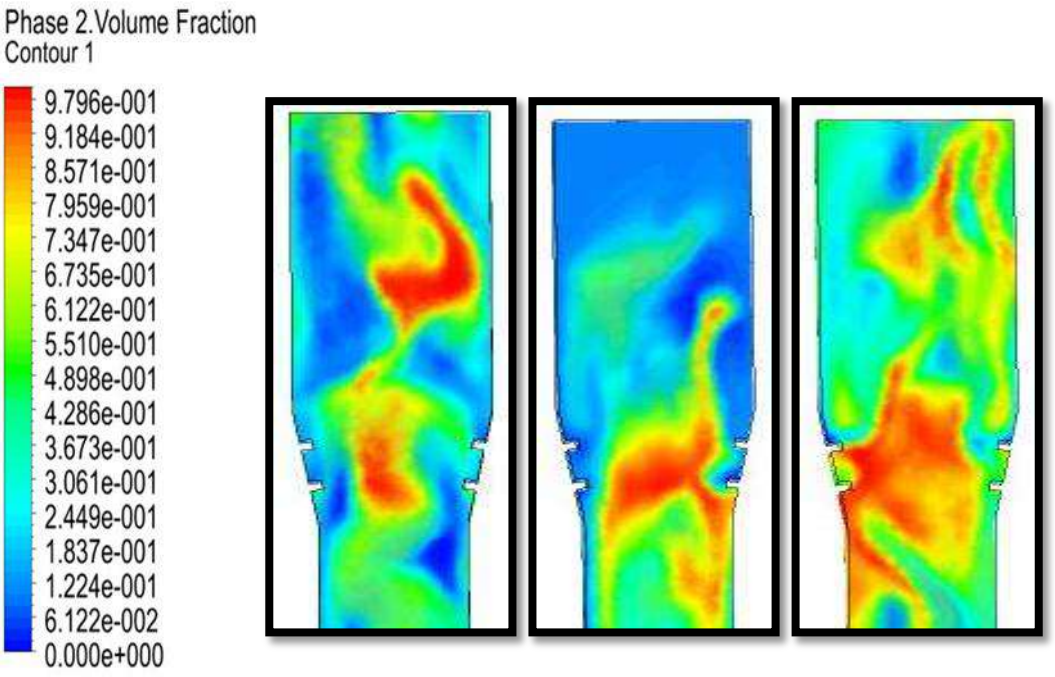

Numerical Q air (a) 5.833 (b) 10.833 (c) 16.666

F

nu

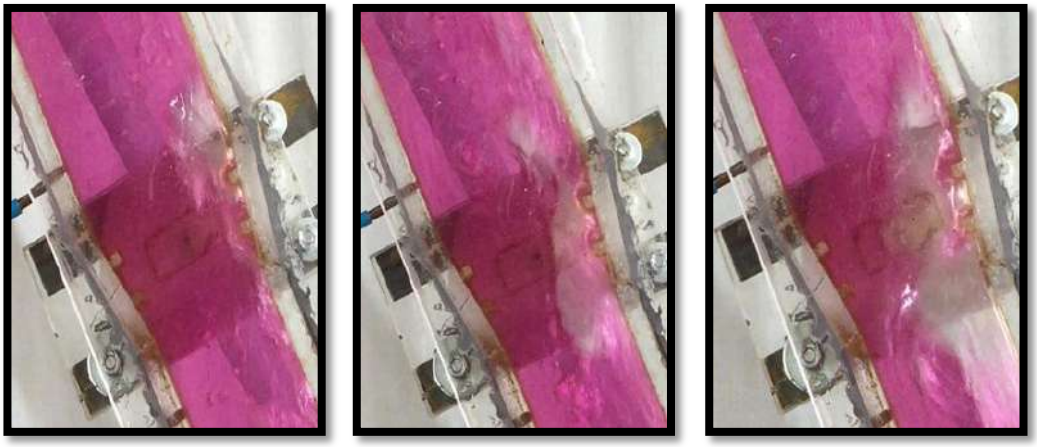

Experimental Q air (a) 5.833 (b) 10.833 (c) 16.666

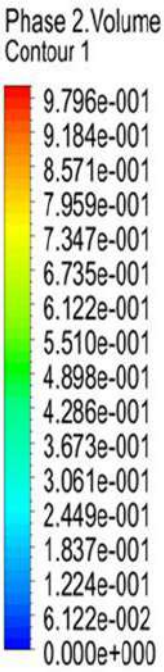

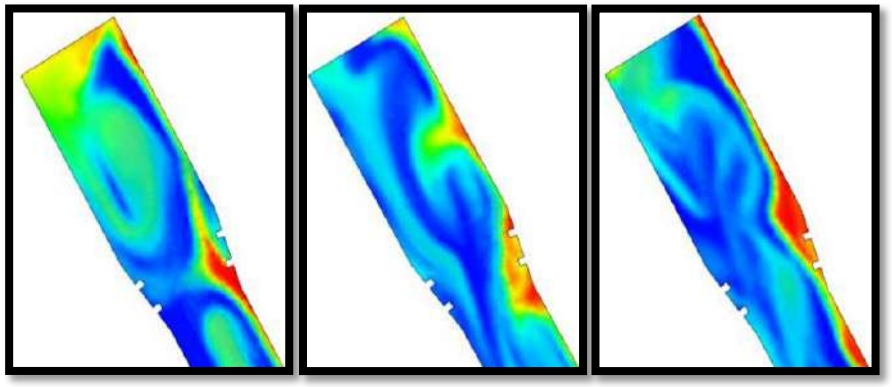

Numerical

Q air (a) 5.833 (b) 10.833 (c) 16.666

Figure (5.36) compression between the experimental and numerical of effect of air discharge on the flow behavior at Q water =5 L/min

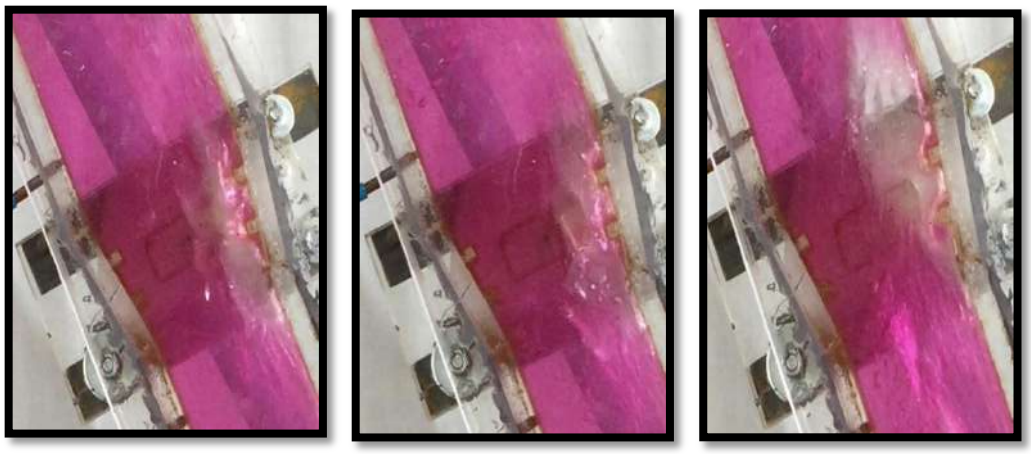

Experimental Q air (a) 5.833 (b) 10.833 (c) 16.666

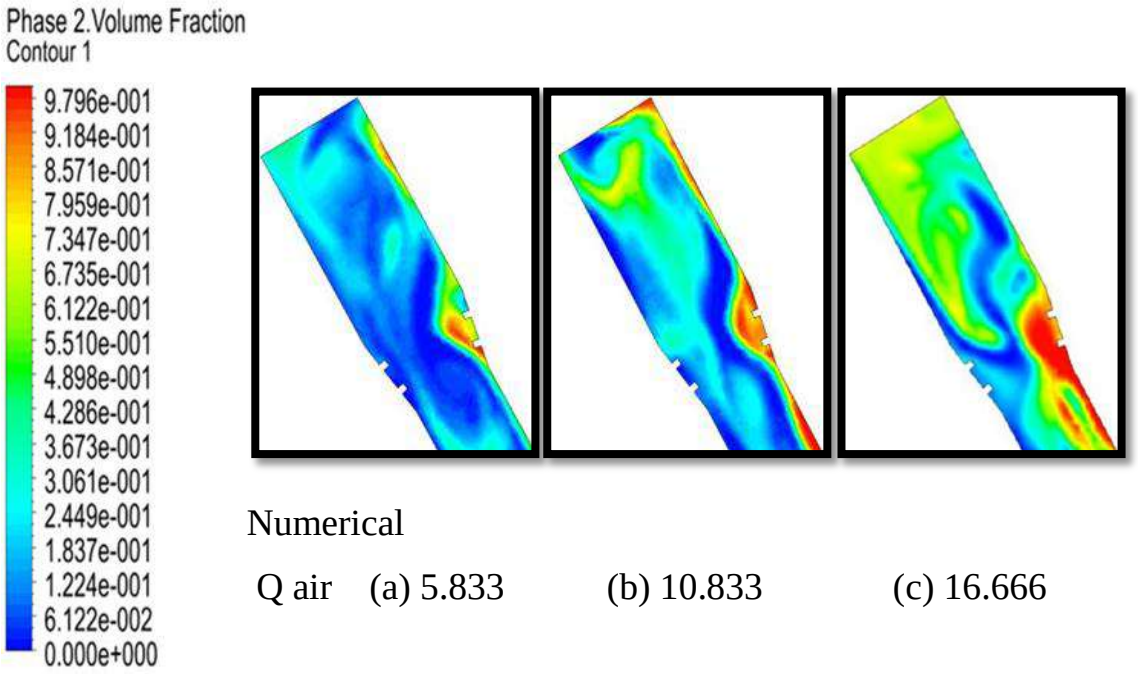

Numerical

Q air (a) 5.833 (b) 10.833 (c) 16.666

Figure (5.37) compression between the experimental and numerical of effect of air discharge on the flow behavior at Q water =15 l/min

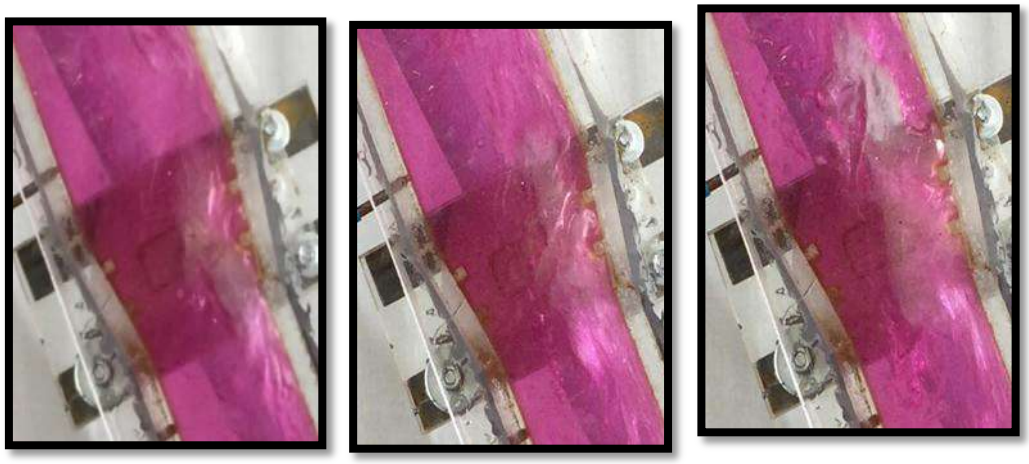

Experimental Q air (a) 5.833 (b) 10.833 (c) 16.666

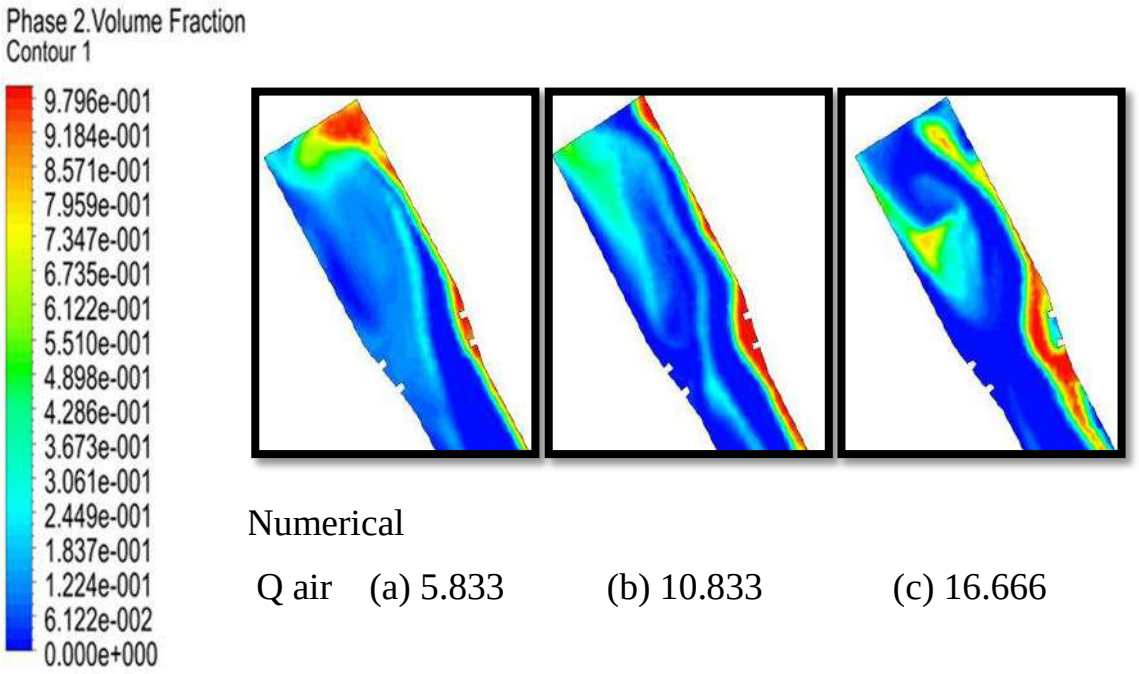

Numerical

Q air (a) 5.833 (b) 10.833 (c) 16.666

Figure (5.38) compression between the experimental and numerical of effect of air discharge on the flow behavior at Q water =20 l/min

5.3.4. Comparison of the pressure values between the vertical and inclined flow

When comparing the experimental and numerical values of pressure for case of vertical flow against inclined flow, observed that the pressure values for case of vertical flow are higher than the inclined flow case of both the experimental and the numerical values because, for the case of vertical flow, the column of the mixture is higher for vertical flow case than inclined flow at same location of pressure traducer.

The Figure (5.39) illustrates a comparison between the values of the experimental and numerical pressure between the state of the vertical and the inclined flow at the value of the discharge of water 5 L/min and different air discharge. observe that the experimental and numerical pressure value for the case of vertical flow is 18.2 and 18.6 kpa respectively, at the location of pressure transducer 0.35 cm and air discharge 5 L/ min, with divergence opening angle 10 degrees. While experimental and numerical pressure value for the case of inclined flow is 16.4 and 16.6 kpa respectively, under the same conditions.

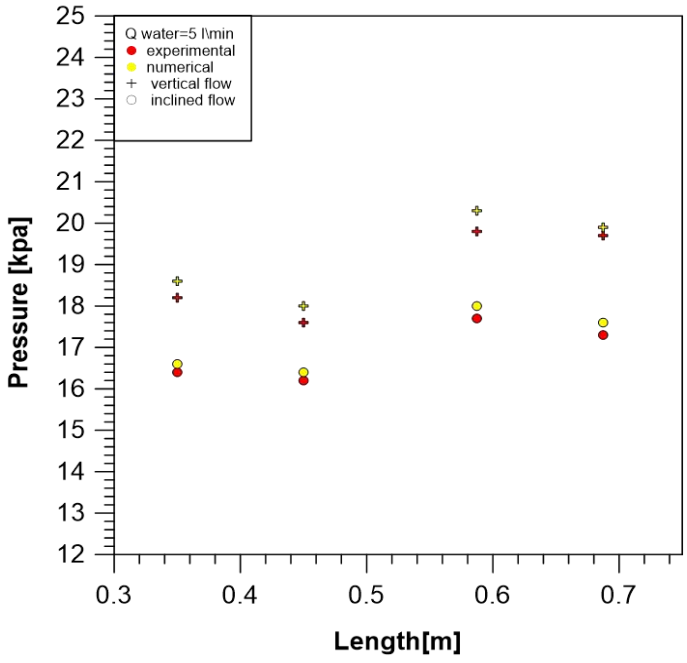

Figure (5.39): Comparison the pressure values between the vertical an inclined flow

5.3.5. Visualization and flow pattern maps

By observing the flow during the vertical divergence test section, we observe that the current flow pattern at the downstream and upstream for the divergence section is the slug flow, While the flow pattern through the divergence section cannot be determined due to the high disturbance caused by the mixing of the phases due to the presence of the ribs, in particular when air or high water discharge, as shown in Figure (5.40). Figure (5.41) shows the flow pattern map at the upstream divergence test channel. A common chart is the one proposed by Hewitt and Roberts (1969)[7] that has been established for vertical flow in pipes of the constant cross section. The flow map for upstream shows that the test cases precedent in (Table 4.6) are residing on the slug and churn, in contrast to the observation during the experiment that showed that the flow pattern is only slug flow. This is because some experiment conditions of the present work do not correspond to the standard conditions of Hewitt and Roberts' (1969)[7] map.

For the inclined flow, the dominant flow pattern is the slug flow too as shown in the figure (5.42). In the present work, has been used the Proposed flow map by Barnea (1960)[6]. Note that it achieves excellent prediction for present work as shown in Figure (5.43), where we note that all points are located in the region of a slug.

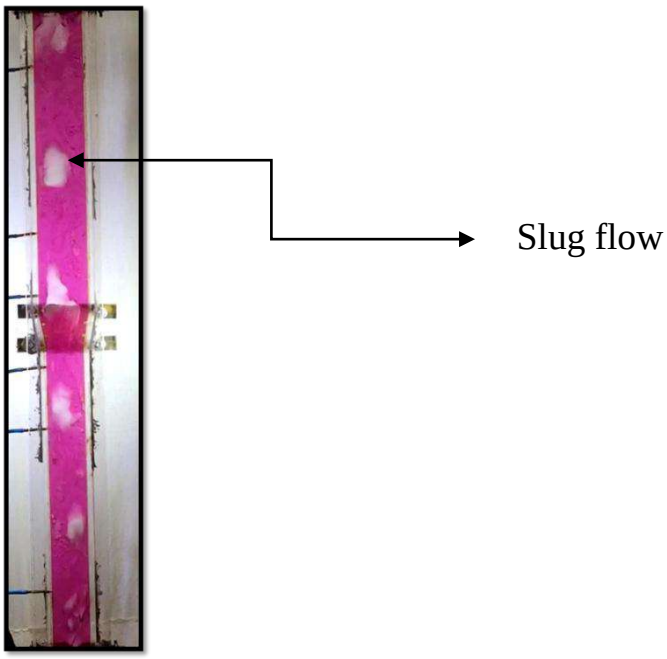

Figure (5.40): flow pattern in vertical channel

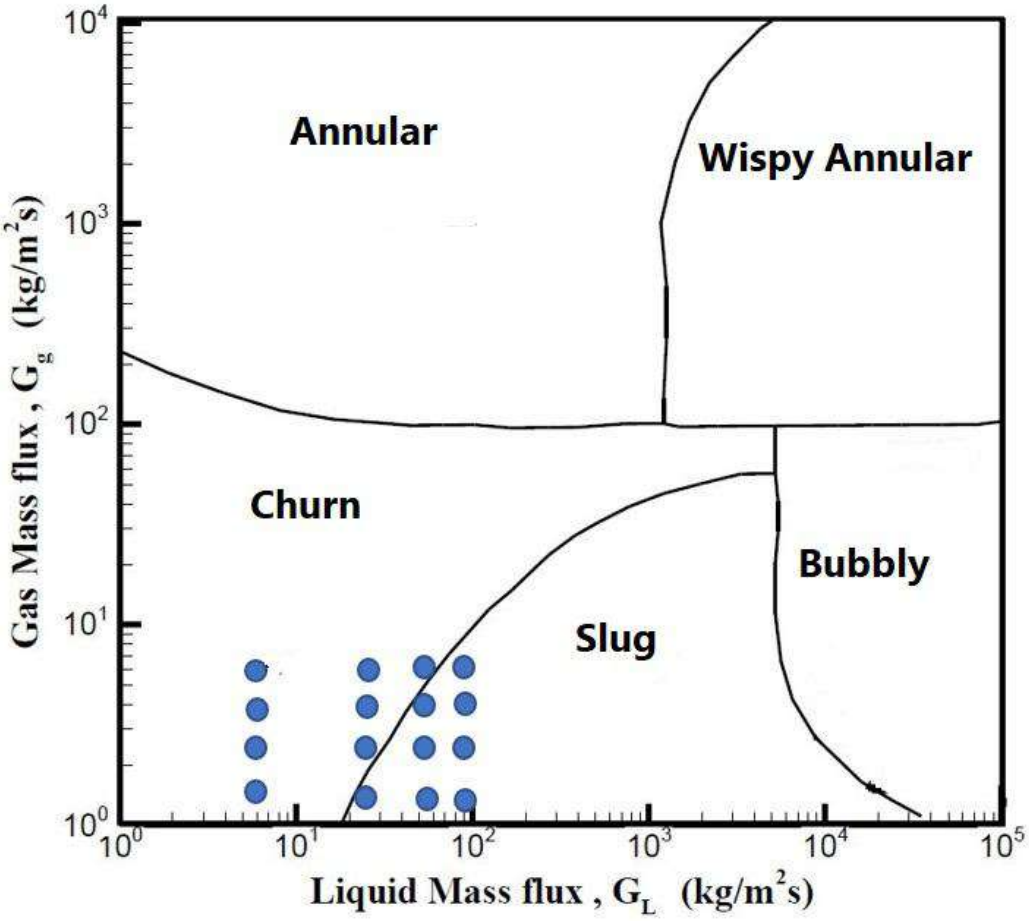

Figure (5.41): Flow pattern map of Hewitt and Roberts (1969) for vertical flow

Figure (5.42): flow pattern in inclined channel

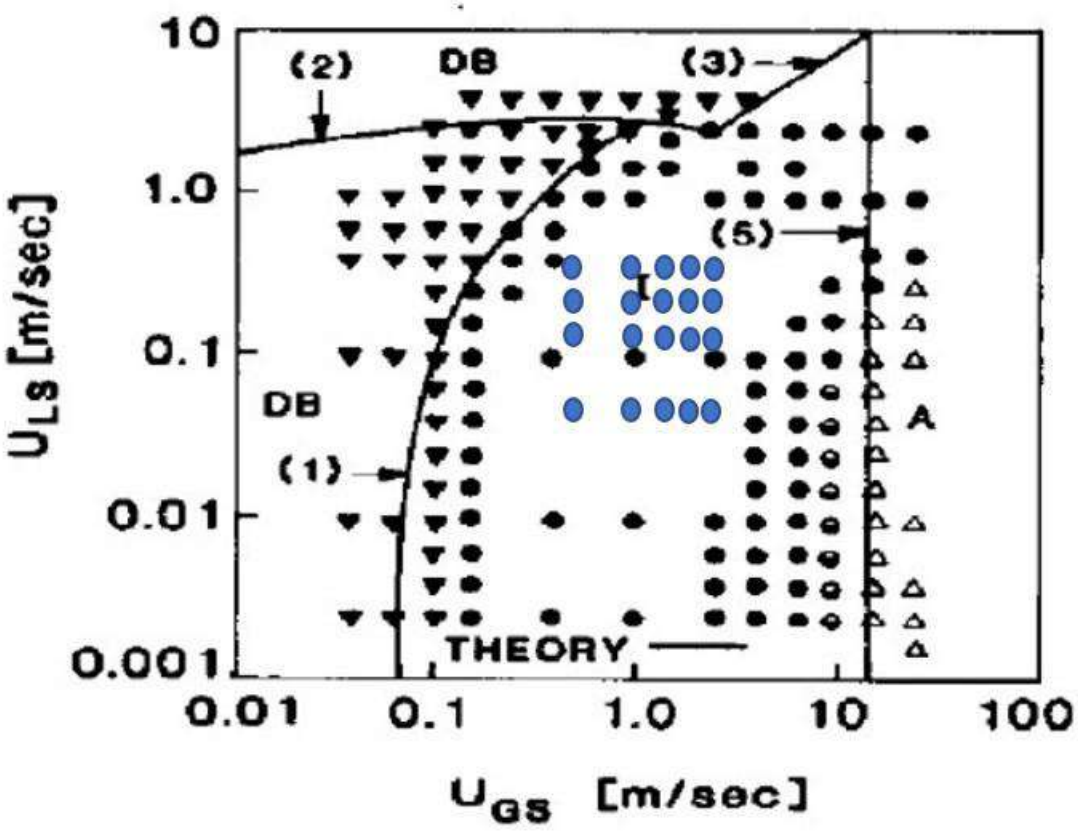

The symbol in this flow patterns map is defined in figure (5.44)

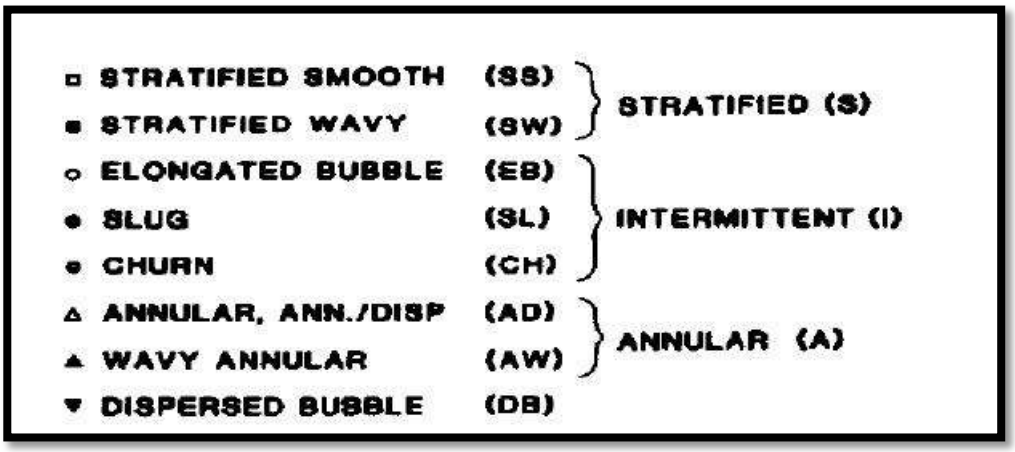

Figure (5.44)

the symbol represents ● the test cases in the present work According to the Table 5.1 for water and Table 5.2 for air

Figure (5.43) Flow pattern map Barnea (1980) for inclined flow

5.4. Two-phase flow through the convergence section for vertical and inclined position

5.4.1 Experimental results

5.4.1. A. Effect of water and air discharge on the pressure profile

The experimental results of the impact of increasing air and water discharge on the pressure profile can be shown in figures (5.45) to (5.48). It can be seen from these figures that the pressure of the test channel decreased from the bottom to the top, especially in the convergence section. Can be seen too, the effect of increased water or air discharge for the case of converge section is similar to that of divergence section, Where observe that pressure profile increases with increased air or water

Figure (5.45) and (5.46), deals the experimental results of the pressure profile for vertical test channel with opening angle 10 and 15 degrees, respectively with different air discharge (5.833,8.333,10.833,13.333 and 16.666 L/min) for water discharge (5,10,15,20 L/min. as the discharge of the water increase from 5 L/min to 20 L/min at same location of pressure transducer and constant air discharge (0.35 m and 5.833 L/min), the value of the experimental pressure increase from 16.1 kpa to 18.5 kpa for opening angle 10 degree, and from 15.9 kpa to 18.8 kpa for opening angle 15 degree.

In figure (5.47) and (5.48), shows the experimental results of the pressure profile for inclined test channel with opening angle 10 degrees, with different air discharge (5.833,10.833 and 16.666 L/min) for water discharge (5,10,15,20 L/min). as the discharge of the water increase from 5 L/min to 20 L/min at same location of pressure transducer and constant air discharge (0.35 m and 5.833 L/min), the value of the experimental pressure increase from 15.1 kpa to 16.8 kpa for opening angle 10 degree ,and from 15.4 kpa to 17.3 for opening angle 15 degree.

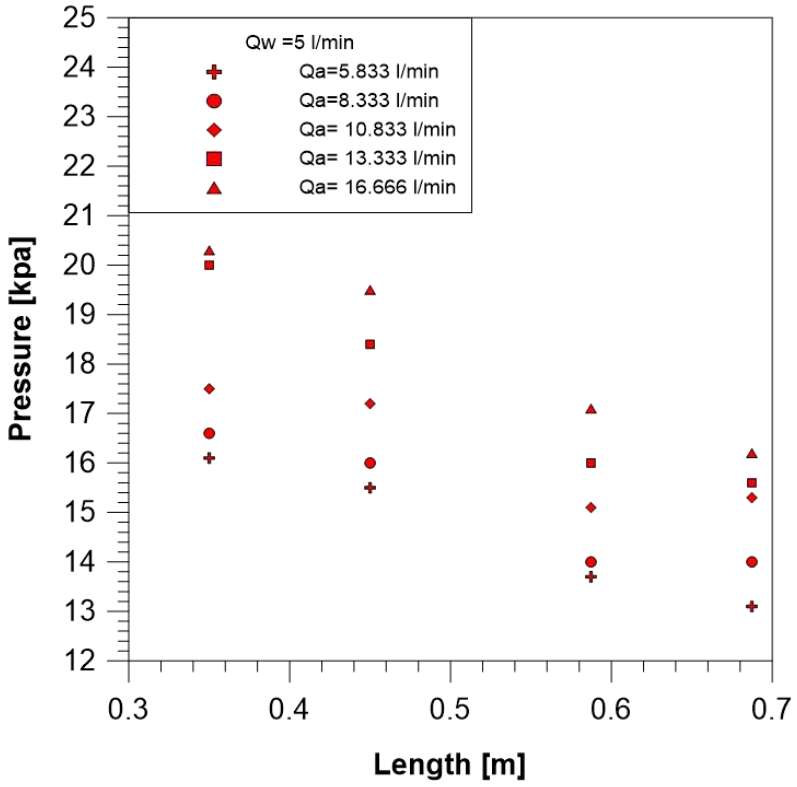

Figure (5.45a)

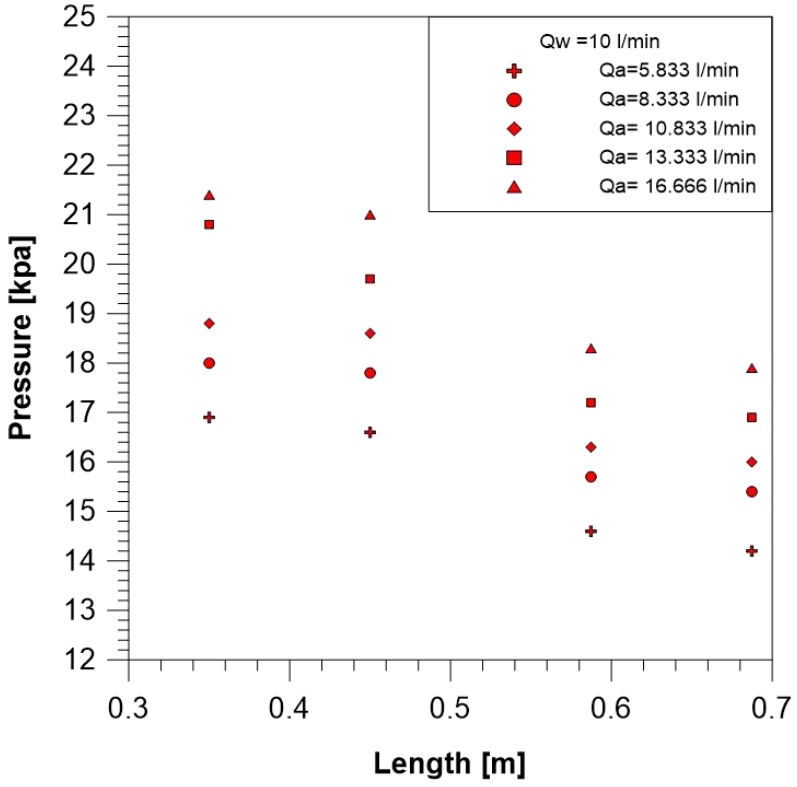

Figure (5.45b)

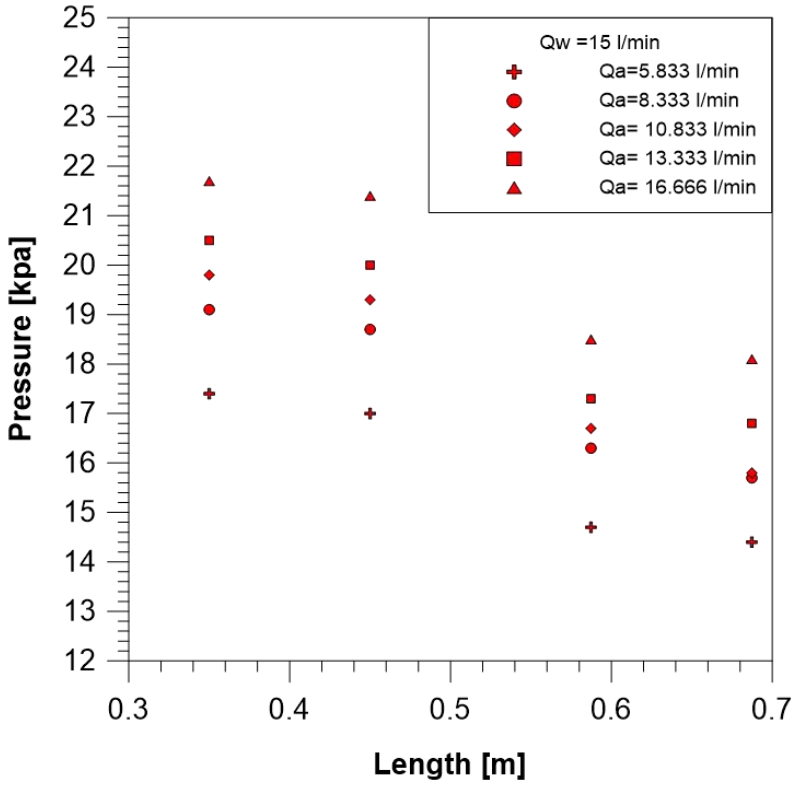

Figure (5.45c)

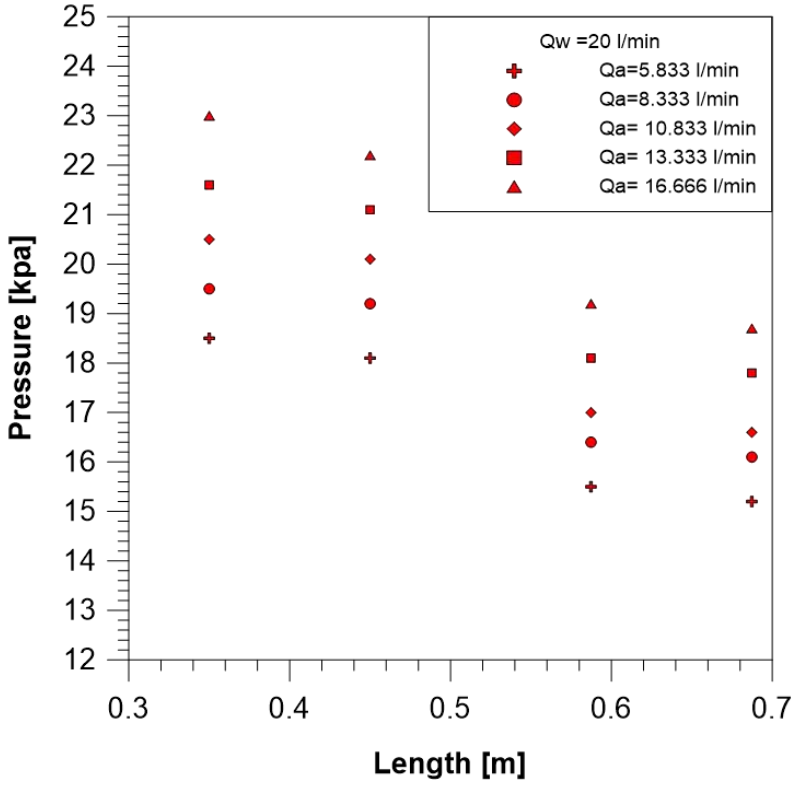

Figure (5.45d)

Figure (5.45): Effect water discharge on
Pressure profile for convergence angle 10 degree (vertical)

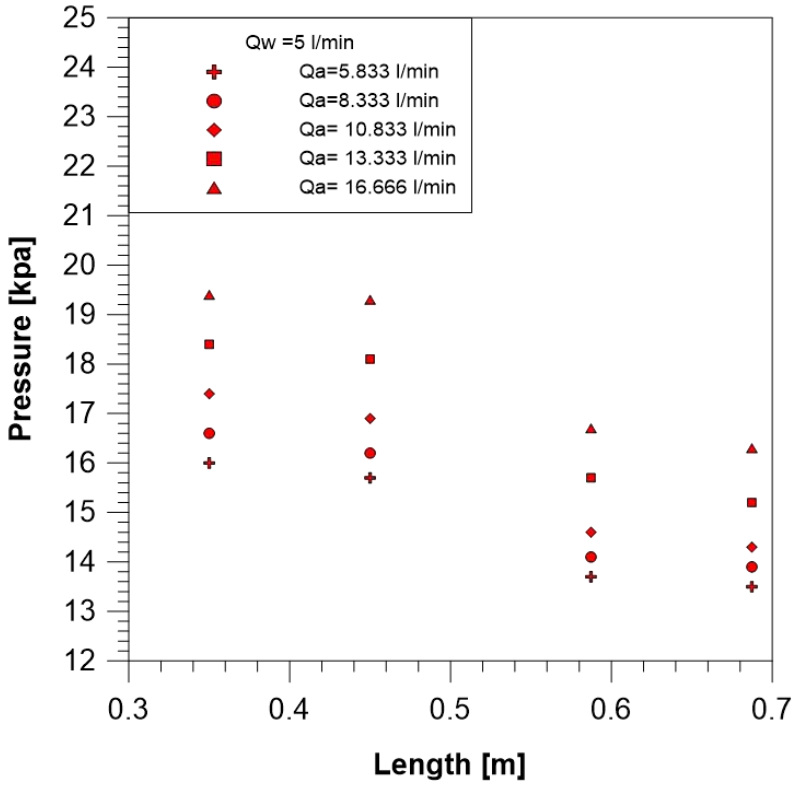

Figure (5.46a)

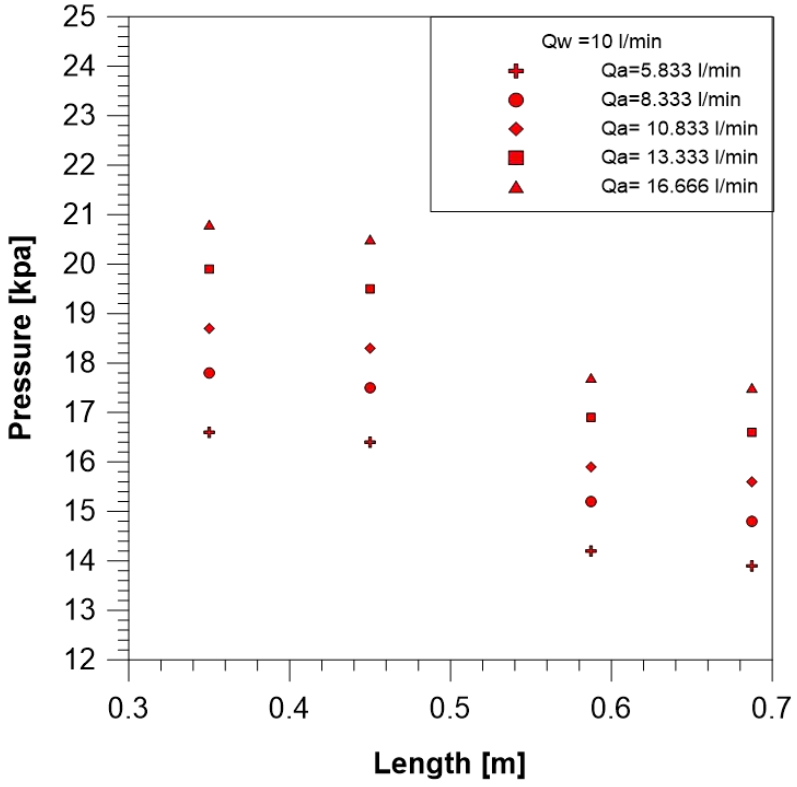

Figure (5.46b)

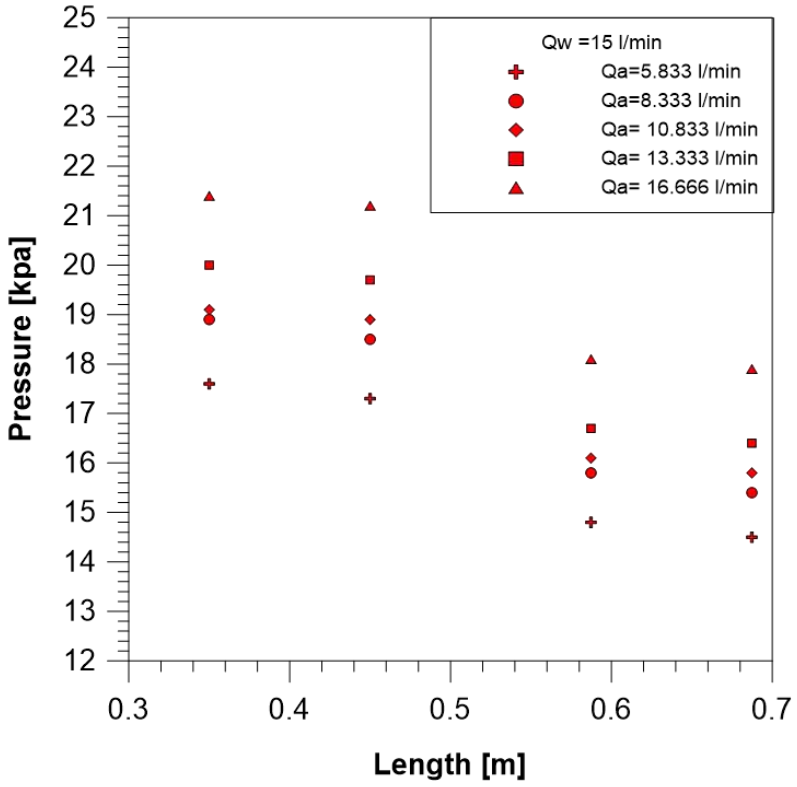

Figure (5.46c)

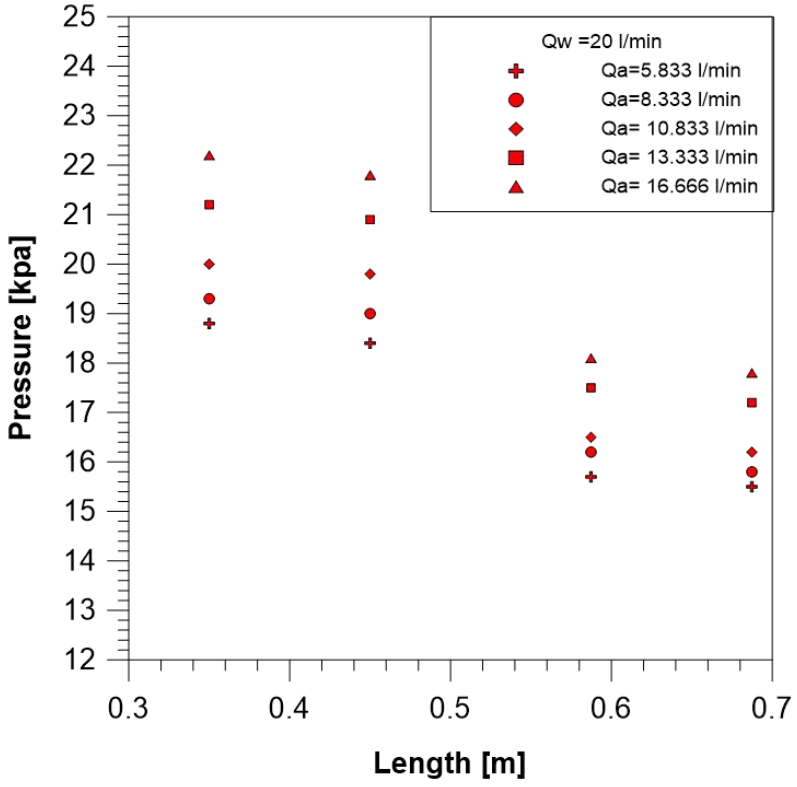

Figure (5.46d)

Figure (5.46): Effect water discharge on
Pressure profile for convergence angle 15 degree (vertical)

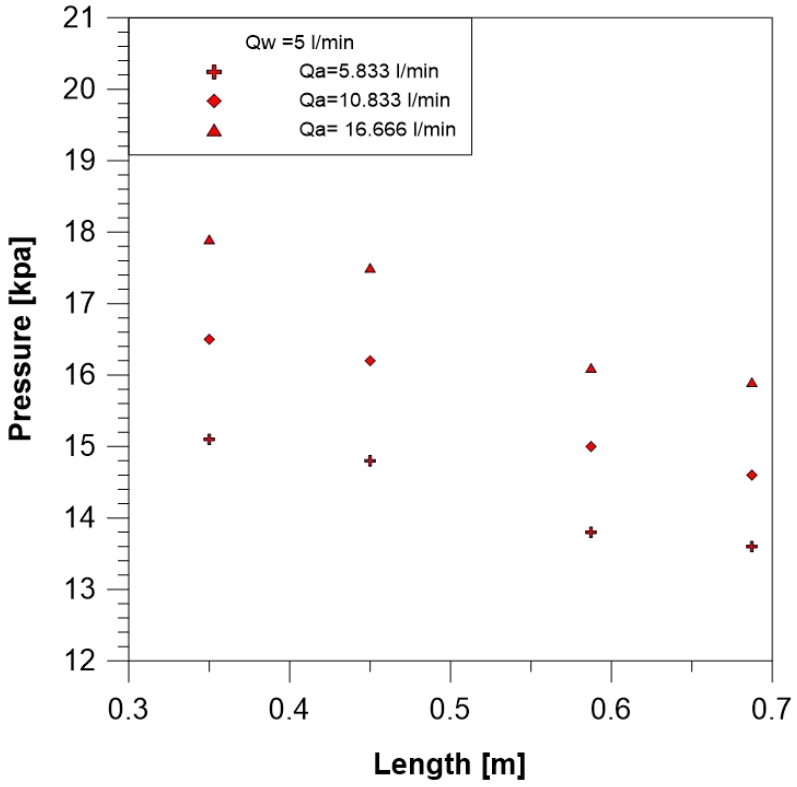

Figure (5.47a)

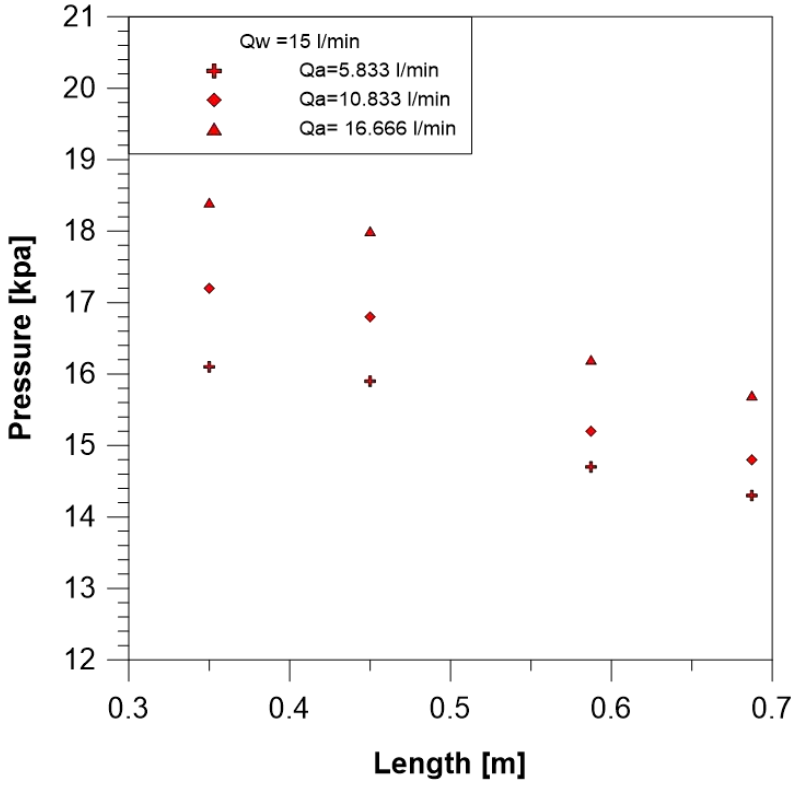

Figure (5.47b)

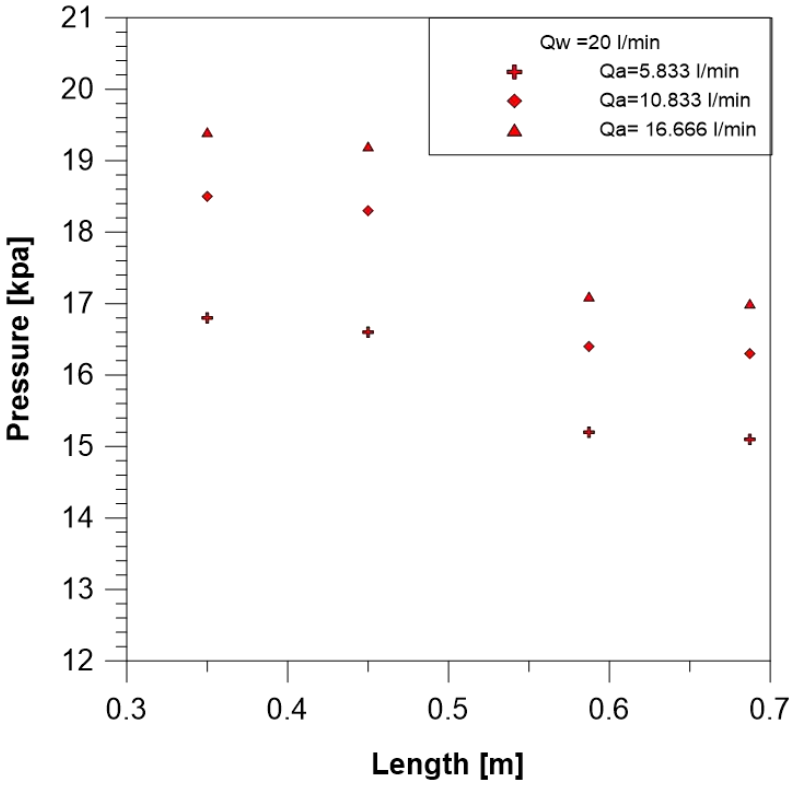

Figure (5.47c)

Figure (5.47): Effect water discharge on
Pressure profile for convergence angle 10 degree (inclined)

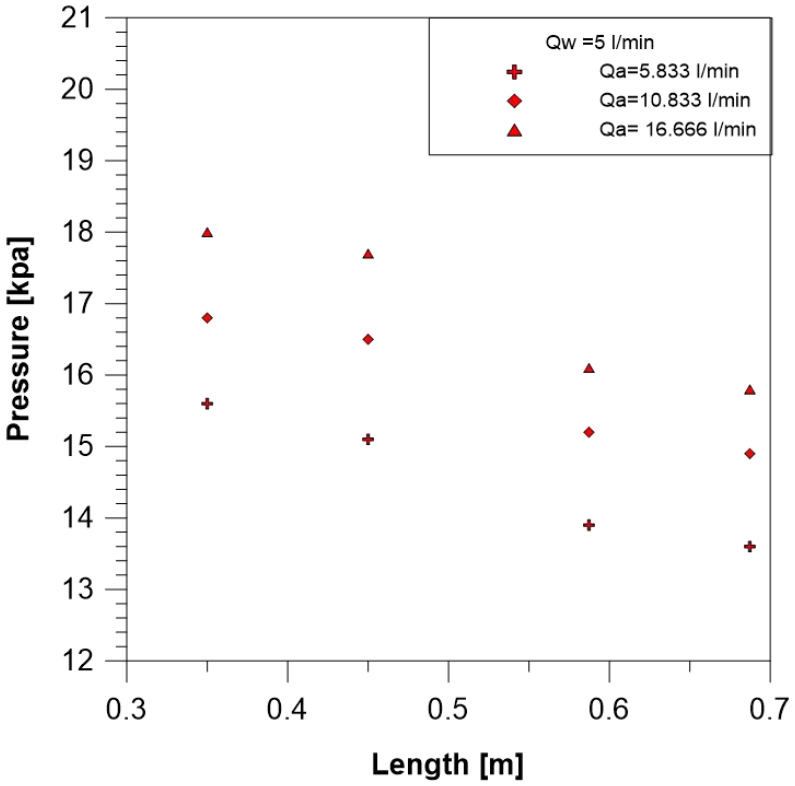

Figure (5.48a)

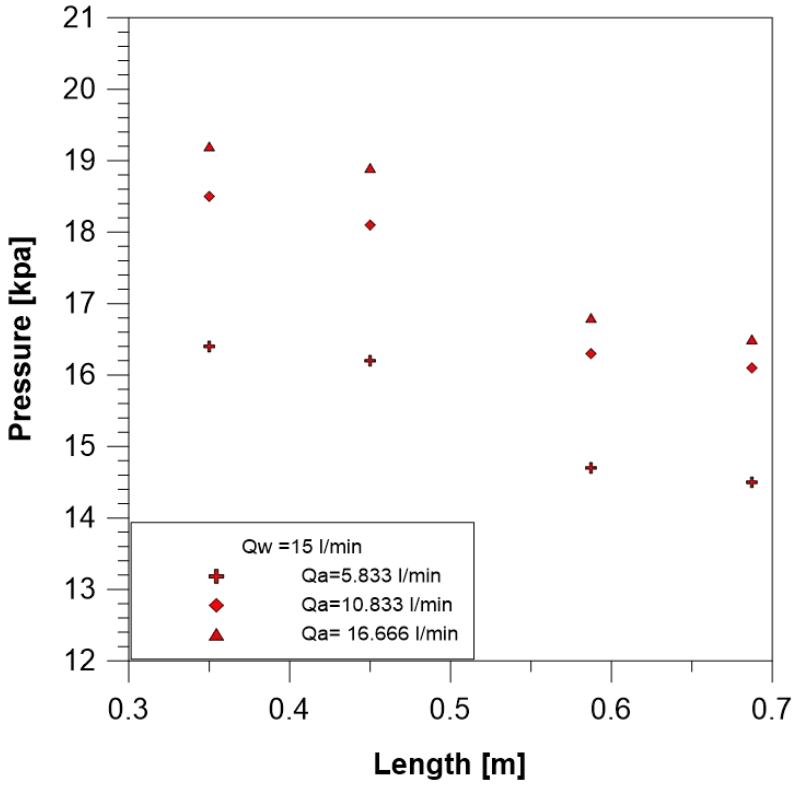

Figure (5.48b)

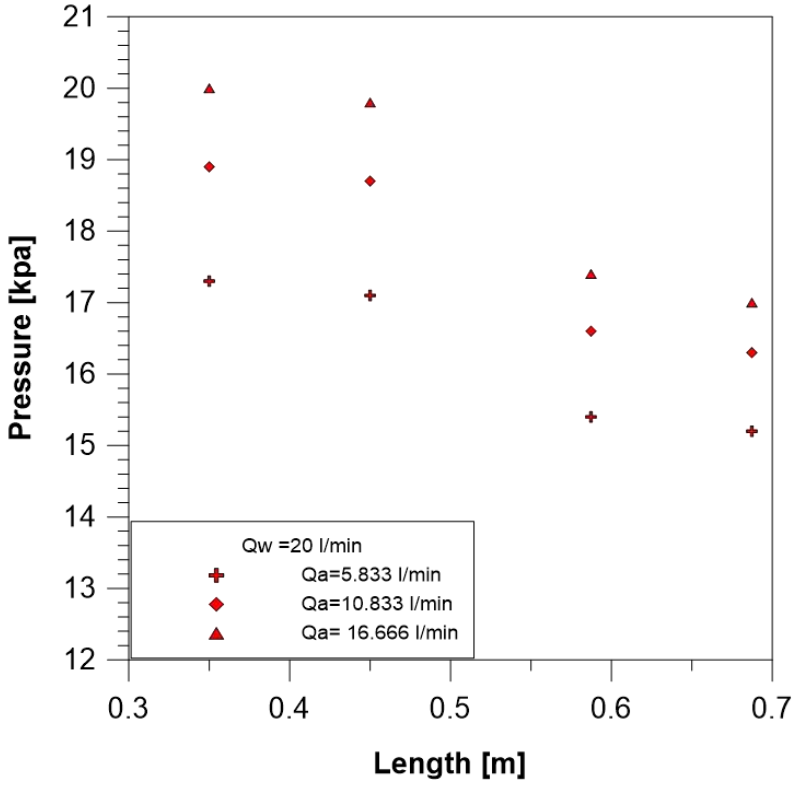

Figure (5.48c)

Figure (5.48): Effect water discharge on
Pressure profile for convergence angle 15 degree (inclined)

5.4.1. B. Effect of water and air discharge and opening angle on the drop pressure

The experimental results of the effect of increasing air and water discharge and effect of increasing of opening angle on the drop pressure through the convergence section can be shown in Figure (5.49) to (5.52). It can be seen from these figures that the drop pressure increases with increasing discharge of air or water for both the 10 and 15 opening angles. It was observed, too, that the effect of increasing the opening angle on the pressure drop in the case of convergence section is contrary to the effect of increasing the angle divergence on the recovery of pressure in the case of divergence section, where note that drop pressure for the opening angle 15 is more than the drop pressure at the opening angle 10 at the same air and water discharge because the eddies are more for the case of angle 15 because of the additional flow area Contributes to the promotion of pressure drop , leading to make the drop pressure more than the case of opening angle of 10 degrees.

Figure (5.49) and (5.50) shows the experimental drop pressure through the vertical convergence section for opening angle 10 degrees and 15 respectively with different air discharge (5.833,8.333,10.833,13.333 and 16.666 L/min) for water discharge (5,10,15,20 L/min) .as the air discharge increased from (5.833 to 16.666 L/min) at constant water discharge (5 L/min),the value recovery pressure increase from (1.8 kpa to 2.4 kpa) for opening angle 10,and from (2 kpa to 2.7 kpa)..

Figure (5.51) and (5.52) shows the experimental drop pressure through the inclined convergence section for opening angle 10 and 15 respectively degree with different air discharge (5.833,8.333,10.833,13.333 and 16.666 L/min) for water discharge (5,10,15,20 L/min) .as the air discharge increased from (5.833 to 16.666 L/min) at constant water discharge (5 L/min),the value recovery pressure increase from (1kpa to 1.5 kpa) for

opening angle 10 ,and from (1.2 kpa to 1.6 kpa) for opening angle 15 degree.

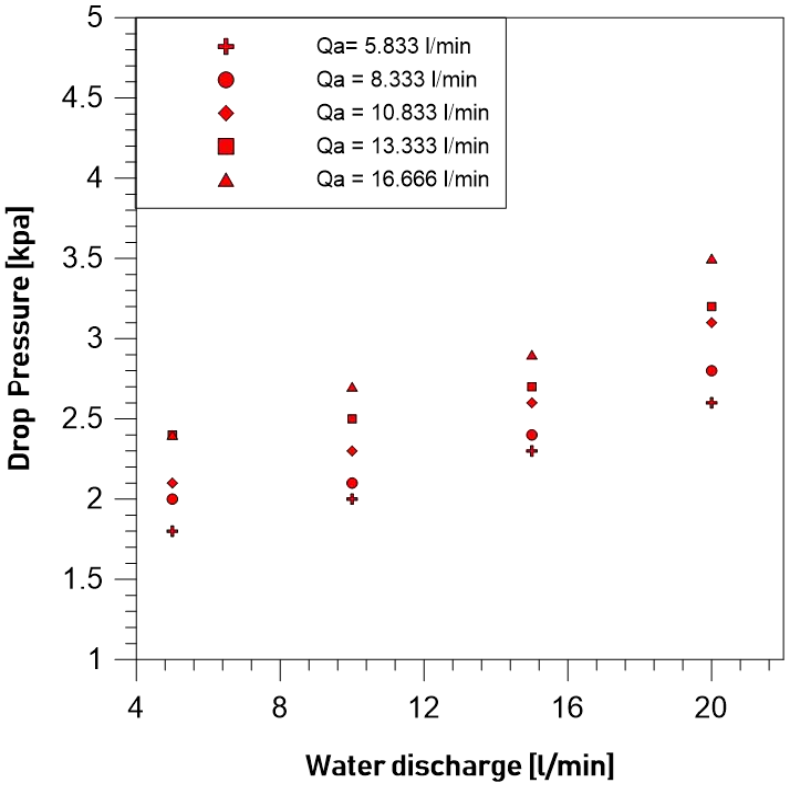

Figure (5.49): Drop pressure for different values of water discharge at convergence angle 10 degree (vertical)

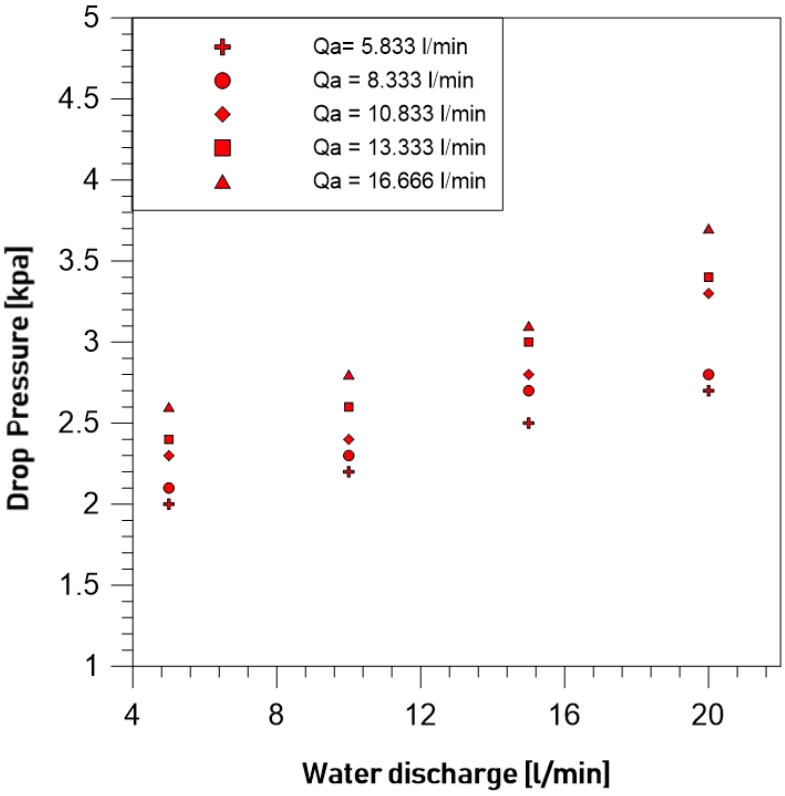

Figure (5.50): Drop pressure for different values of water discharge at convergence angle 15 degree (vertical)

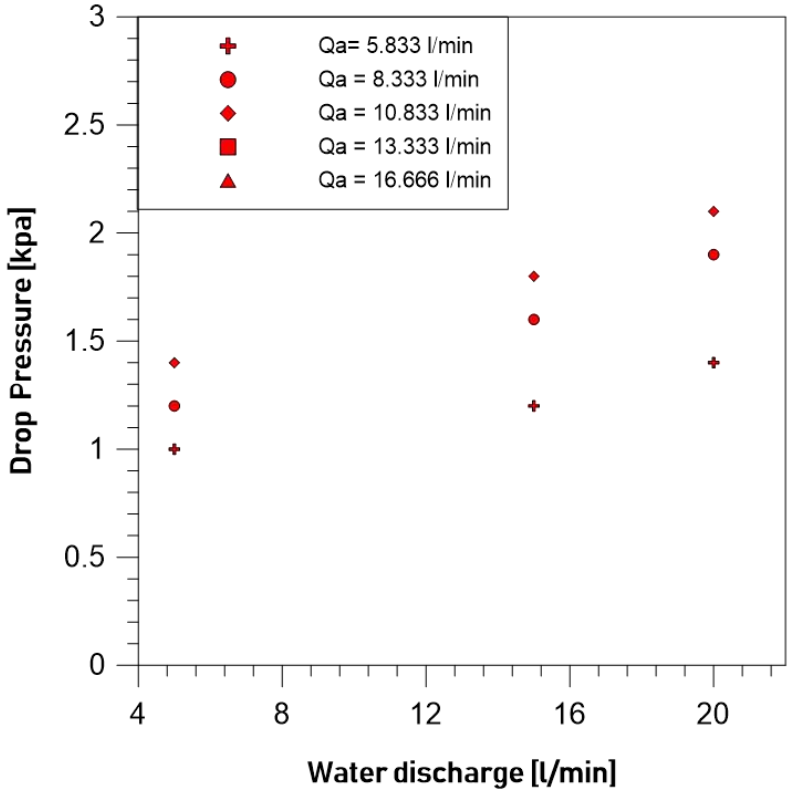

Figure (5.51): Drop pressure for different values of water discharge at convergence angle 10 degree (inclined)

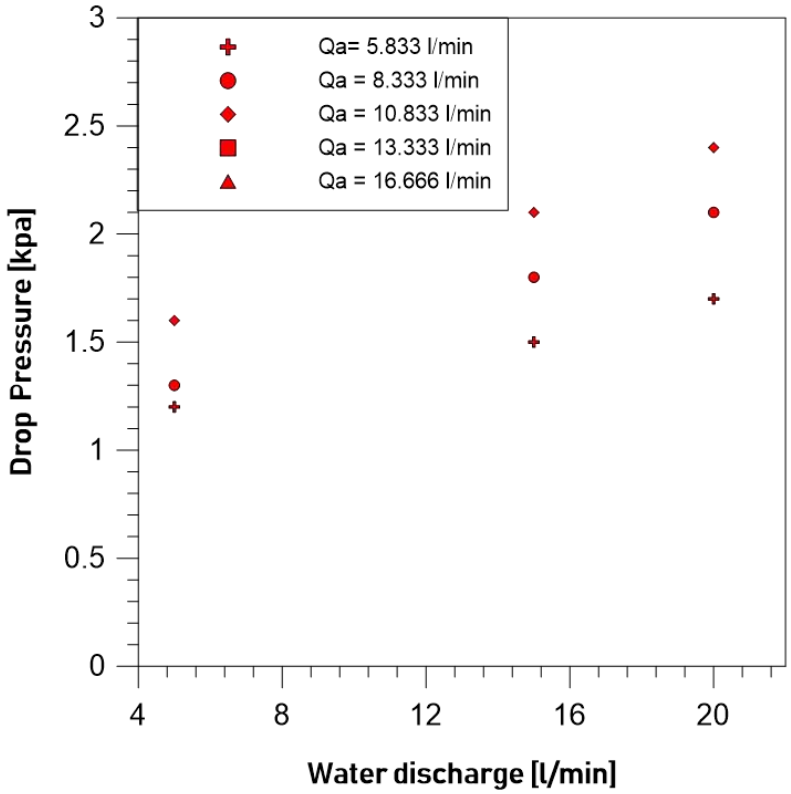

Figure (5.52): Drop pressure for different values of water discharge at convergence angle 15 degree (inclined)

5.4.2. Numerical results

5.4.2. A. Pressure contour

Figures (5.53) to (5.56), show the contours of pressure distribution for two-phase flow through the vertical ribs convergence test channel with opening angle 10 degrees, at various values of water (5,10,15 and 20 L/min). Each figure is five values of air discharge (5.833, 8.333, 10.833, 13.333 and 16.666 L/min)

Figures (5.57) to (5.59), show the contours of pressure distribution for two-phase flow through the inclined ribs convergence test channel with opening angle 10 degrees, at various values of water (5, 15 and 20 L/min). Each figure is three values of air discharge (5.833, 10.833and 16.666 L/min).

The figures show the effect of air discharge on contours of pressure at various values of water. It can be observed that the air discharge increased from 5.833 L/min to 16.666 L/min

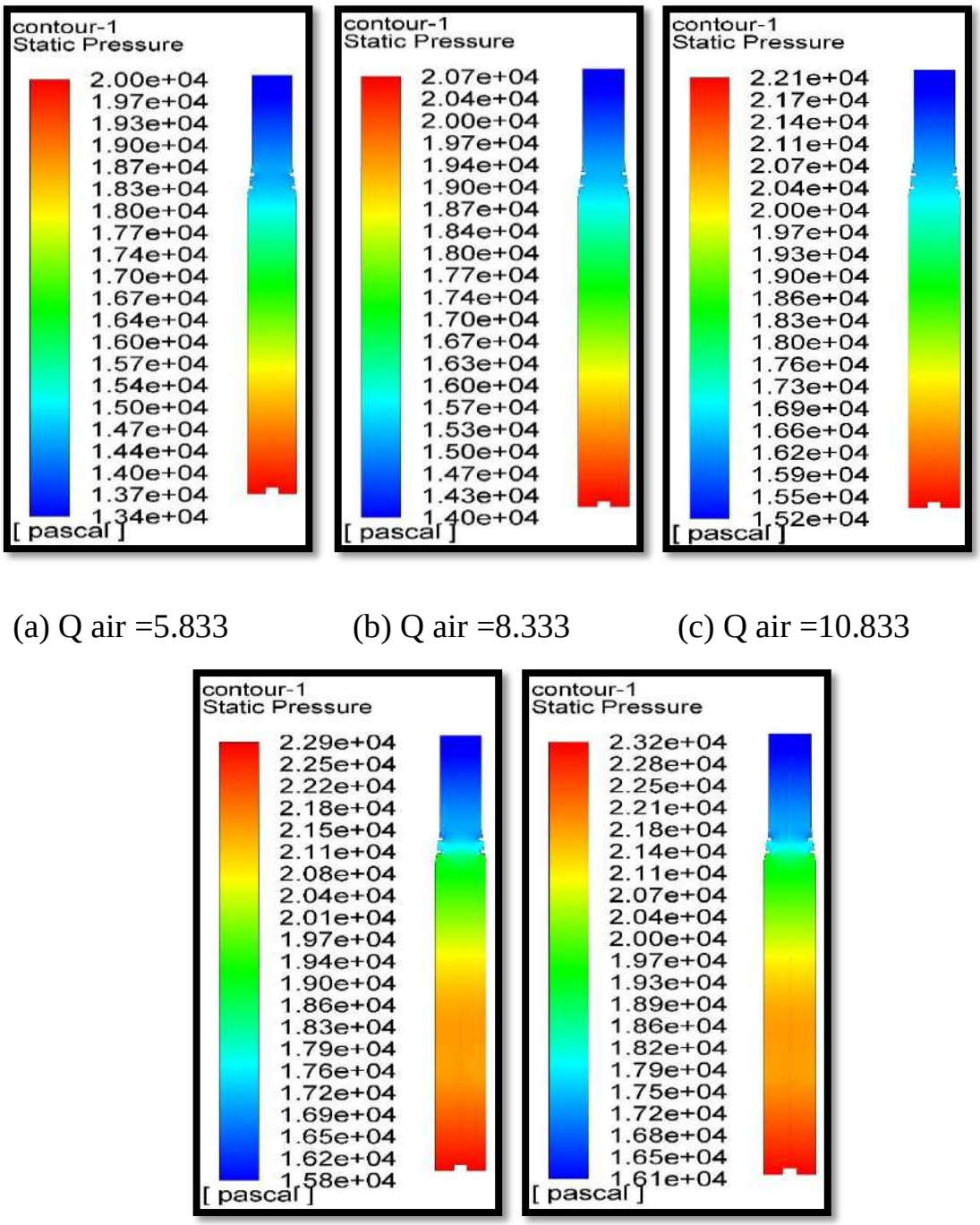

(a) Q air =5.833 (b) Q air =8.333 (c) Q air =10.833

(d) Q air =13.333 (e) Q air =16.666

Figure (5.53): Effect of air discharge on pressure distribution at 5 l/min water discharge (convergence angle10 degree)

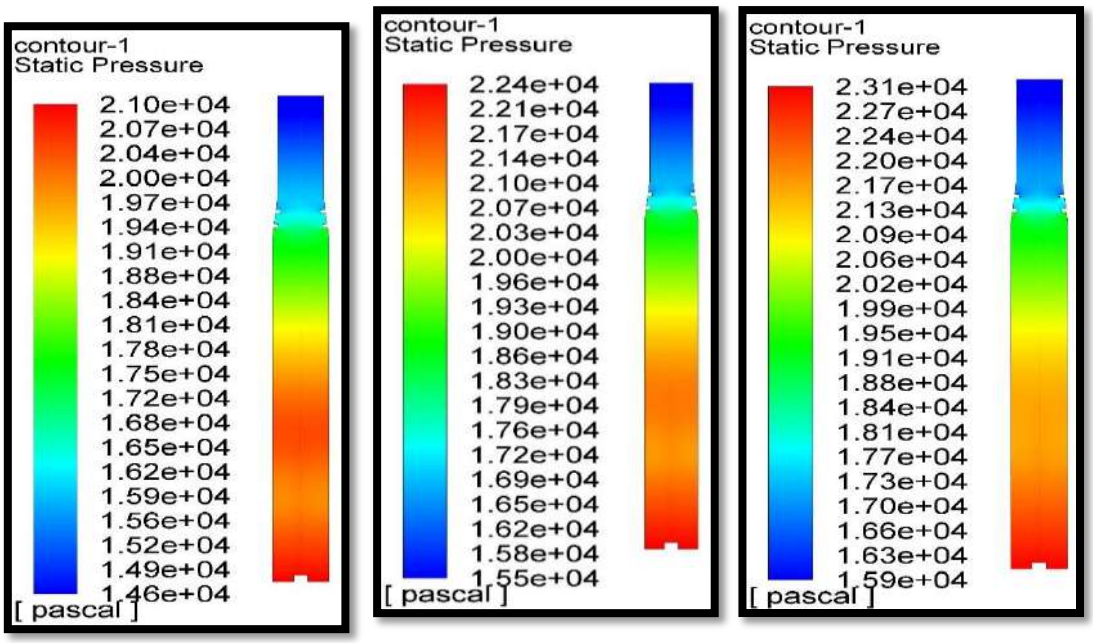

(a) Q air =5.833 (b) Q air =8.333 (c) Q air =10.833

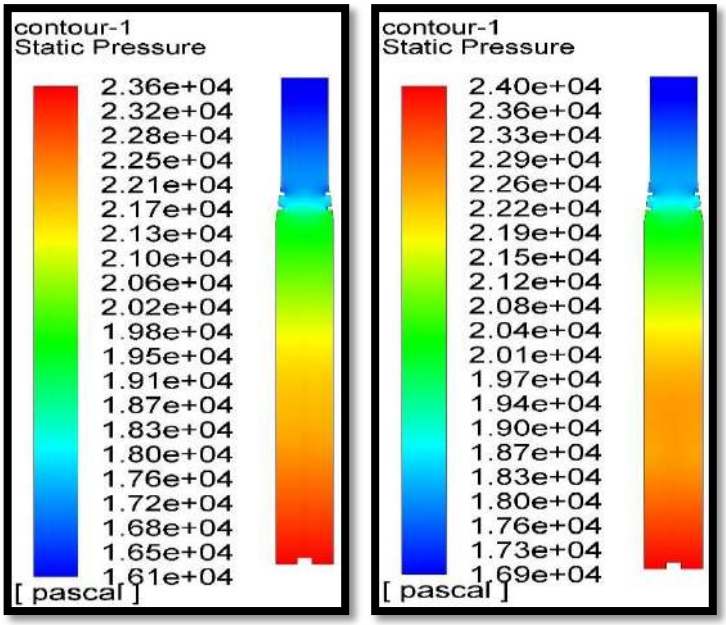

(d) Q air =13.333 (e) Q air =16.666

Figure (5.54): Effect of air discharge on pressure distribution at 10 l/min water discharge (convergence angle10 degree)

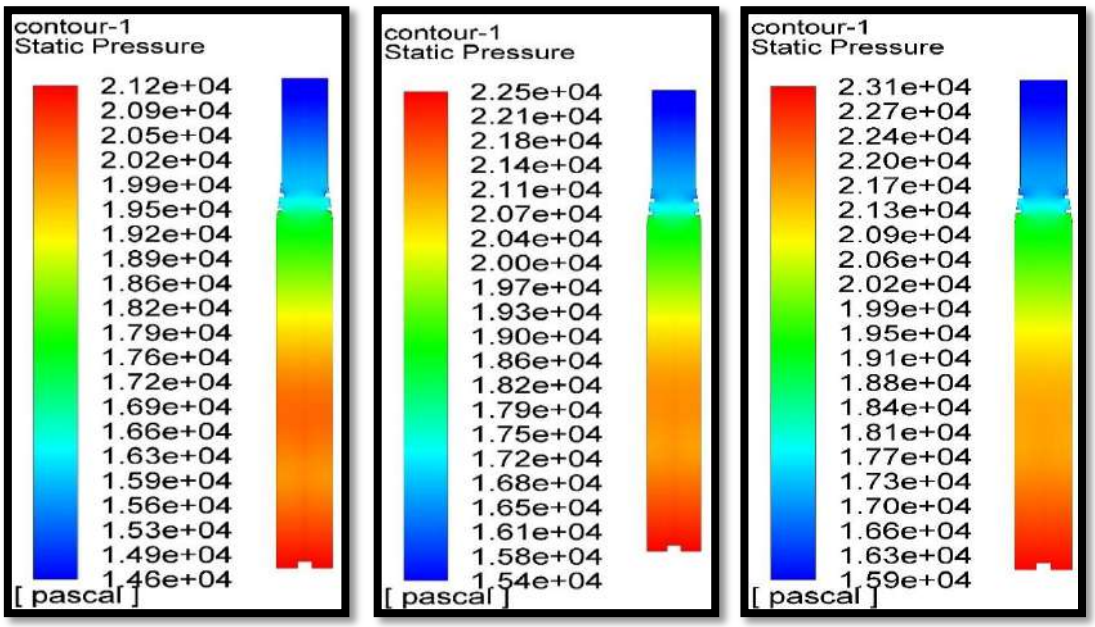

(a) Q air =5.833 (b) Q air =8.333 (c) Q air =10.833

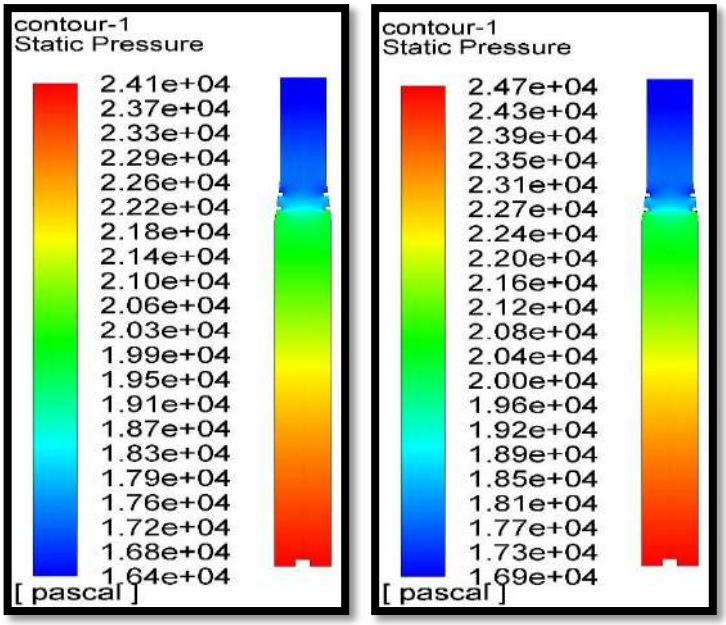

(d) Q air =13.333 (e) Q air =16.666

Figure (5.55): Effect of air discharge on pressure distribution at 15 l/min water discharge (convergence angle10 degree)

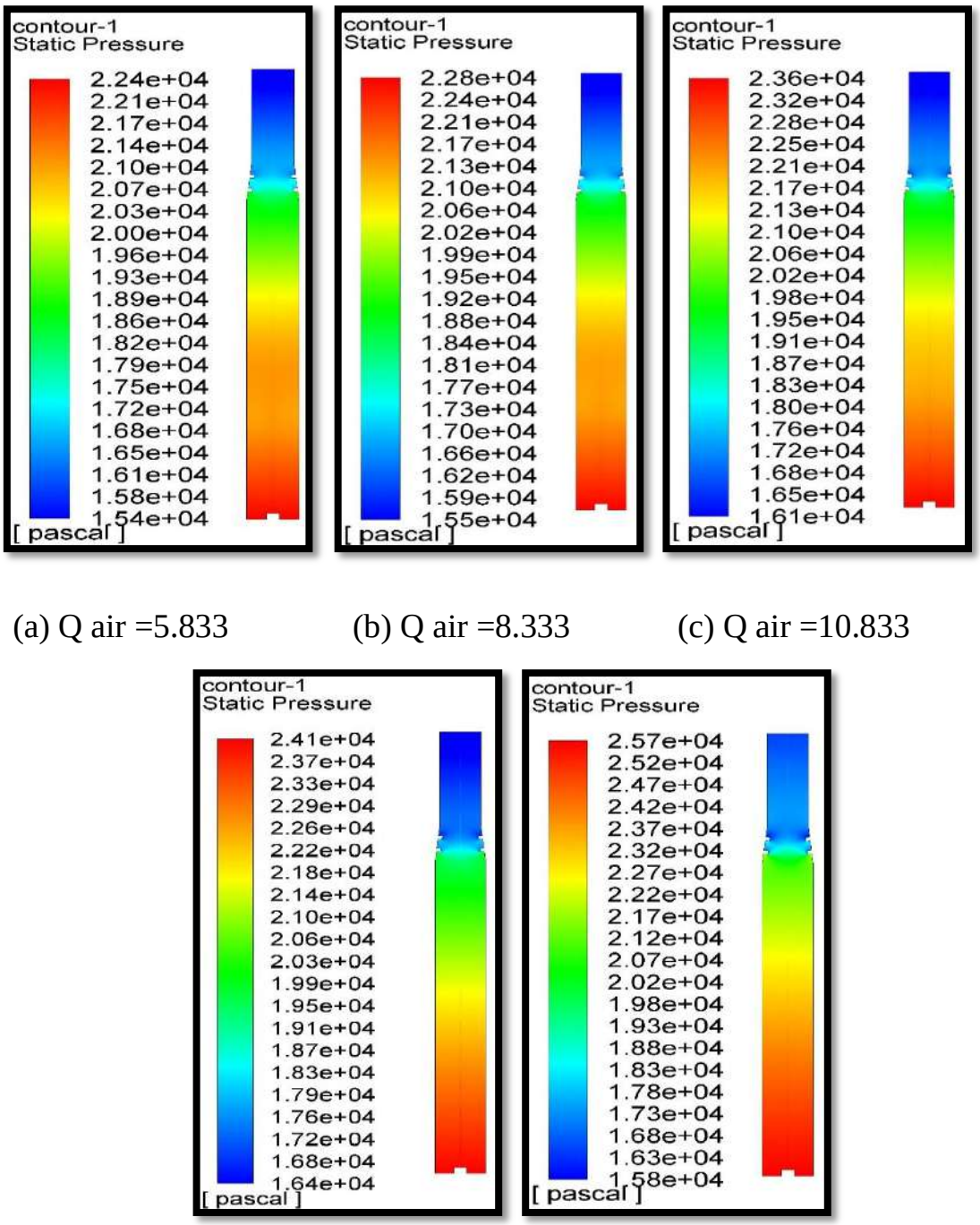

(a) Q air =5.833 (b) Q air =8.333 (c) Q air =10.833

(d) Q air =13.333 (e) Q air =16.666

Figure (5.56): Effect of air discharge on pressure distribution at 20 l/min water discharge (convergence angle10 degree)

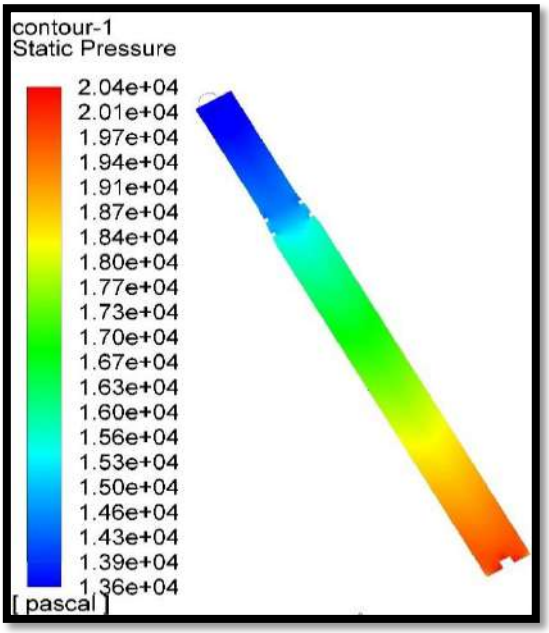

(a) Q air =5.833

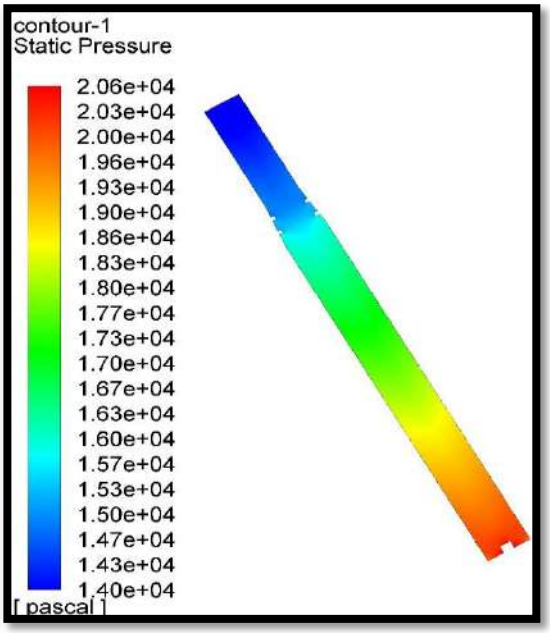

(b) Q air =10.833

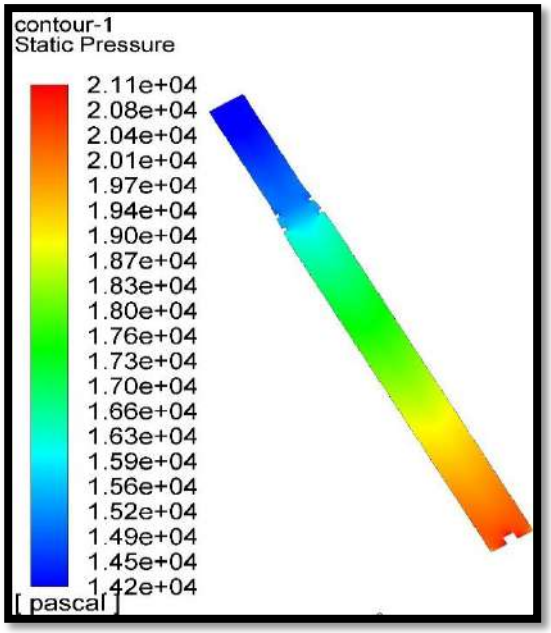

(c) Q air =16.666

Figure (5.57): Effect of air discharge on pressure distribution at 5 L/min water discharge (convergence angle10 degree)

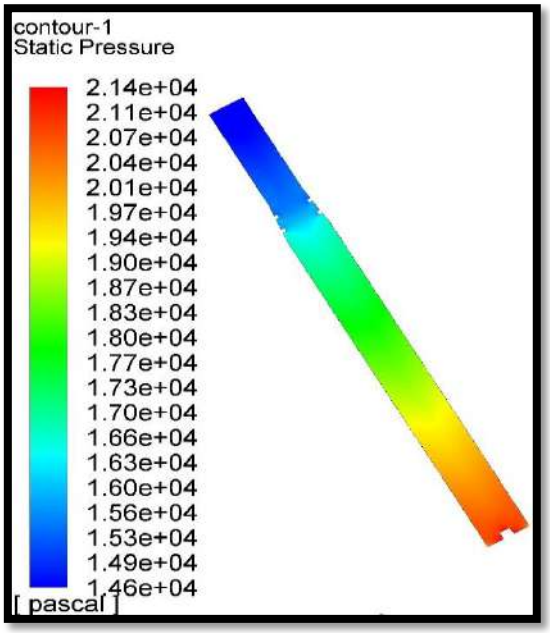

(a) Q air =5.833

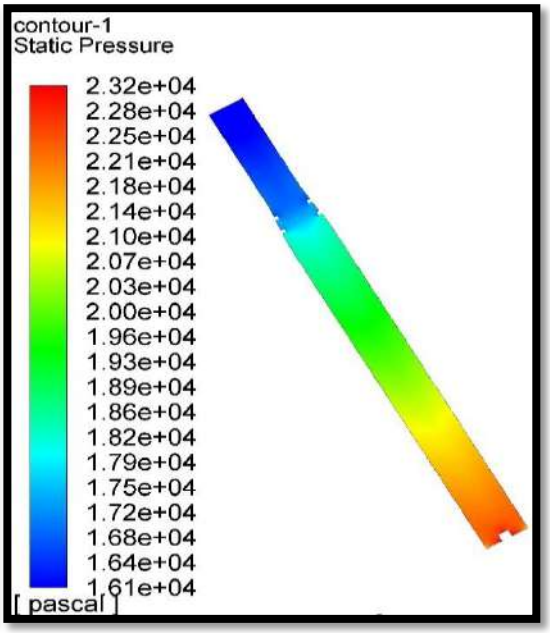

(b) Q air =8.333

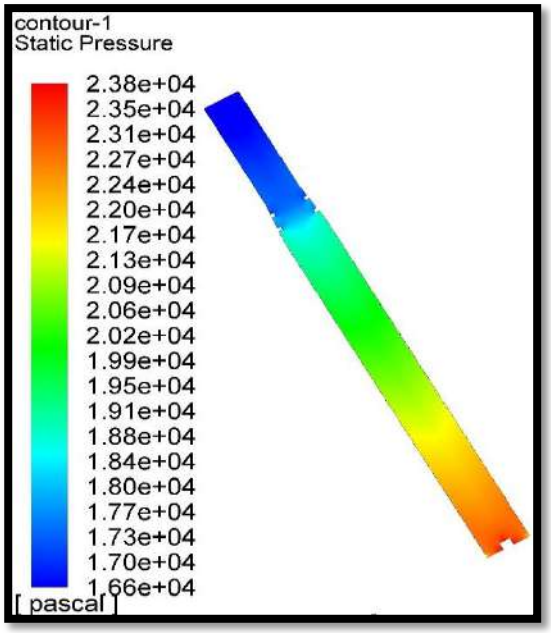

(c) Q air =16.666

Figure (5.58): Effect of air discharge on pressure distribution at 15 l/min water discharge (convergence angle10 degree)

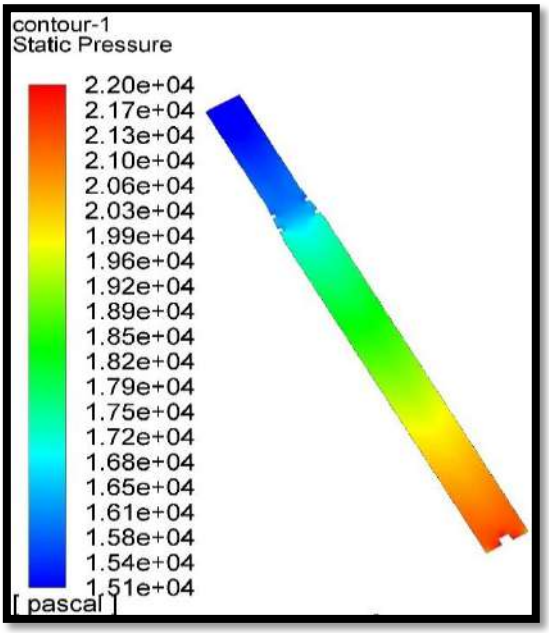

(a) Q air =5.833

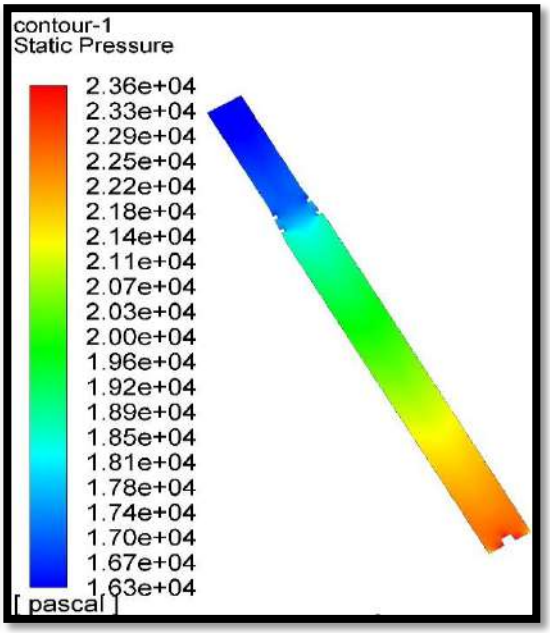

(b) Q air =10.833

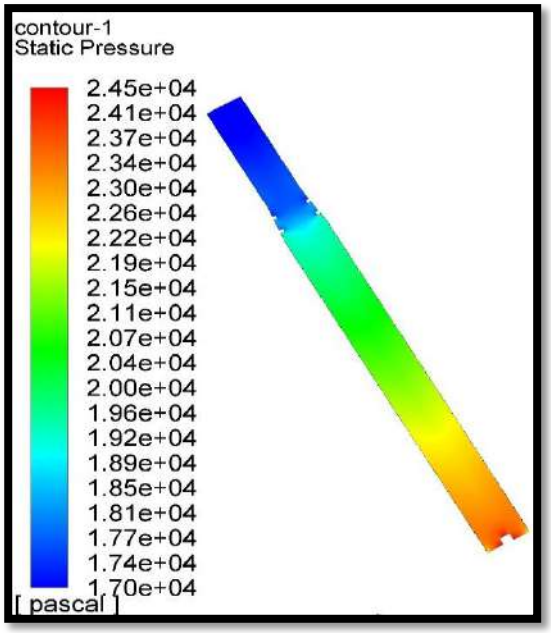

(c) Q air =16.666

Figure (5.59): Effect of air discharge on pressure distribution at 20 l/min water discharge (convergence angle10 degree)

5.4.2. B. Velocity Vector

The figures (5.60) and (5.61) shown the velocity vector, note that the generated vortexes are affected by the increased discharge of air and water which leads to increased turbulence, also notice that the ribs have a role in changing the direction of velocity and thus generate further turbulence.

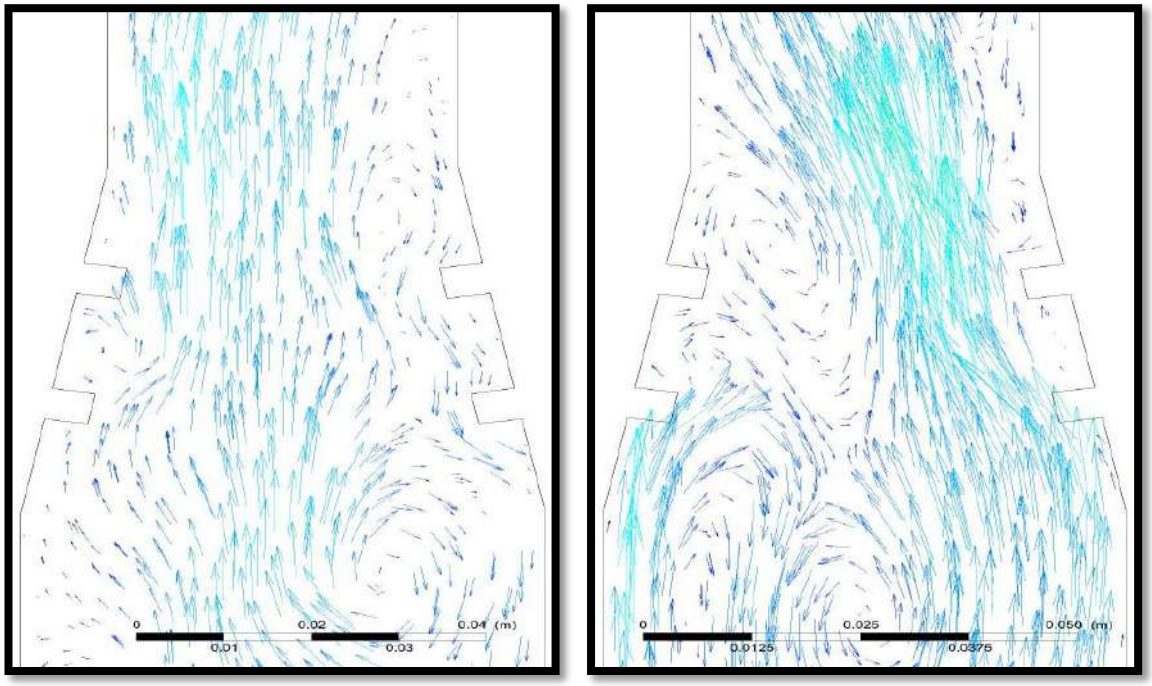

(a) Qair=5.833 L/min (b) Qair=16.666 L/min

Figure (5.60): velocity vector at 5 L/min water discharge (convergence angle10 degree)

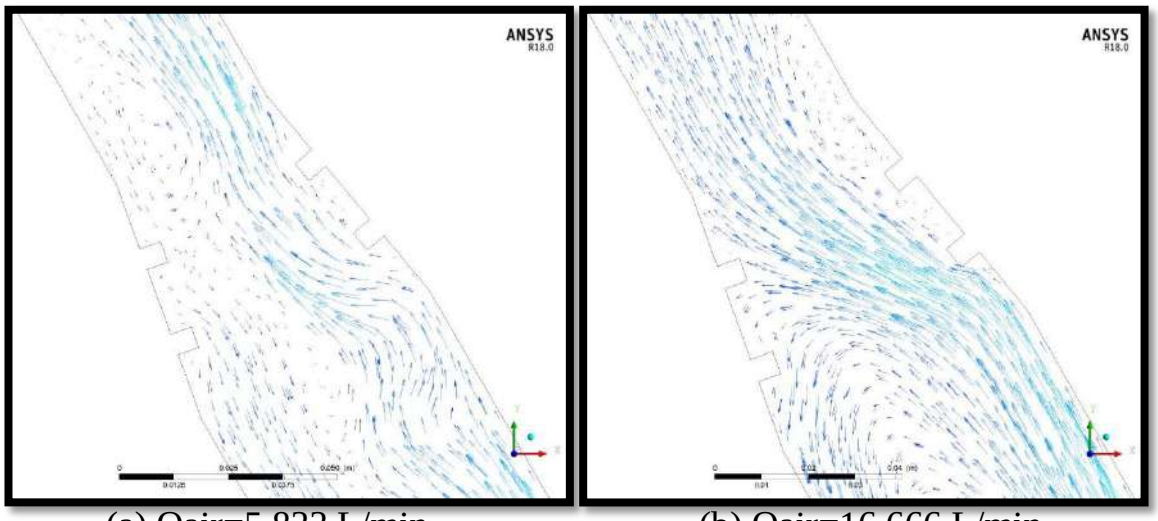

(a) Qair=5.833 L/min (b) Qair=16.666 L/min

Figure (5.61): velocity vector at 5 L/min water discharge (convergence angle10 degree)

5.4.3. Comparison between experimental and numerical results

5.4.3. A. Effect of water and air discharge on the pressure profile

The figures (5.62) and (5.63) is shown a comparison between of experimental and numerical results. Can observe that the behavior of the numerical results was similar to the experimental results. As observed that the values of experimental and numerical results were close and the maximum deviation was (9%).

Figure (5.62) demonstrate the compression between Effect of increasing water discharge on the experimental and numerical results of the pressure profile at four different points along the vertical test channel with opening angle 10 degrees for various values of air discharges (5.833,8.333,10.833,13.333 and 16.666)

Figure (5.63) show the compression between Effect of increasing water discharge on the experimental and numerical results of the pressure profile at four different points along the inclined test channel with opening angle 10 degrees for various values of air discharges (5.833, 10.833 and 16.666).

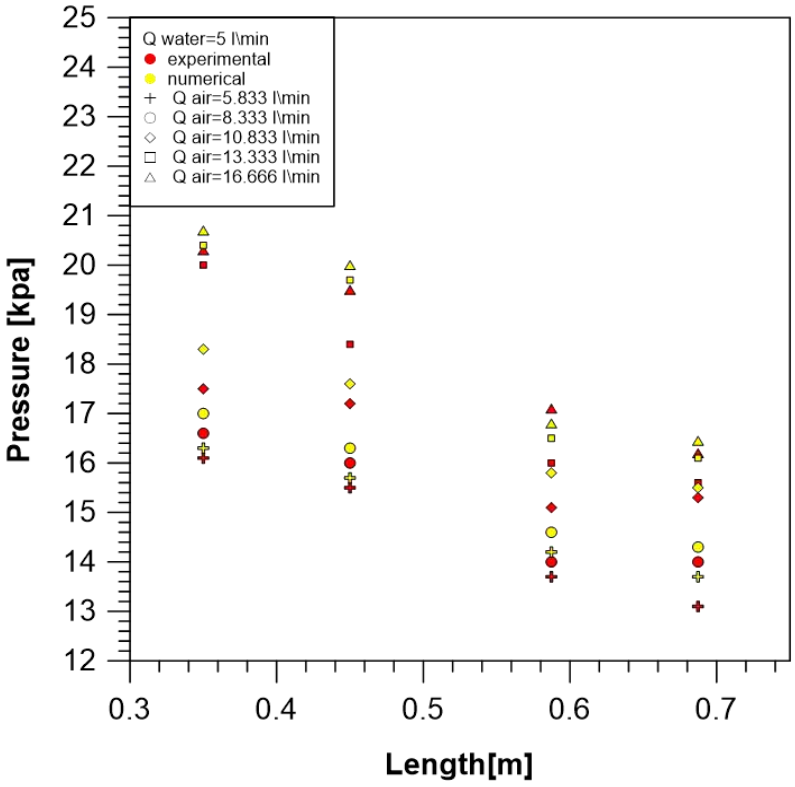

Figure (5.62a)

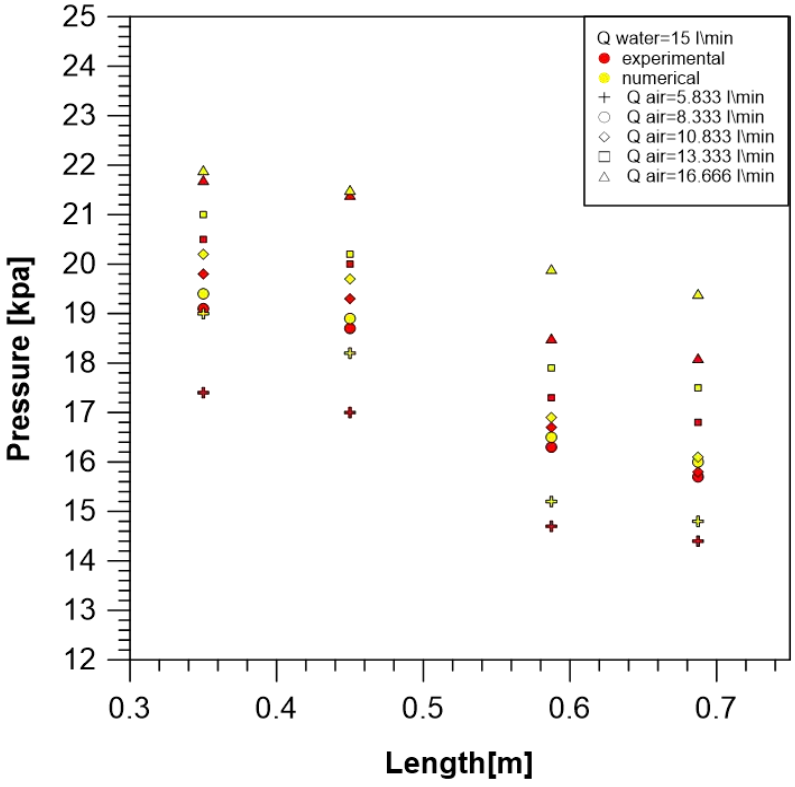

Figure (5.62): compression between Effect water discharge on Experimental and numerical pressure profile for convergence angle 10 degree (vertical)

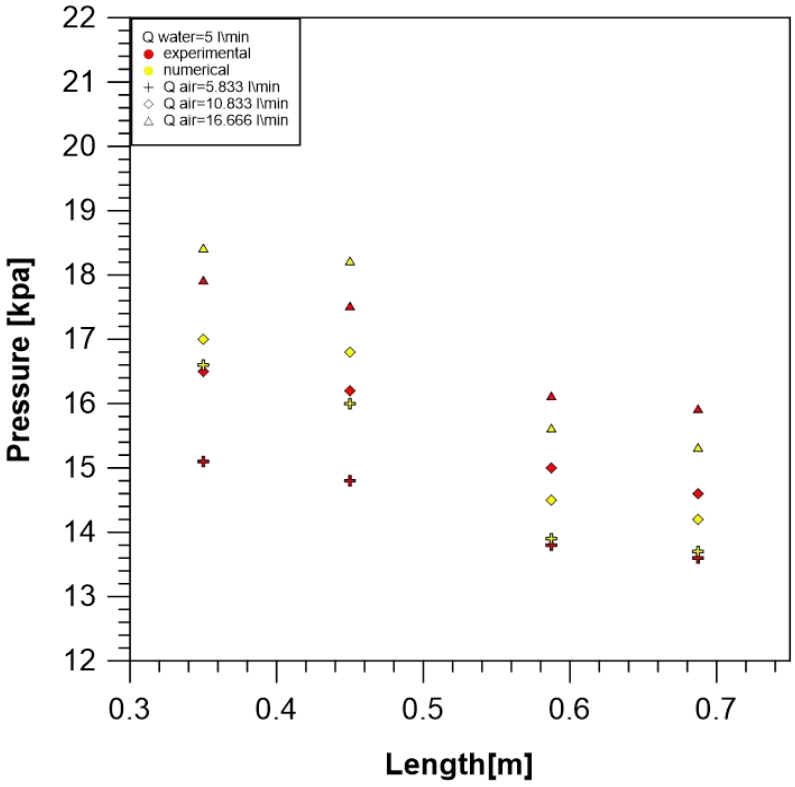

Figure (5.63a)

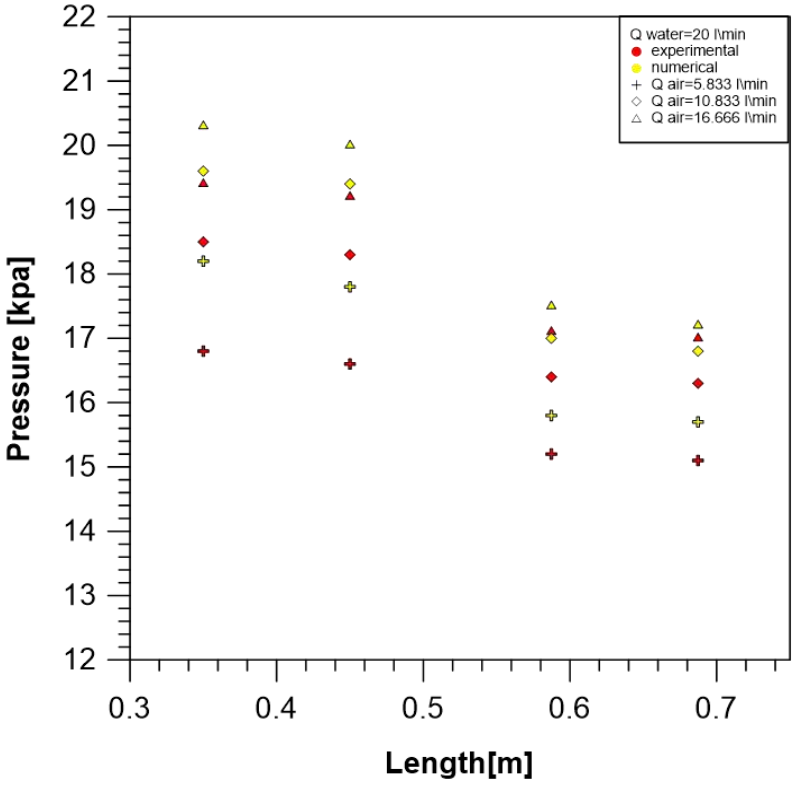

Figure (5.63b)

Figure (5.63): compression between Effect water discharge on Experimental and numerical pressure profile for convergence angle 10 degree (inclined)

5.4.3. B.The influence of water and air discharge on the flow behavior

The figures from (5.64) to (5.70) show the experimental flow behavior through the photographs that were taken for ribs convergence section and numerical simulation. A close similarity for the behavior of flow between

Visually compared it with the contour of air volume fraction found by the experimental photos and the images of air volume fraction found with ANSYS 18.

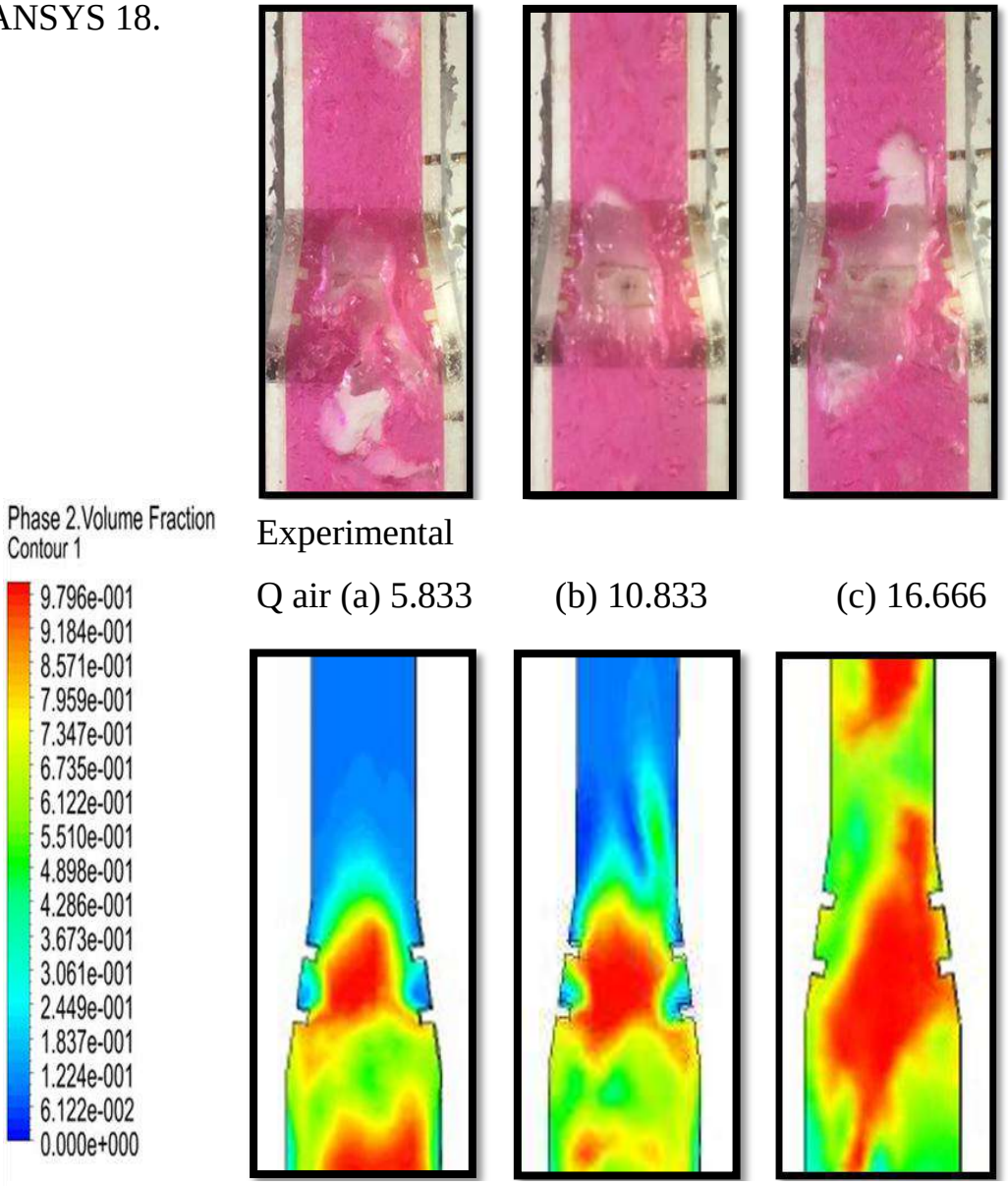

Figure (5.64) compression between the experimental and numerical of effect of air discharge on the flow behavior at Q water =5 L/min

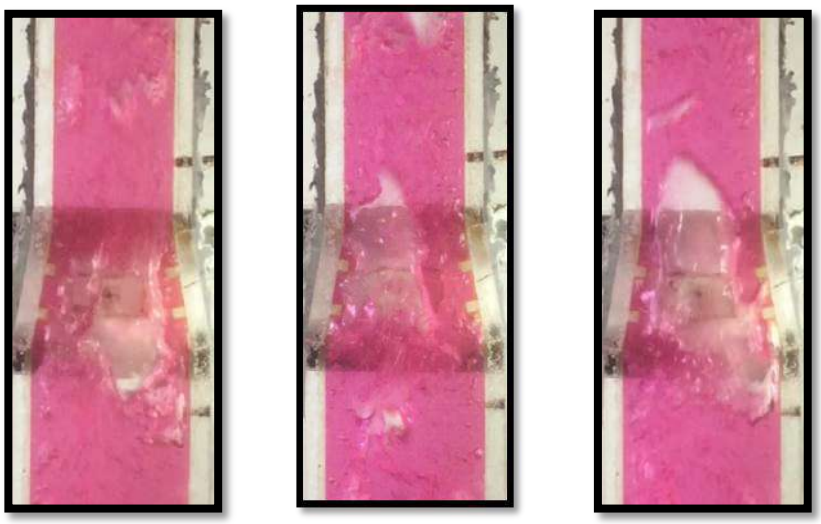

Experimental Q air (a) 5.833 (b) 10.833 (c) 16.666

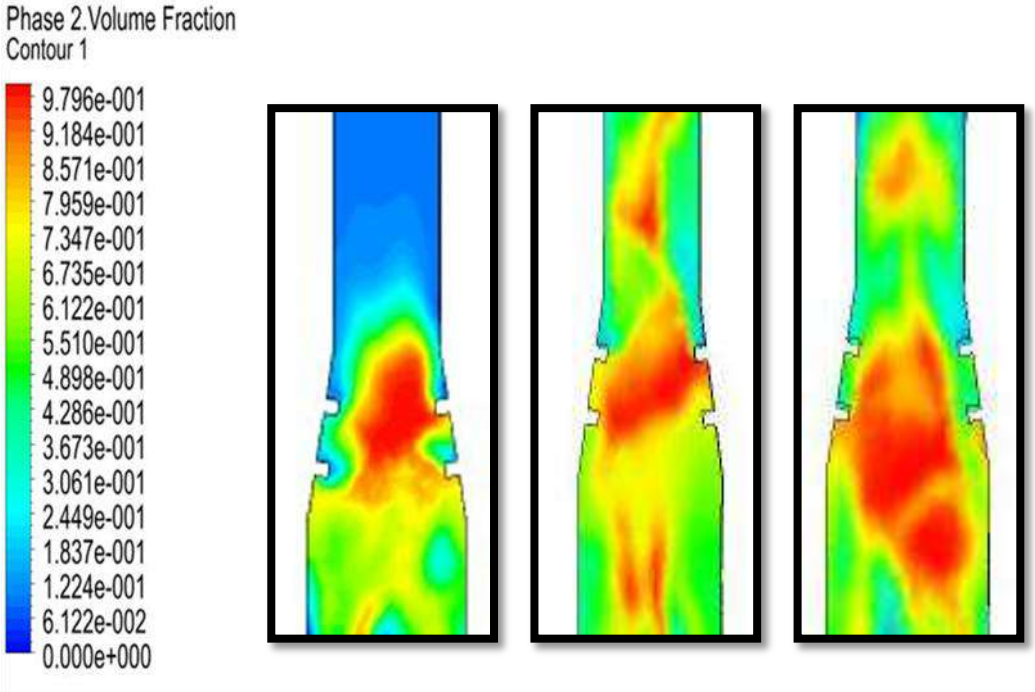

Numerical Q air (a) 5.833 (b) 10.833 (c) 16.666

Figure (5.65) compression between the experimental and numerical of effect of air discharge on the flow behavior at Q water =10 l/min

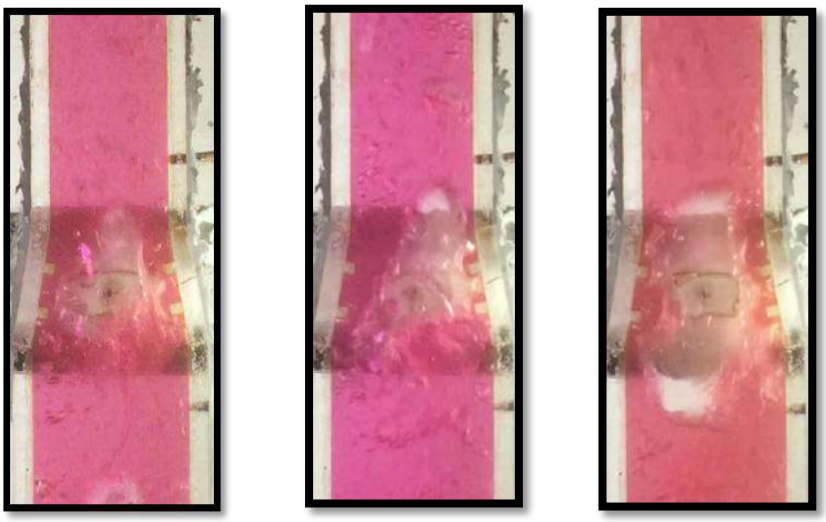

Experimental Q air (a) 5.833 (b) 10.833 (c) 16.666

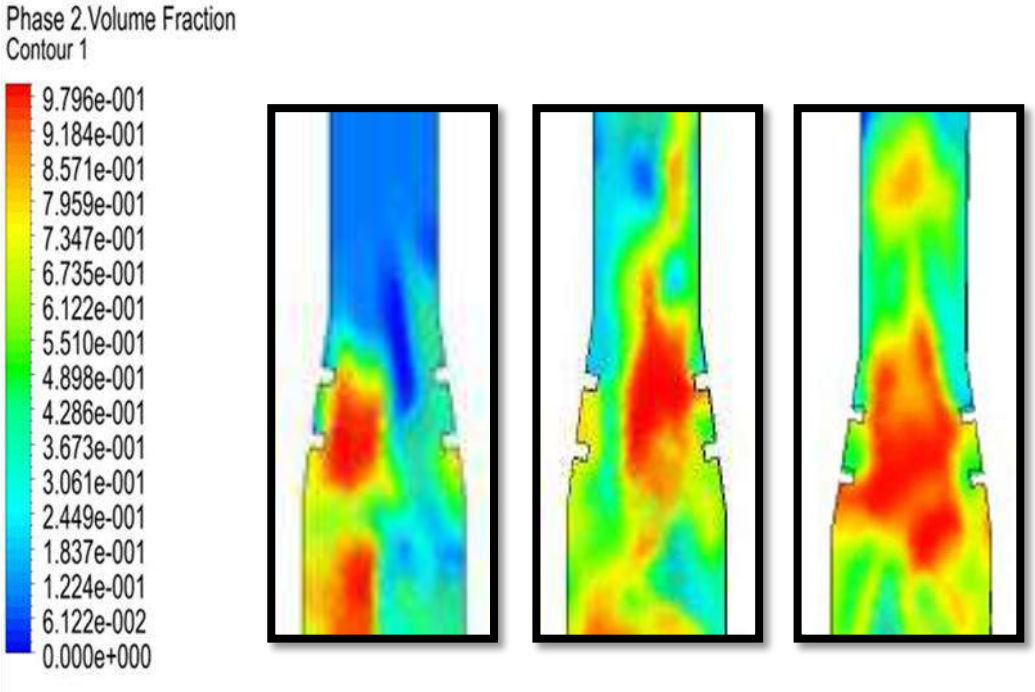

Numerical Q air (a) 5.833 (b) 10.833 (c) 16.666

Figure (5.66) compression between the experimental and numerical of effect of air discharge on the flow behavior at Q water =15 l/min

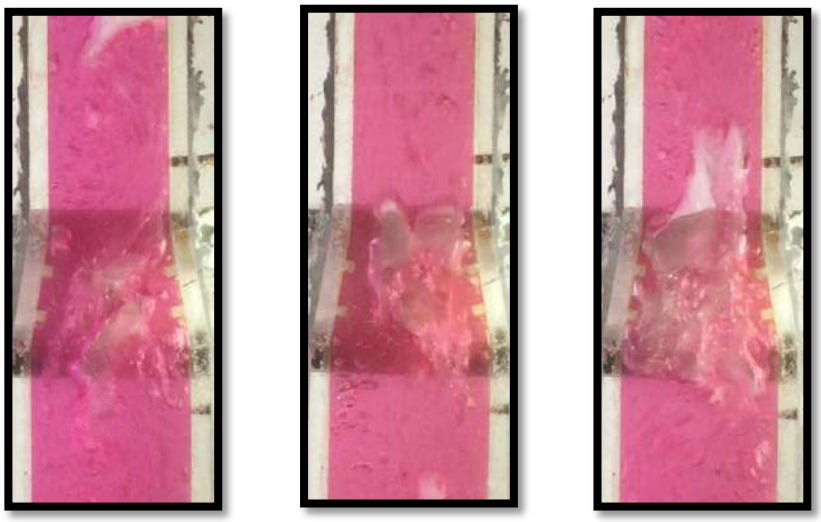

Experimental Q air (a) 5.833 (b) 10.833 (c) 16.666

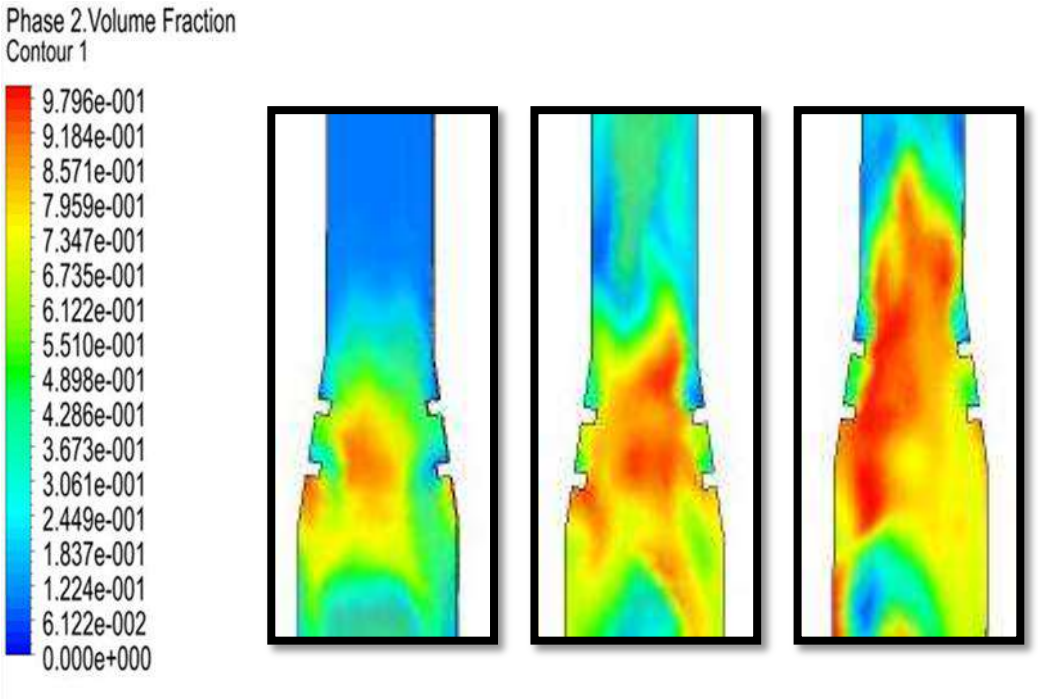

Numerical Q air (a) 5.833 (b) 10.833 (c) 16.666

Figure (5.67) compression between the experimental and numerical of effect of air discharge on the flow behavior at Q water =20 l/min

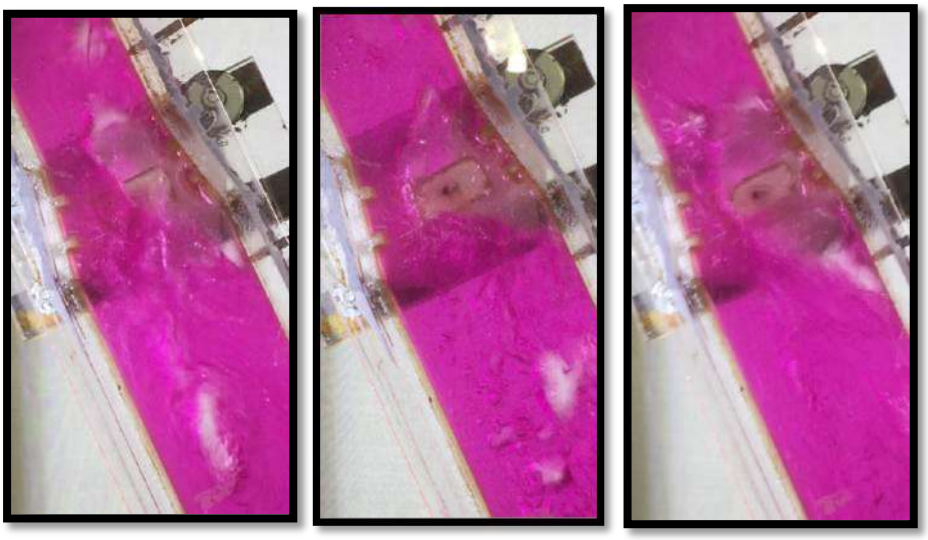

Experimental Q air (a) 5.833 (b) 10.833 (c) 16.666

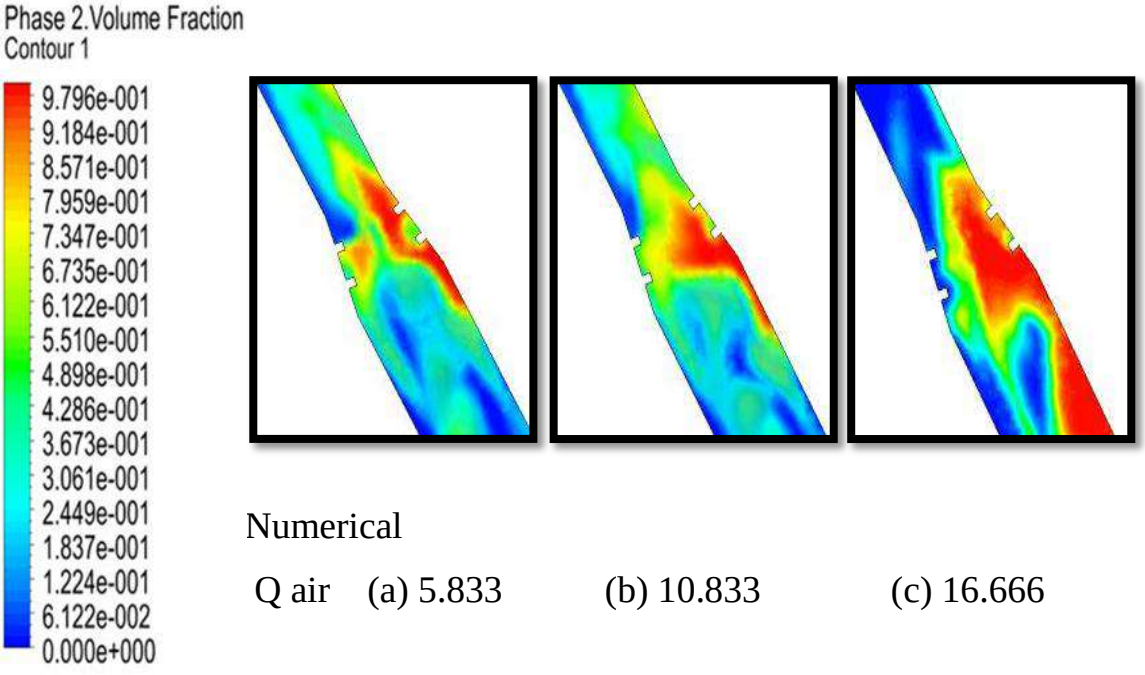

Numerical

Q air (a) 5.833 (b) 10.833 (c) 16.666

Figure (5.68) compression between the experimental and numerical of effect of air discharge on the flow behavior at Q water =5 l/min

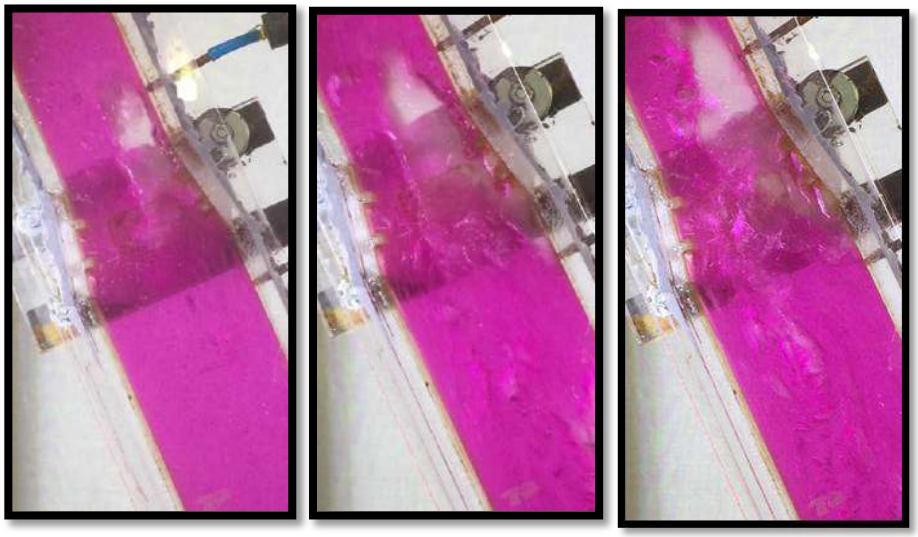

Experimental Q air (a) 5.833 (b) 10.833 (c) 16.666

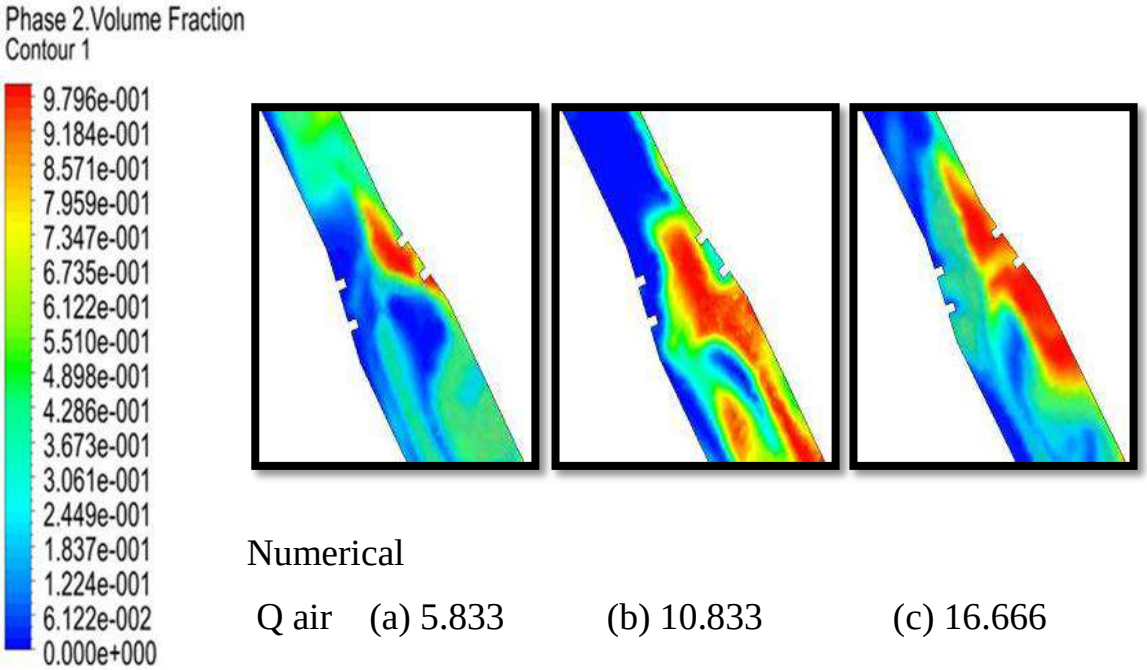

Numerical

Q air (a) 5.833 (b) 10.833 (c) 16.666

Figure (5.69) compression between the experimental and numerical of effect of air discharge on the flow behavior at Q water =15 L/min

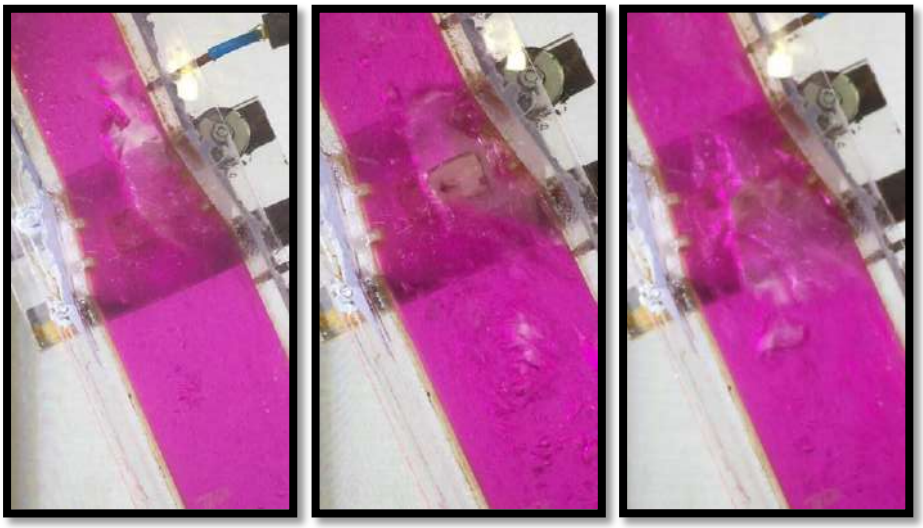

Experimental Q air (a) 5.833 (b) 10.833 (c) 16.666

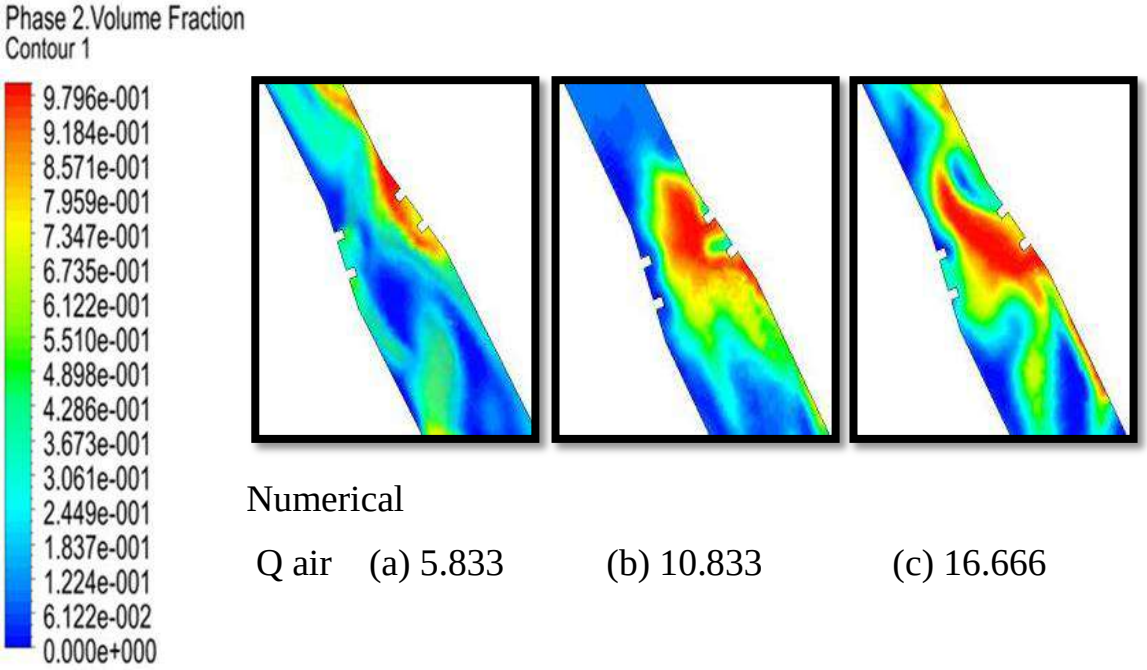

Numerical

Q air (a) 5.833 (b) 10.833 (c) 16.666

Figure (5.70) compression between the experimental and numerical of effect of air discharge on the flow behavior at Q water =20 l/min

5.5. Numerical study of effect the ribs the pressure recovery

A numerical study was carried out to show the effect of ribs on the pressure recovery across the divergent section; a case was studied with ribs and without ribs as shown in Figure (5.71) and (5.72).

The figure (5.71) represents the case of the flow through the divergence section with opening angle 10 and the air and water discharges were 5 L/min and 16.666 L/min with the absence of ribs, while the figure (5.72) represents the flow within the same divergence section and same discharges of air and water with the presence of ribs. We note that the values of the recovery of pressure across the divergence section of the absence of ribs are higher than the case of presence ribs, where the pressure increased in the absence of ribs case from 17.2 kpa to 22 kpa while in the presence of ribs, the pressure increased from 17.3 kpa to 21.7 kpa because more vortex occur as a result of the presence of ribs thus leading to reduced pressure, as shown in figure (5.73) and (5.74).

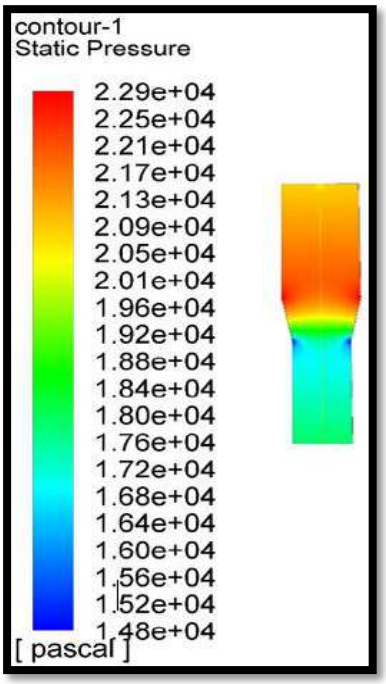

Figure (5.71)

Divergence section without ribs

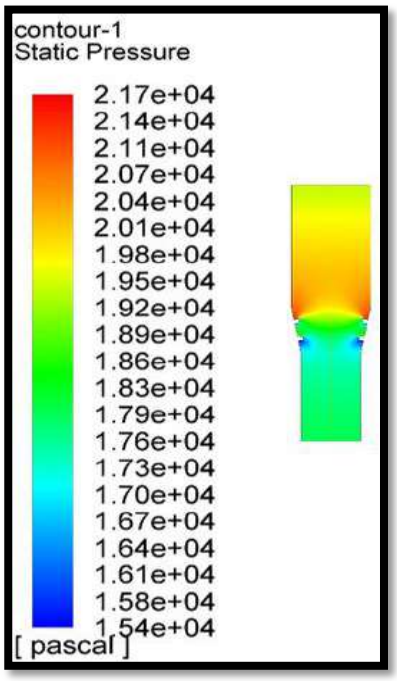

Figure (5.72)

Divergence section with ribs

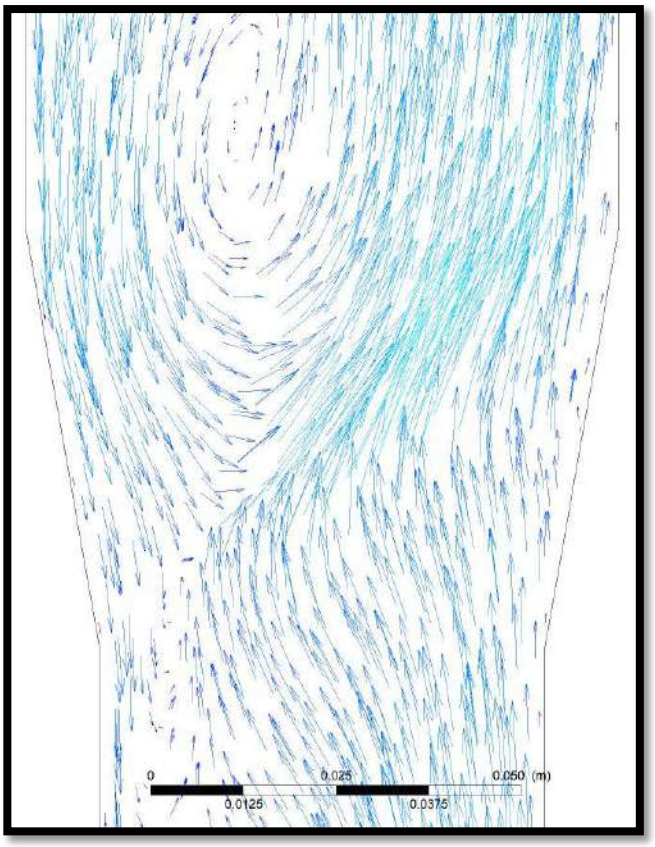

Figure (5.73): Velocity vector at divergence section without ribs

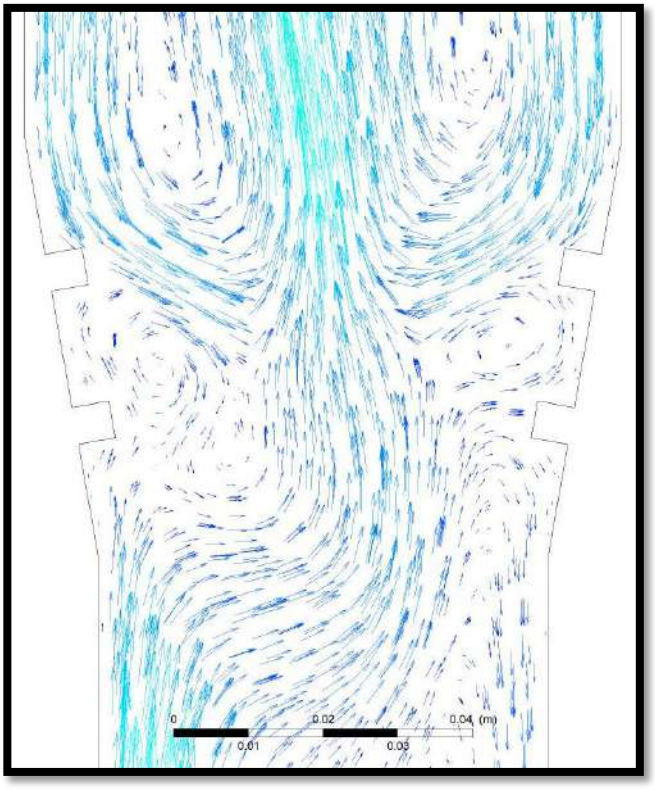

Figure (5.74): Velocity vector at divergence section without ribs

الخلاصة

تم دراسة الجريان ثنائي الطور في قناة مستطيلة تحتوي على مقطع متباعد/متقارب يحتوي على مضلعات وتمت الدراسة بحالتين للجريان: جريان تصاعدي عمودي ومائل. تم استخدام الهواء والماء كمواد للتم اجراء دراسة عملية وعددية لاختبار تأثير زيادة تصريف الهواء والماء على توزيع الضغط على طول قناة الاختبار وتأثيره على فرق الضغط عبر مقطع التباعد/التقارب وكذلك تأثير زيادة زاوية التباعد/التقارب على فرق الضغط عبر المقطع.

تم تحديد خصائص أنماط الجريان عن طريق المشاهدة البصرية. وتم استخدام متحسسات الضغط وكاميرا تصوير فديو لدراسة أنماط الجريان خلال قناة الاختبار. تصاريف الماء المستخدمة في هذا العمل كانت (5-20 لتر/دقيقة) و تصاريف الهواء كانت (5.833-16.666 لتر/دقيقة) . وتم استخدام قناتي اختبار بزوايا تباعد/تقارب كانت ١٠و١٥ درجة.

تم تصنيع قناة الاختبار بأبعاد (٢*٦ سم) بالنسبة لمساحة المقطع العرضي للقناة قبل مقطع التباعد/التقارب و بطول 50 سم بينما مساحة المقطع العرضي للقناة بعد مقطع التباعد/التقارب كانت (٢*٨ سم) و بطول ٥٠ سم ايضاً.

تم عمل محاكاة CFD لنموذج ثلاثي الابعاد باستخدام برنامج ANSYS FLUENT 18 الذي يعتمد على شرط حدود الدخول التي يتم اخذها من الجانب العملي والمحكومة بمعادلات نموذج اويلر للجريان متعدد الاطوار.

لوحظ ان هناك تطابق بين قيم الضغط العملي والنظري وان اعلى انحراف كان ٩% وكذلك لوحظ بوجود تشابه في سلوك الجريان بين الجانب العملي و النظري.

بينت النتائج ان الضغط على طول القناة يزداد مع زيادة تصريف الهواء او الماء. بالنسبة للقناة العمودية ذات مقطع المقطع التباعدي بزاوية ١٠ درجة نلاحظ انه عندما يزداد تصريف الماء م 5 لتر/دقيقه الى ٢٠ لتر/دقيقة عند نفس موقع متحسس الضغط و تصريف الهواء (٣٥ سم و ٥.٨٣٣ لتر/دقيقة) على التوالي ،فأن الضغط يزداد من 14.6 kpa الى 16.7 kpa

بالنسبة للمقطع المتباعد نلاحظ انه عندما تزداد زاوية الانفتاح فأن قيمة استرجاع الضغط يقل بينما في حالة المقطع المتقارب فأن هبوط الضغط يزداد مع زيادة زاوية التقارب للمقطع.

كذلك لوحظ ان نمط الجريان السائد ضمن مديات التصريف المستخدمة كان من نوع slug وان قيم تصاريف الهواء و الماء تم تمثيلها على خريطة الجريان Hewitt and Roberts flow.

maps(1969) وكذلك استخدمت خريطة الجريان Barnea flow map (1980) للجريان المائل قد لوحظ ان هناك تطابق جيد بين نمط الجريان الذي ظهر خلال تجارب العملي و بين نمط الجريان في خريطه نمط الجريان.

تم إجراء دراسة رقمية فقط لدراسة تأثير المضلعات على سلوك التدفق واستعادة الضغط، وقد لوحظ أن قيمة استرداد الضغط عبر قسم التباعد في حالة عدم وجود أضلاع أعلى من حالة وجود الأضلاع بنسبة 8.333%.

جمهورية العراق

وزارة التعليم العالي والبحث العلمي

جامعة كربلاء - كلية الهندسة

قسم الهندسة الميكانيكية

دراسة تجريبية وعددية لجريان ثنائي الطور في قناة توسعية مستطيله مضلعة

رسالة مقدمة الى كلية الهندسة - جامعة كربلاء كجزء من متطلبات نيل درجة ماجستير علوم في الهندسة الميكانيكية

من قبل

علي عبد الائمة حسن

بأشراف

أ.م.د. عباس ساهي شريف

أ.م.د. رياض صباح الطريحي

٢٠١٨ م ١٤٤٠ هـ